SYNTHESIS AND CHARACTERIZATION OF EXTRUDED ALKALI ACTIVATED EARTH-BASED COMPOSITES FOR SUSTAINABLE BUILDING CONSTRUCTION

DISSERTATION

Submitted to the Graduate Faculty
in Partial Fulfillment of the Requirement for the
Degree of **Doctor of Philosophy** in the
Department of Materials Science and Engineering
African University of Science and Technology, Abuja-Nigeria

EMESO BECKLEY OJO
70107

Ph.D Dissertation Committee:
Professor Holmer Savastano Jr. (University of São Paulo, Brazil)
Professor Peter A. Onwualu (African University of Science and Technology, Abuja)
Professor Winston O. Soboyejo (Worcester Polytechnic Institute, Massachusetts, USA)
Dr. Kabiru Mustapha (Kwara State University, Malete Nigeria)

SYNTHESIS AND CHARACTERISATION OF EXTRUDED ALKALI ACTIVATED EARTH-BASED COMPOSITES FOR SUSTAINABLE BUILDING CONSTRUCTION

By

Emeso Beckley Ojo

A THESIS APPROVED BY THE MATERIALS SCIENCE AND ENGINEERING DEPARTMENT

RECOMMENDED: …….
Supervisor, Professor Holmer Savastano Jr.

……
Co-Supervisor, Professor Peter A. Onwualu

……..

…….
Head, Dept. of Materials Science and Engineering

Approved:……..……
Vice President, Academics

Date:……

DEDICATION

This thesis is dedicated to Almighty God; thank you for making a way for me.

ABSTRACT

Alkali activation is a rapidly developing area in the global materials research and development community. It is based on alkali aluminosilicate chemistry with primary focus on the activation of solid aluminosilicate materials under alkaline conditions to produce three-dimensional network of inorganic polymer binders. However, little research has been conducted to harness this technology in the development of earth-based composites. This work provides insights on the application of alkali activation in the synthesis of in situ binders in earth-based composites using uncalcined clays and low molarity alkaline solutions for the development of low-impact extruded building materials. To evaluate the effect of these alkaline soil matrices on the reinforcing effects of natural fibres, two ligno-cellulosic fibres were selected (sisal and eucalyptus pulp) as well as a synthetic fibre (polypropylene) as reinforcements. The compositional dependence on extrudability of the fresh pastes was studied by characterizing bulk and interfacial rheology behavior induced by fibres using the Benbow-Bridgwater model to evaluate the feasibility of extrusion moulding as a processing method. Physico-mechanical evaluation as well as microstructural analysis was conducted to evaluate reinforcing efficiency of fibres. The underlying strengthening and toughening mechanisms associated with the fibres were explored using a combination of in situ/ex situ observations of crack propagation and micro-mechanical models. The results show that with low molarity alkali activator solutions, partial dissolution of aluminosilicates in the soil result in the formation of amorphous sodium aluminosilicate gels which provide satisfactory binding within the soil matrix. Variation of synthesis conditions shows that initial curing temperatures plays a critical role in the synthesis of these binders. Mechanical and physical properties of plain earth matrices incorporating these binders were comparable and in some cases higher than other stabilized earth building materials. Interactions between the alkaline matrix and ligno-cellulosic fibres resulted in improved flexural strengths as well as reduced water absorption capacities of the composites. On the other hand, weak interactions between polypropylene fibre and the alkaline matrix resulted in marginal increase in flexural strengths but transformed brittle earth matrices into deflection hardening composites. Whilst, strengthening mechanism of composites reinforced with ligno-cellulosic fibres was via elastic shear stress transfer at the fibre-matrix interface, polypropylene fibres strengthened the matrix via frictional slip after debonding at the fibre-matrix interface. Predominant toughening mechanisms for all composites was via crack bridging as prediction of

resistance curve behavior of composites was comparable to measured resistance curve in short scale and long scale bridge regimes. The implications of these results are discussed as potential building materials to meet increasing housing demands in line with targets set by the sustainable development goals (SDGs).

ACKNOWLEDGEMENTS

I wish to extend my sincere appreciation to my Ph.D Dissertation Committee; Prof. Holmer Savastano Jr., Prof. Peter A. Onwualu, Prof. Winston O. Soboyejo and Dr Kabiru Mustapha for their technical guidance and support throughout the course of the program. Particularly, I wish to appreciate the efforts and technical support of Prof. Holmer Savastano Jr. His encouragement and technical guidance was instrumental to the successful completion of this program. My gratitude also goes to Research Nucleus for Biosystems at the University of São Paulo, Pirassununga, Brazil for their contribution and useful suggestions.

I would like to thank the Pan African Materials Institute under the World Bank African Centres of Excellence Program as well as the African Development Bank for their financial support. I also wish to thank the staff and Management of the Nigerian Building and Road Research Institute for support. Special thanks goes to Prof. D.S. Matawal, the immediate past Director General/CEO as well as Prof. Duna Samson, Acting Director General/CEO.

This academic pursuit would have been impossible without the continuous guidance, emotional support, prayers and mentorship from my parents, Prof. Paul and Mrs. Rose Idornigie. They set me on this path to academic excellence and I'm truly grateful to God to be blessed with such supportive parents. I also wish to thank my siblings Emo, Obo, Tony and Imoudu.

Finally, a special thank you goes to my 'Sweets of Life', Mr. Beckley Ojo for the love, encouragement and support from the onset of the Ph.D program. This program would have been impossible if I wasn't married to such a strong, confident and understanding man. And to my lovely children Isabel, Michelle and David, thank you for understanding and bearing with my absence during the program.

TABLE OF CONTENTS

List of Tables

List of Figures

Peer Reviewed Publications

1. **Ojo E.B.,** Mustapha K., Teixeira R.S., & Savastano H. (2019). Development of unfired earthen building materials using muscovite rich soils and alkali activators, *Case Studies in Construction Materials* 11 (2019) doi:https://doi.org/10.1016/j.cscm.2019.e00262.

2. **Ojo E.B.,** Bello O.K., Mustapha K., Teixeira R.S., Santos S.F. & Savastano H. (2019). Effects of fibre reinforcements on properties of extruded alkali activated earthen building materials, *Construction and Building Materials* 227 (2019) 116778. doi:https://doi.org/10.1016/j.conbuildmat.2019.116778.

3. **Ojo E.B.,** Bello O.K., Teixeira R.S., Onwualu P.A., & Savastano H. (2019). Statistical Data on the Physical and Mechanical Properties of Fibre Reinforced Alkali Activated Uncalcined Earth-based Composite, *Data in Brief* 28 (2020) https://doi.org/10.1016/j.dib.2019.104839

4. **Ojo E.B.,** Bello O.K., Ngasoh O.F., Stanislas T.T., Mustapha K., Savastano H. & Soboyejo W.O. (2019). Mechanical Performance of Fibre-Reinforced Alkali Activated Un-Calcined Earth-Based Composites, *Construction and Building Materials* (Under Review)

5. **Ojo E.B.,** Bello O.K., Ngasoh O.F., Stanislas T.T., Teixeira R.S., Onwualu P.A., & Savastano H. (2019). Rheology and Extrudability of Fibre Reinforced Alkali Activated Earth Based Composites *Materials and Structures* (Under Review)

Conference Presentations

1. **Ojo E.B.,** Stanislas T.T., Ngasoh O.F., Onwualu P.A., Savastano H. & Soboyejo W.O. (2019). Influence of Fibres on Strength and Resistance Curve Behaviour of Extruded Alkali Activated Natural Clays**.** *10th AMRS Conference Arusha Tanzania December 2019*

2. **Ojo E.B.,** Forioni C.A & Savastano H. (2018). Durability of Alkali Activated Clay Based Composites. 72nd RILEM Annualweek: *Proceedings of 4th International Conference on Service Life Design for Infrastructures SLD4. Delft, Netherlands(August 2018) pp467-478* RILEM Publications S.A.R.L ISBN 978-2-35158-213-8

3. **Ojo E.B.,** Adamu K.I., Teixeira R.S., Matawal D.S., & Savastano H. (2018). Geopolymer Stabilisation of Earth Building Materials for Sustainable Building Construction. *Proceedings of NBRRI International Conference:* Sustainable Development Goals and the Nigerian Construction Industry – Challenges and The Way Forward. *NBRRI Abuja, Nigeria*. (June 2018)

4. Yola A.M., Abdulmumin M. M., Makwin H.L., **Ojo E. B.,** & Matawal D.S. (2018). Assessing the Potential of Selected Kaolin for the Synthesis of Metakaolin Based Geopolymer. *Proceedings of NBRRI International Conference:* Sustainable Development Goals and the Nigerian Construction Industry – Challenges and the Way Forward. *NBRRI Abuja, Nigeria*. (June 2018)

5. **Ojo E.B.,** Adamu K.I., Teixeira R.S., Matawal D.S., & Savastano H. (2018) Low Temperature Geopolymeric Setting for the Stabilisation of Earthen Masonry Units. 42nd International Conference & Exposition on Advanced Ceramics & Composites. Daytona Beach, Florida, U.S.A January 2018. (http://ceramics.org/wp-content/uploads/2018/01/ICACC18_Abstracts-WebFinal.pdf)

6. **Ojo E.B.,** Tyoden J.N & Adamu I.K. (2017). Experimental Feasibility Studies of Low Temperature Geopolymer Stabilised Earth Blocks. Proceedings of 3rd KEYS Symposium: Applicable Cement and Concrete Technology for Sub-saharan Africa. University of Witswatersrand, Johannesburg, South Africa, (June 2017) (https://opus4.kobv.de/opus4-bam/frontdoor/index/index/docId/41037

1.0 Chapter One: INTRODUCTION

1.1 Introduction

This chapter introduces earth as an attractive candidate in the development of sustainable construction materials and the need to investigate alternative binding mechanisms (such as alkali activation) and reinforcements in a bid to improve its resilience/robustness. Unresolved issues arising from the use of these modifications are considered. The aim and structure of thesis are presented at the end of the chapter.

1.2 Background and Motivation

The increase in world population continues to place an increasing demand for buildings and other related infrastructure particularly in view of rapid urbanization taking place in major cities across the world (UN SDGs, 2019). With the ongoing consensus to achieve sustainable development globally by 2030, Goal 11 of the sustainable development goals (SDGs) seeks to provide sustainable cities and communities (UN SDGs, 2019). This could be an ambitious target as current statistics showed that in 2018, about half of the world's population lived in cities (UN SDGs, 2019). The statistics also show that in the coming decades, 90% of urban expansion will be in the developing world (UN SDGs, 2019). Consequently, the need for research on building materials has never been more critical as materials make an integral contribution to the sustainability of the built environment [1]. The use of more sustainable construction materials and innovative processing techniques presents a major contribution to the eco-efficiency of the construction industry and thus sustainable development [2]. This is because building materials account for about half of materials extracted for human activities [3]. Hence there is need for appropriate and sustainable building materials which minimize impact on the ecosystem. In this context, earthen construction is an extremely competitive candidate for sustainable building construction in comparison with conventional construction materials. For instance, it has been reported that unfired earth bricks require only 14% of the embodied energy required for the production of fired bricks and 25% of the energy required for the production of lightweight concrete[4]. In addition, earthen construction possesses excellent thermal and moisture buffering properties[5] which reduce the heating and cooling loads required in buildings[6].

Interestingly, earthen construction is as old as civilization itself. However, despite being a more sustainable option, a number of disadvantages have been associated with building with earth which has limited its application over the years. These include its strength and durability, particularly in the presence of high moisture conditions[2,7]. This has been attributed to strong attraction of water to soil mineral surfaces particularly clay minerals[8]. Furthermore, from a mechanical point of view, earth-based composites demonstrate brittle behavior and low resistance to flexural/tensile stresses limiting its structural application to scenarios where only compressive strength is required.

These adverse characteristics associated with earthen construction have stimulated researchers to develop several techniques for the improvement of properties of earthen construction. Current research is now being tailored towards the adoption of recent advances in materials science to promote the use of this vast resource in the provision of more sustainable and ecofriendly construction materials. Traditional methods of stabilisation have focused on the use of additives such as lime and cement[9–11]. More recent efforts have focused on alternative additives to encourage a more widespread use of earthen construction; biopolymers[12–14]; and other pozzolans such as Coal ash[15]; Metakaolin[16]; Lime activated granulated blast furnace slag [17]; Agricultural by-products -Rice husk ash/bagasse ash[18]. Most of these solutions involve the use of natural or synthetic additives which bind the soil particles via cementation which involves creating a solid matrix to bind the soil together; chemical linkage which generates bond between soil mineral particles; and/or water-proofing which introduces a waterproof film around soil particles to improve imperviousness.

Alkali activation is a rapidly developing area in the global materials research and development community. It is based on alkali aluminosilicate chemistry with primary focus on the activation of solid aluminosilicate materials under alkaline conditions to produce three dimensional network of inorganic polymers[19–21]. Extensive studies have shown that they are an attractive alternative to Portland cement as they possess excellent mechanical properties, durability characteristics whilst possessing lower embodied energy[22,23]. Historically, alkali activation of clays has been explored since the late 1950’s. Glukhovsky[24] developed cementitious binders from low-basic-calcium or calcium-free aluminosilicates and alkali metal solutions and termed them soil silicates. Since then, extensive studies have focused on the formulation of alkali

activated aluminosilicates from metallurgical slags, clays, aluminosilicate rocks, fuel ashes etc, for the development of Alkali Activated Cements (AAC's) and AAC based concretes. The alkaline cations act as catalysts in the destruction of Si-O-Si, Al-O-Al and Si-O-Al bonds[25] and subsequently serve as partners in the formation of water resistant alkaline or alkaline-alkaline earth aluminosilicate hydrates analogous to natural zeolites and micas[26]. Presently, extensive studies have demonstrated the improved properties of AAC's and AAC based concretes relative to Portland cement concrete[27].

Previous work by Davidovits[28] proposed the Low Temperature Geopolymeric Setting (LTGS) as a stabilization mechanism for the production of high mechanical strength and water stable building units at drying temperatures of 50-250°C. The authors reported that kaolinite mineral in clay/lateritic soils can be transformed into a three dimensional compound producing water stable building blocks with satisfactory mechanical properties using the geopolymer technology. The alkaline solution acts as a catalyst enabling argillaceous components of soils to react and set at relatively lower temperatures (50-250°C)[21,28]. In other words, it is the argillaceous material itself that manufactures, in situ, the binder for agglomeration.

Whereas Alkali Activated Materials (AAMs) refer to the broadest classification comprising any binder system derived from the reaction of any aluminosilicate solid and alkali metal source[29], geopolymers are a subset of AAMs where the binder phase is sourced exclusively from aluminosilicates with highly coordinated products[30]. Aluminosilicates predominantly used are metakaolin (or other calcined clay minerals), blast furnace slag, fly ash etc; with the amorphous nature of the materials making them susceptible to dissolution by alkaline solution. However, according to Kriven[31], most studies in geopolymers actually produce Alkali Activated Binders and not geopolymers with the major difference between both materials being that geopolymers are amorphous inorganic nano precipitates whereas alkali activated binders are hydrated crystalline precipitates. Hence, although the stabilisation mechanism adopted in this study was based on the LTGS proposed by Davidovits, the crystalline nature of the source materials suggests that the binding mechanism may fall into the broader classification of alkali activation and hence the term alkali activation was adopted in this study instead of geopolymerisation.

Presently, research into alkali activation technology is increasing as studies have shown that they are viable economical alternatives to organic polymers and inorganic cements in various applications such as low energy ceramics tiles, high tech composites for aircraft interior and automobile, hazardous waste containment, cements and concretes, thermal insulating foams, fire-proof building materials, protective coatings, refractory adhesives etc[32]. However, very little work has been conducted to harness this technology for the improvement of earthen masonry given that the major composition of earth are aluminosilicates. This technique has the potential to open up the vista of low cost eco-friendly construction materials particularly in the developing world.

1.3 Unresolved Issues

A review of literature reveals conflicting reports on the alkali activation of natural aluminosilicates as binding mechanism for earthen construction. A study by Xu and van Deventer [22] demonstrated that a wide number of clay minerals can be used as source materials for alkali activation. They emphasized the need to optimise the concentration of alkaline solution for each mineral type as each aluminosilicate demonstrated varying dissolution rates. However, a study by Maskell et al.[33] showed that alkali activation was ineffective for the stabilisation of a predominantly silty soil containing kaolinite mineral. They argued that given the variable mineralogical composition of soils, it is not possible to know if alkali activation would provide a sufficient mechanism for the stabilisation of soils. Nonetheless, given the availability of earth in various parts of the world and its potential to provide sustainable construction materials, the presence of aluminosilicates in earth triggers interest as to whether alkali activation can be harnessed for the production of building products.

Phase composition of these aluminosilicates has been identified as a critical variable which determines their reactivity and thus the degree of dissolution [34] in alkaline environment. This has necessitated the de-hydroxylation of clay minerals to break down the crystalline structure in order to increase reactivity [35–38] or intensive mechanical attrition to increase surface area of particles[39]. These energy intensive processes increase the embodied energy associated with production which may ultimately negate eco-friendly benefits of earth construction. Other authors have employed the use of high molarity alkali activator solutions[20,40] to increase dissolution rates as the quantity of alkaline activator added to the argillaceous material

determines the level of crosslinking resulting in the formation of water stable units[21,28]. According to Maskell et al.[41] the inclusion of chemical additives to unfired earth has a detrimental effect on embodied energies and global warming potentials. The production of alkali activators constitutes the most energy intensive component of the alkali activation process [42]. In a bid to harness the use of alkali activation as binder mechanisms for earthen building units, there is a need to explore synthesis routes which still preserve eco-friendly indices of earth-based construction.

Furthermore, like other quasi-brittle materials, low energy absorption capacity and poor fracture resistance of this class of materials has necessitated the need to reinforce earthen matrices with fibres. It is well documented that the presence of fibres in soil matrices enhances ductility of the composite [43–45]. The mechanical properties of fiber-reinforced composites depend on the fiber-matrix interface, since the strength of such a composite is obtained by transferring the stress between the fibers and the matrix. Studies have shown that fibre-matrix interactions which could be based on physical/chemical adhesion, friction and/or mechanical anchorage; largely determine the effectiveness of fibres in enhancing the mechanical performance of brittle matrices[46]. However, it is not clear how this alkali activated earth-based matrix will interact with ligno-cellulosic fibres, which are typically used in the reinforcement of earth-based matrices and how these interactions would ultimately control composite property. Whilst significant effort has been made to characterize enhanced ductility of earth-based matrices as a result of fibre reinforcements, the underlying strengthening and toughening mechanisms induced by fibre reinforcements within the binder systems are still partly understood. There are relatively few studies that involve the application of micromechanical continuum theories to the prediction of mechanical properties of earth-based composites. The understanding of the mechanisms of stress transfer provides a basis for the development of improved composites through the tailoring of fibre-matrix interactions.

Furthermore, extrusion has shown great potential in the production of fibre reinforced cementitious composites for various applications. Various studies have demonstrated high mechanical performance and durability associated with extruded fibre reinforced cementitious products as a result of improved packing and good interfacial bonds[47–49]. With a properly designed extrusion system and well controlled rheology, fibre reinforcements can be aligned in preferred directions, which is necessary for achieving high performance in the extruded

products[50]. Despite its great potential, extrusion processing has not been widely adopted for the production of earth-based building products. Particularly studies on the constitutive behaviour of fresh fibre reinforced earthen pastes have not been extensively researched on. A successful extrusion process is a function of the paste bulk flow properties as well as the interfacial flow behaviour between the bulk material and the equipment wall[48]. Consequently, it is essential to know how different fibre types and contents control rheology of fresh pastes and determine extrudability.

1.4 Research Objectives

Earth-based building materials can be considered as engineered structures whose properties are a function of composition and processing. From a materials science point of view, an understanding of how these variables inter-relate would lead to a more effective use of this abundant resource in meeting increasing demands for sustainable building infrastructure. This study proposes to develop a novel fibre reinforced earth-based composite, which takes advantage of alkali activation of natural aluminosilicates within soil for the production of sustainable building materials. Using extrusion processing technique, the study seeks to elucidate the synthesis-processing-property relationship of these composites and how this inter-relationship controls composite property with a view to expanding the scope of application of earth-based composites. The scope of work entails a combination of experimental and computational analysis to:

- Provide insight on synthesis-property relationship by evaluating effect of curing conditions on extruded alkali activated un-calcined soils using low molarity alkali activator solutions;
- Evaluate effect of various fibre types/contents on extrudability and rheology characteristics of extruded alkali activated earthen composites;
- Evaluate effect of various fibre types/contents on physico-mechanical and microstructural properties of extruded alkali activated earthen composites;
- Elucidate reinforcing/toughening mechanisms associated with various fibre types via micromechanical modeling and nano-indentation;

- Ascertain resistance of composites to alternate wet-dry cycles and implications on durability for building construction.

A fundamental tenet of materials science is that the properties of materials can be engineered as a function of processing and composition. Figure 1.1 presents a schematic illustration of study approach.

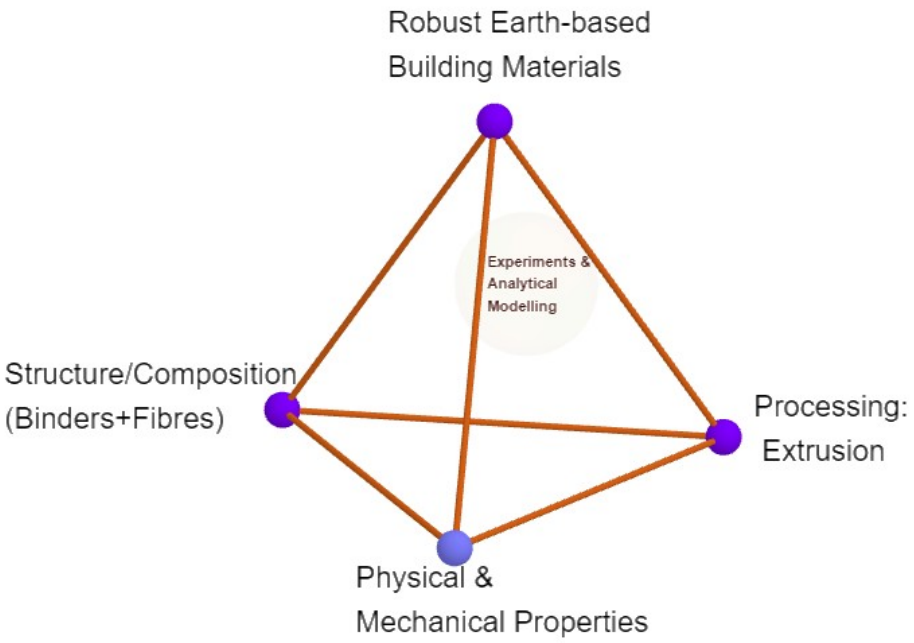

Figure 1:1: Schematic illustration of study approach adopted from materials science paradigm

1.5 Dissertation Layout

This dissertation comprises of eight chapters which is majorly based on papers that have been published, submitted to peer-reviewed journals or presented at conferences.

Chapter 2 provides a state of the art literature review which focuses on the raw materials used in the study, description of characterization techniques used, micro-mechanical models used and the mechanism of alkali activation.

Chapter 3 demonstrates a baseline study that investigates the synthesis-property relationship of an extruded earth-based matrix producing using muscovite rich soil and activated with low molarity alkali activator solutions. Effect of varying curing conditions on binding phases is

characterized via XRD, SEM/EDX and FTIR. Environmental impact analysis was conducted to quantify savings in embodied energy associated with this mechanism.

Chapter 4 studies the effects of different fibre reinforcements and volume composition on rheological properties. Inclusion of varying fibres modifies the rheology of the fresh paste in different ways with attendant effect on extrusion pressures, which has implications from a process control point of view.

Chapter 5 evaluates effect of various fibres/contents on physical (density, water absorption), mechanical (flexural response in the dry and saturated conditions) and microstructure with a view to establishing reinforcing efficiency of different fibres for this class of materials. Optimum fibre volume fractions are presented to provide a satisfactory balance of strength, energy absorption and low density for the development of robust building materials.

Chapter 6 elucidates strengthening and toughening mechanisms associated with different fibre reinforcements. Micromechanical models are used to satisfactorily predict strengthening and toughening contributions which provide guidelines which can be used for the tailoring of specific composite properties.

Chapter 7 presents major conclusions arising from this study and highlights areas for future work.

References

[1] B. Vale, 3 - Building materials, in: E.K. Petrović, B. Vale, M.P.B.T.-M. for a H. Zari Ecological and Sustainable Built Environment (Eds.), Woodhead Publ. Ser. Civ. Struct. Eng., Woodhead Publishing, 2017: pp. 67–112. doi:https://doi.org/10.1016/B978-0-08-100707-5.00003-4.

[2] F. Pacheco-Torgal, S. Jalali, Earth construction: Lessons from the past for future eco-efficient construction, Constr. Build. Mater. 29 (2012) 512–519. doi:10.1016/j.conbuildmat.2011.10.054.

[3] M.P. E., Sustainability literacy: the future paradigm for construction education?, Struct. Surv. 25 (2007) 7–23. doi:10.1108/02630800710740949.

[4] T. Morton, Feat of clay Moves to develop UK production of unfired clay bricks are driven by the growing demand for sustainable construction materials to, (2006) 2–3.

[5] F. McGregor, A. Heath, E. Fodde, A. Shea, Conditions affecting the moisture buffering

measurement performed on compressed earth blocks, Build. Environ. 75 (2014) 11–18. doi:10.1016/j.buildenv.2014.01.009.
[6] C. Rode, K. Grau, Moisture buffering and its consequence in whole building hygrothermal modeling, J. Build. Phys. 31 (2008) 333–360. doi:10.1177/1744259108088960.
[7] V. Sharma, B.M. Marwaha, H.K. Vinayak, Enhancing durability of adobe by natural reinforcement for propagating sustainable mud housing, Int. J. Sustain. Built Environ. 5 (2016) 141–155. doi:10.1016/j.ijsbe.2016.03.004.
[8] J.K. Mitchell, K. Soga, Fundamentals of soil behavior., John Wiley & Sons Ltd, Chichester, 2005.
[9] E.B. Ojo, D.S. Matawal, A.K. Isah, Statistical analysis of the effect of mineralogical composition on the qualities of compressed stabilized earth blocks, J. Mater. Civ. Eng. 28 (2016). doi:10.1061/(asce)mt.1943-5533.0001609.
[10] D. Maskell, A. Heath, P. Walker, Inorganic stabilisation methods for extruded earth masonry units, Constr. Build. Mater. 71 (2014) 602–609. doi:10.1016/j.conbuildmat.2014.08.094.
[11] F.G. Bell, Lime stabilization of clay minerals and soils, Eng. Geol. 42 (1996) 223–237. doi:10.1016/0013-7952(96)00028-2.
[12] J. Nakamatsu, S. Kim, J. Ayarza, E. Ramírez, M. Elgegren, R. Aguilar, Eco-friendly modification of earthen construction with carrageenan: Water durability and mechanical assessment, Constr. Build. Mater. 139 (2017) 193–202. doi:10.1016/j.conbuildmat.2017.02.062.
[13] C.A. Dove, F.F. Bradley, S. V. Patwardhan, Seaweed biopolymers as additives for unfired clay bricks, Mater. Struct. Constr. 49 (2016) 4463–4482. doi:10.1617/s11527-016-0801-0.
[14] C. Galán-Marín, C. Rivera-Gómez, J. Petric, Clay-based composite stabilized with natural polymer and fibre, Constr. Build. Mater. 24 (2010) 1462–1468. doi:10.1016/j.conbuildmat.2010.01.008.
[15] M.C.N. Villamizar, V.S. Araque, C.A.R. Reyes, R.S. Silva, Effect of the addition of coal-ash and cassava peels on the engineering properties of compressed earth blocks, Constr. Build. Mater. 36 (2012) 276–286. doi:10.1016/j.conbuildmat.2012.04.056.
[16] D. Maskell, A. Heath, P. Walker, Use of metakaolin with stabilised extruded earth masonry units, Constr. Build. Mater. 78 (2015) 172–180. doi:10.1016/j.conbuildmat.2015.01.041.
[17] J.E. Oti, J.M. Kinuthia, R.B. Robinson, The development of unfired clay building material using Brick Dust Waste and Mercia mudstone clay, Appl. Clay Sci. 102 (2014) 148–154. doi:10.1016/j.clay.2014.09.031.
[18] S.A. Lima, H. Varum, A. Sales, V.F. Neto, Analysis of the mechanical properties of compressed earth block masonry using the sugarcane bagasse ash, Constr. Build. Mater. 35 (2012) 829–837. doi:10.1016/j.conbuildmat.2012.04.127.
[19] P. Duxson, A. Fernández-Jiménez, J.L. Provis, G.C. Lukey, A. Palomo, J.S.J. Van Deventer, Geopolymer technology: The current state of the art, J. Mater. Sci. 42 (2007) 2917–2933. doi:10.1007/s10853-006-0637-z.
[20] F. Slaty, H. Khoury, J. Wastiels, H. Rahier, Characterization of alkali activated kaolinitic clay, Appl. Clay Sci. 75–76 (2013) 120–125. doi:10.1016/j.clay.2013.02.005.
[21] J. Davidovits, Geopolymer : chemistry and applications, Institut G�opolym�re, Saint-Quentin, 2011.
[22] H. Xu, J.S.J. Van Deventer, The geopolymerisation of alumino-silicate minerals, Int. J.

Miner. Process. 59 (2000) 247–266. doi:10.1016/S0301-7516(99)00074-5.
[23] M. Steveson, K. Sagoe-Crentsil, Relationships between composition, structure and strength of inorganic polymers, J. Mater. Sci. 40 (2005) 2023–2036.
[24] V.D. Glukhovsky, Soil silicates (Gruntosilikaty), USSR Kiev Budivelnik Publ. (1959).
[25] S. Ahmari, L. Zhang, J. Zhang, Effects of activator type/concentration and curing temperature on alkali-activated binder based on copper mine tailings, J. Mater. Sci. 47 (2012) 5933–5945. doi:10.1007/s10853-012-6497-9.
[26] P. Krivenko, Why alkaline activation - 60 years of the theory and practice of alkali-activated materials, J. Ceram. Sci. Technol. 8 (2017) 323–333. doi:10.4416/JCST2017-00042.
[27] F. Pacheco-Torgal, Z. Abdollahnejad, A.F. Camões, M. Jamshidi, Y. Ding, Durability of alkali-activated binders: A clear advantage over Portland cement or an unproven issue?, Constr. Build. Mater. 30 (2012) 400–405. doi:10.1016/j.conbuildmat.2011.12.017.
[28] J. Davidovits, C. James, Low Temperature Geopolymeric Setting (LTGS) and Archaeometry, Geopolymer ’88. 1 (1988) 69–78.
[29] C. Shi, A. Fernández-Jiménez, Stabilization/solidification of hazardous and radioactive wastes with alkali-activated cements, J. Hazard. Mater. 137 (2006) 1656–1663. doi:10.1016/j.jhazmat.2006.05.008.
[30] P. Duxson, J.L. Provis, G.C. Lukey, F. Separovic, J.S.J. Van Deventer, 29Si NMR study of structural ordering in aluminosilicate geopolymer gels, Langmuir. 21 (2005) 3028–3036. doi:10.1021/la047336x.
[31] W.M. Kriven, 5.9 Geopolymer-Based Composites BT - Comprehensive Composite Materials II, in: Elsevier, Oxford, 2018: pp. 269–280. doi:https://doi.org/10.1016/B978-0-12-803581-8.09995-1.
[32] J.L. Provis, J.S.J. Van Deventer, Geopolymers : structure, processing, properties and industrial applications, 2009. http://www.sciencedirect.com/science/book/9781845694494.
[33] D. Maskell, A. Heath, P. Walker, Geopolymer Stabilisation of Unfired Earth Masonry Units, Key Eng. Mater. 600 (2014) 175–185. doi:10.4028/www.scientific.net/KEM.600.175.
[34] S. Ahmari, L. Zhang, The properties and durability of mine tailings-based geopolymeric masonry blocks, Elsevier Ltd, 2014. doi:10.1016/B978-1-78242-305-8.00013-9.
[35] F. Pacheco-Torgal, J. Castro-Gomes, S. Jalali, Tungsten mine waste geopolymeric binder: Preliminary hydration products investigations, Constr. Build. Mater. 23 (2009) 200–209. doi:10.1016/j.conbuildmat.2008.01.003.
[36] M.B. Ogundiran, S. Kumar, Synthesis and characterisation of geopolymer from Nigerian Clay, Appl. Clay Sci. 108 (2015) 173–181. doi:10.1016/j.clay.2015.02.022.
[37] S. Omar Sore, A. Messan, E. Prud’homme, G. Escadeillas, F. Tsobnang, Stabilization of compressed earth blocks (CEBs) by geopolymer binder based on local materials from Burkina Faso, Constr. Build. Mater. 165 (2018). doi:10.1016/j.conbuildmat.2018.01.051.
[38] A. Buchwald, M. Hohmann, K. Posern, E. Brendler, The suitability of thermally activated illite/smectite clay as raw material for geopolymer binders, Appl. Clay Sci. 46 (2009) 300–304. doi:10.1016/j.clay.2009.08.026.
[39] A.D. Hounsi, G.L. Lecomte-Nana, G. Djétéli, P. Blanchart, Kaolin-based geopolymers: Effect of mechanical activation and curing process, Constr. Build. Mater. 42 (2013) 105–113. doi:10.1016/j.conbuildmat.2012.12.069.

[40] C.Y. Heah, H. Kamarudin, A.M. Mustafa Al Bakri, M. Bnhussain, M. Luqman, I. Khairul Nizar, C.M. Ruzaidi, Y.M. Liew, Kaolin-based geopolymers with various NaOH concentrations, Int. J. Miner. Metall. Mater. 20 (2013) 313–322. doi:10.1007/s12613-013-0729-0.
[41] D. Maskell, A. Heath, P. Walker, Appropriate structural unfired earth masonry units, Proc. Inst. Civ. Eng. - Constr. Mater. 169 (2016) 261–270. doi:10.1680/jcoma.15.00034.
[42] J.L. Provis, A. Palomo, C. Shi, Advances in understanding alkali-activated materials, Cem. Concr. Res. 78 (2015) 110–125. doi:10.1016/j.cemconres.2015.04.013.
[43] J.-C. Morel, K. Ghavami, A. Mesbah, Theoretical and Experimental Analysis of Composite Soil Blocks Reinforced with Sisal Fibres Subjected to Shear by, Mason. Int. 13 (2000) 54–62.
[44] S.M. Hejazi, M. Sheikhzadeh, S.M. Abtahi, A. Zadhoush, A simple review of soil reinforcement by using natural and synthetic fibers, Constr. Build. Mater. 30 (2012) 100–116. doi:10.1016/j.conbuildmat.2011.11.045.
[45] V. Sharma, H.K. Vinayak, B.M. Marwaha, Enhancing compressive strength of soil using natural fibers, Constr. Build. Mater. 93 (2015) 943–949. doi:10.1016/j.conbuildmat.2015.05.065.
[46] A. Bentur, S. Mindess, Fibre Reinforced Cementitious Composites, Second Edition, Taylor & Francis, 2006.
[47] S. Srinivasan, D. Deford, P.S. Shah, The use of extrusion rheometry in the development of extrudate fibre-reinforced cement composites, Concr. Sci. Eng. 1 (1999) 26–36.
[48] X. Zhou, Z. Li, Characterization of rheology of fresh fiber reinforced cementitious composites through ram extrusion, Mater. Struct. Constr. 38 (2005) 17–24. doi:10.1617/14064.
[49] R.S. Teixeira, S.F. Santos, A.L. Christoforo, H. Savastano, F.A.R. Lahr, Extrudability of cement-based composites reinforced with curauá (Ananas erectifolius) or polypropylene fibers, Constr. Build. Mater. 205 (2019) 97–110. doi:https://doi.org/10.1016/j.conbuildmat.2019.02.010.
[50] Y. Akkaya, A. Peled, S.P. Shah, Parameters related to fiber length and processing in cementitious composites, Mater. Struct. 33 (2000) 515–524. doi:10.1007/BF02480529.

.

2.0 Chapter Two: Literature Review

2.1 Introduction

Concepts on the development of earth-based composites, as building materials are presented in this section. Attention is given to its unique material properties as well as efforts to improve on major drawbacks with focus on binding mechanisms as well as strengthening/toughening improvements using fibre reinforcements, which have been studied. Description of characterization techniques typically used in evaluating these modifications as well as micromechanical models, which describe strengthening and toughening contributions, are also discussed. Rheological characterisation techniques associated with fibre reinforcements which control extrudability of fresh paste with respect to extrusion moulding as a processing technique is discussed. The chapter concludes by highlighting research gaps and areas for future work.

2.2 Earth as a Building Material

Historically, earthen construction has been reported to have started about 9,000-10,000 years ago with primarily early agricultural societies [1,2]. Presently, studies have shown that about 50% of the world's population lives in earth-based structures[3]. Although the majority of these earthen constructions are located in less developed countries, earth-based buildings can also be found in Germany, France and the United Kingdom[4]. Earthen construction comprises several techniques such as wattle and daub, rammed earth and adobe or compressed earth bricks; the most popular being stabilized earth blocks. Earth is a cheap, environmentally friendly, easy to work with and abundantly available construction material [5,6]; and this has resulted in a resurgence in its use as a construction material in line with the present global drive towards sustainable construction materials[3]. Environmental benefits associated with earthen construction include reduced embodied energy, reduced CO_2 emissions and possible reuse of earthen materials at the end of life cycle[7].

Soils used in earth construction typically consists of varying sized particles of clays, silts and sands; the nature and proportions of these particles ultimately controls its properties as a construction material[8]. Various studies have recommended ideal particle size distributions to guide the selection of soils for earthen construction[9]. However, as soils are naturally occurring materials, it is difficult to control particle size distribution. These particles make up a solid

skeleton with pores in between which may be filled with water and/or air depending on the level of saturation of the soil. As highlighted in the previous section, a main drawback for raw earth is its affinity for water. Water binds to the solid skeleton via three mechanisms [10]:

- adhesion to solid surfaces by very strong but short-range London-van der Waals forces,
- capillary binding of water due to cohesive forces between water molecules and
- osmotic binding of water in double layers

Based on these mechanisms, soils as construction materials are highly sensitive to moisture; swelling when water is absorbed and shrinking when the soil dries out which may lead to structural failures[11]. Consequently, they possess high stiffness in the dry state but loose this stiffness completely when in contact with moisture[11] . Hence, the main purpose for introducing binders to earthen materials is not only to improve the mechanical properties, but also improve their resistance to detrimental effects of water[12].

2.3 Binding mechanisms in Earthen Building Materials

Binders are necessary to improve the strength and durability of earth-based materials to impart improved resistance to load and adverse weather conditions[1]. Binding typically involves the introduction of chemical stabilisers which are broadly classified into three groups: traditional stabilisers (cement, lime and fly ash); non-traditional stabilisers (sulfonated oils, ammonium chloride, enzymes, polymers etc.); and by-product stabilisers (cement kiln dust, lime kiln dust etc.)[13]. Binding mechanisms may vary widely from the formation of new compounds binding the finer soil particles to coating particle surfaces by additives to limit the moisture sensitivity. Extensive literature review conducted by Danso et al.[14] on various binders used in earthen construction shows that most studies (about 95%) evaluated the effect cement and lime on earthen materials; other studies investigated effect of pozzolanic materials (coal ash, volcanic ash, metakaolin etc) as well as natural polymers. Discussions in this section would focus on typical binding mechanisms associated with calcium-based stabilisers (cement and lime) given their prominent use for various applications.

2.3.1 Hydration reaction

Hydration reactions are associated with the use of cement in soils stabilization. However, the use of cement has been associated with higher energy consumption costs as well as adverse

environmental impacts with respect to CO_2 emissions[15,16]. Notwithstanding, Portland cement is the most commonly and widely used binder for various types of soil stabilization applications. It is usually preferred over lime (or other calcium based stabilisers) due to its faster and higher strength enhancements [17–20].

When the pore water within the soil interacts with cement in a cement-soil mix, each cement particle is covered with water and forms a gel-like film which coat soil particles as well as illustrated in Figure 2.1.

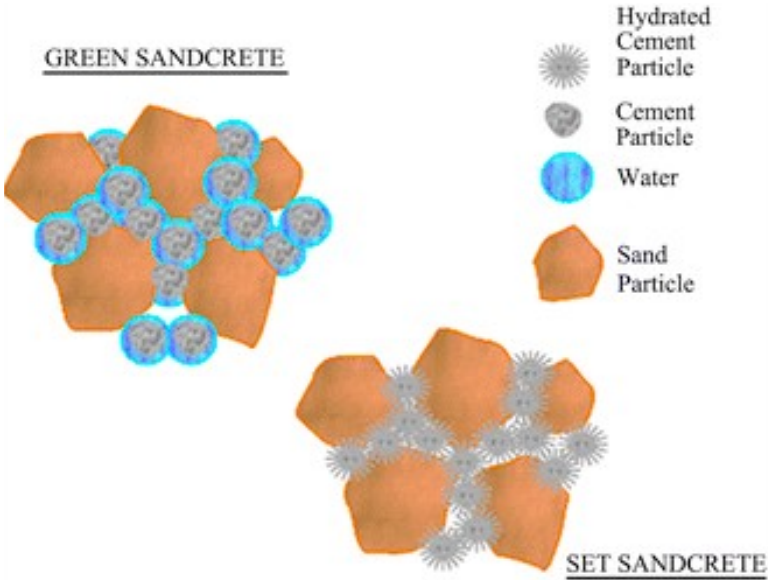

Figure 2:2 Bonding process between cement particles and soil particles [21]

Hydration reactions transform cement particles into products which bind soil particles and continue to gain strength as long as there is water to hydrate all cement particles. Four main phases found in Portland cement are C_3S, C_2S, C_3A, and C_4AF. When C_3S and C_2S interact with water, they are transformed into calcium silicate hydrate and (C-S-H) and hydrated lime ($Ca(OH)_2$, also known as portlandite) and is represented schematically using the equation below[22]

(C_3S, C_2S) + water $\rightarrow$ C-S-H + $(Ca(OH)_2)$

Similarly, in the presence of water and calcium sulphate, C_3A, and C_4AF (referred to as the interstitial phases) are transformed into ettringite and monosulphoaluminate according to the equation below [22]

(C_3A, C_4AF) + calcium sulphate + water $\rightarrow$ ettringite + monosulphoaluminate

With the development of hydration, formation of CSH and CAH occurs when crystals begin to grow and are attracted to adjoining crystals by van der Waals forces forming a crystalline network.[21]

Horpibulsuk et al.[23] investigated the evolution of strength as a function of cement content in cement stabilized silty clay and observed three distinct zones. At cement contents less than 10%, which was called the active zone, increase in cement content resulted in significant increase in the unconfined compressive strength values due to the rapid development of hydration products. In the second zone (referred as to the inert zone), the rate of strength development with increase in cement content was much slower where the hydration products were relatively similar irrespective of cement content (cement contents between 11 and 30%). Beyond the inert zone, a deterioration zone was identified corresponding to cement contents greater than 30% where strength values decrease with increasing cement contents due to insufficient moisture for the complete hydration of cement particles. Apart from cement content, studies have also demonstrated the significance of compaction energies [24] as well as soil moisture content [25] on strength development of cement-stabilized soils.

2.3.2 Cation Exchange

Cation exchange is the primary reaction associated with lime stabilization. As a soil stabilizer, lime can be used in the form of ground quick lime, (calcium oxide), hydrated lime (calcium hydroxide) or milk of lime suspension[26]. It is typically preferred over cement for soils with high plasticity index (i.e. P.I $\geq$ 30). When hydrated lime is mixed with soil in the presence of sufficient moisture, calcium ions and hydroxyl ions dissociate into pore solution increasing the soil solution pH. This favors the exchange of Ca^{2+} ions from lime with the monovalent cations (Na^+, K^+ etc.) present in the diffused double layer of the soil minerals [27]. These divalent calcium cations possess a smaller hydration radius thereby exerting a greater attractive force

towards the soil particle surface compared to monovalent cations which have been replaced leading to shrinkage of the thickness of the diffuse double layer[28]. This promotes a flocculated positive/negative charge causing agglomeration of particles as illustrated in Figure 2.2 [29].

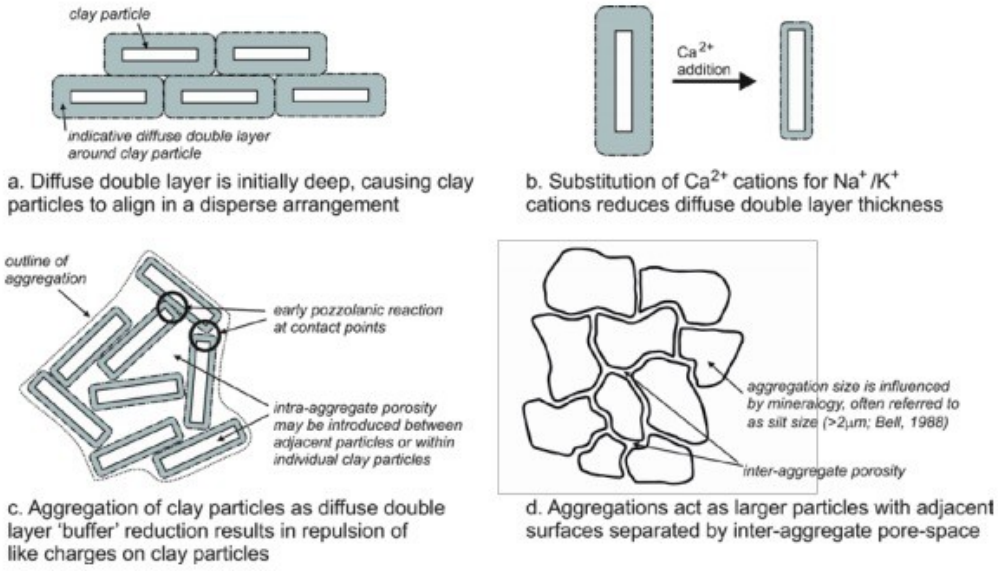

Figure 1 Sequence illustrating influence of early lime-clay reactions upon clay particle arrangements and soil structure

Figure 2:3 Illustration of cation exchange and agglomeration associated with lime stabilization from[29]

This reduces the effective surface area of particles in contact with pore water and accounts for immediate change in physical properties of lime-soil mixes[29]. Consequently, plasticity index drops with improved workability and immediate strength enhancement.

Bell [30] investigated the lime stabilization of major occurring minerals in clay soils namely kaolinite, montmorillonite and quartz and observed that cation exchange capacity of these minerals controlled the degree of modification of plasticity obtained with lime stabilization. For instance, montmorillonite with the highest (CEC) demonstrated the highest reduction in plastic limits relative to kaolinitic clays.

2.3.3 Pozzolanic reaction

Pozzolanic reactions are typically secondary reactions associated with calcium based binders. It entails the dissolution of silicates and aluminates from the soil matrix under high pH conditions

which react with calcium and water to form additional calcium silicate hydrates and calcium aluminate hydrates[30]. The presence of cement hydration product, portlandite is responsible for high pH conditions in soil-cement mixes and results in long term strength development associated with cement stabilization through these pozzolanic reactions. Similarly, the dissolution of OH^- ions in lime soil mixtures increases pH to about 12.4 inducing the dissolution of reactive silica and alumina ions present in the soil mineral[31]. Reactions occur between free calcium ions and dissolved silica and alumina ions from to soils to form calcium silicates and aluminates which later transforms into hydrates and form cementitious compounds as shown below

Ca^{2+} + OH^- + Soluble Clay Silica → Calcium Silicate Hydrate (CSH)
Ca^{2+} + OH^- + Soluble Clay Alumina → Calcium Alumina Hydrate (CAH)

These pozzolanic reactions are dependent on the nature and availability of reactive clay minerals in the soil and extend over a prolonged duration. Studies have shown that the use of additional reactive pozzolanic materials as partial replacements or in combination with calcium based binders can further take advantage of pozzolanic reactions for soil improvement. For instance, metakaolin is one of the additives that has typically been used in combination with Portland cements for the stabilization of a wide range of soils[32–34] Metakaolin is an amorphous aluminosilicate obtained from the calcination of kaolinite mineral at temperature range of 500-900C. Addition of MK to soil-cement mixes has been reported to significantly increase UCS and split tensile strengths[32,33] . Other pozzolanic materials which have been used as supplementary cementitious materials include fly ash[35,36], granulated blast furnace slag[37], ceramic waste[38] and agricultural wastes such as rice husk ash[39] and palm oil fuel ash[40] .

2.3.4 Carbonation

Carbonation reactions may also constitute secondary reactions associated with calcium based binders. For instance, in lime stabilized soils, reaction of lime with carbon dioxide from the atmosphere to form calcium carbonate leads to improve binding within the soil composites[30]. With cement-stabilised soils, CO_2 from the atmosphere reacts with cement hydrates such as calcium hydroxides (portlandite, Ca(OH)2) and calcium–silicate–hydrate (C–S–H) gel in the

cement paste matrix to form calcium carbonates ($CaCO_3$)[41]. A study by Haas & Ritter [42] demonstrated that both pozzolanic reactions and carbonation can lead to long-term increase in strength in lime stabilized soils.

2.3.5 Alkali Activation

Recent years have witnessed significant strides around the world with respect to the development of a novel class of binders termed alkali activated binders[43]. This can be attributed to the fact that they provide an avenue for the full elimination of traditional calcium-based binders owing to the environmental challenges associated with their use in construction. Essentially, alkali activated binders are synthesized by the reaction of aluminosilicate precursors under high pH conditions to form three dimensional aluminosilicate gels[44]. One of the most significant features of alkali activated binders is that both natural materials (clays or feldspars) and industrial by-products (slag, fly ash and paper sludge) can be utilized as precursors [45]. In the last few decades, a wide variety of alkali activated binders have been synthesized and have been broadly classified into two main categories: (i) high calcium and (ii) low calcium binders. With respect to this study, alkali activation as binding mechanism for natural clays soils falls into the latter category. Hence, mechanism for this class of binders is presented. These systems require higher alkaline media and curing temperatures of 60-200°C to develop a three dimensional inorganic alkali polymer, an alkaline aluminosilicate hydrate (N-A-S-H) gel that can be regarded as a zeolite precursor[46–48].

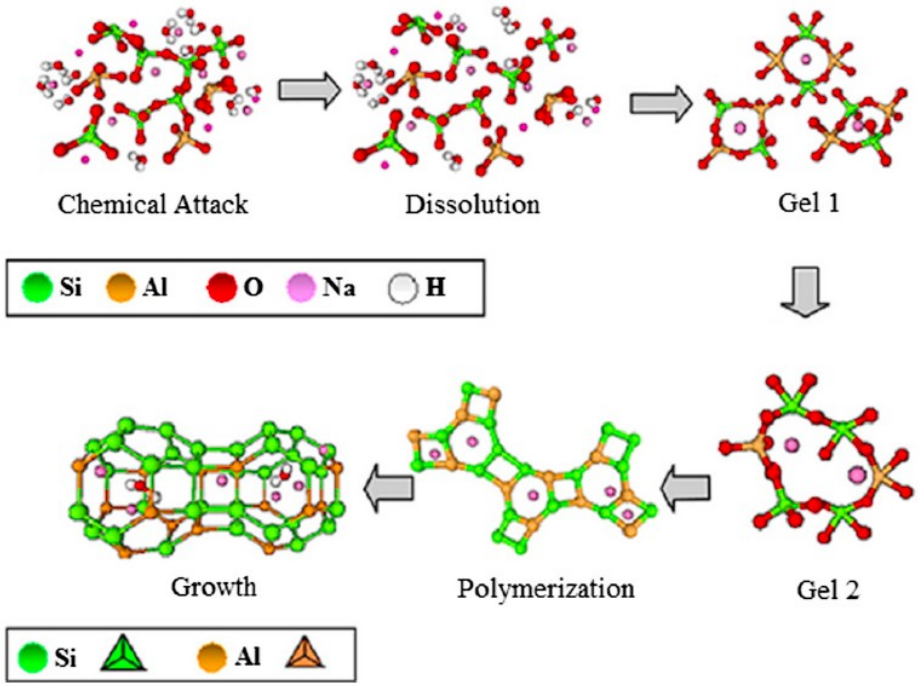

Figure 2:4 Schematic illustration of alkali activation process[47]

Previous work by Davidovits[49] proposed the Low Temperature Geopolymeric Setting (LTGS) as a stabilization mechanism for the production of high mechanical strength and water stable building units at drying temperatures of 50-250°C. The authors reported that kaolinite mineral in clay/lateritic soils can be transformed into a three dimensional compound producing water stable building blocks with satisfactory mechanical properties using the geopolymer technology. However, results from Maskell et al. [16] demonstrated that the LTGS was ineffective for the stabilisation of a predominantly silty soil containing kaolinite under varying NaOH conditions. Whereas Alkali Activated Materials (AAMs) refer to the broadest classification comprising any binder system derived from the reaction of any aluminosilicate solid and alkali metal source[17], geopolymers are a subset of AAMs where the binder phase is sourced exclusively from aluminosilicates with highly coordinated products [18]. Aluminosilicates predominantly used are metakaolin (or other calcined clay minerals), blast furnace slag, fly ash etc.; with the amorphous nature of the materials making them susceptible to dissolution by alkaline solution. However, according to Kriven [19] , most studies in geopolymers actually produce Alkali Activated Binders and not geopolymers with the major difference between both materials being that

geopolymers are amorphous inorganic nano precipitates whereas alkali activated binders are hydrated crystalline precipitates. Hence, although the stabilisation mechanism adopted in this study was based on the LTGS proposed by Davidovits, the crystalline nature of the source materials suggests that the binding mechanism may fall into the broader classification of alkali activation and hence the term alkali activation was adopted in this study instead of geopolymerisation.

According to Glukhovsky[50], the mechanism of alkali activation process for low calcium systems is divided into the following phases;

- Destruction-Coagulation: the reaction begins when OH^- ions from the alkaline hydroxide break the Si-O-Si bonds by redistributing their electronic density around the silicon atoms. This reaction produces silanol (-Si-OH) and sialate (-Si-O^-) species. Alkaline cation neutralizes the negative charge on the sialate species forming Si-O—Na^+ which prevents the reversion to siloxane.

  $$\equiv Si-O-Si\equiv +OH^- \rightarrow \equiv Si-OH+O-Si\equiv \underset{\rightarrow}{Na^+} \equiv Si-O^{-}{}_{-Na^+}$$

Similarly, the OH^- groups break up the Si-O-Al bonds to form complex species of $Al(OH)_4^-$ ions. In the dissolution stage, 5- and 6-coordinated Al is converted to 4-corindation[51]. Studies by Weng and Sagoe-Crenstil[52] have proposed that the initial release of Al may be more rapid than that of Si)

- Coagulation-Condensation stage: in this stage the interaction of dissolved species as well silicates supplied from the alkali activator solutions leads to the formation of aluminosilicates oligomers[53]. Silica monomers react to form dimers which also react with other monomers to build polymers. This process is catalyzed byOH^- ions. In this process, aluminates isomorphically replace the silicon tetrahedral.

- Condensation-Crystallisation stage: where the presence of particles of the original solid phase encourages further product precipitation

The main reaction products associated with the alkaline activation of aluminosilicates is an amorphous alkaline aluminosilicate hydrate ($M_{n}^{-}(SiO_2)-(AlO_2)_n.wH_2O$ known as N-A-S-H gel[54]

where M is an alkali metal and n is the degree of polymerisation. Secondary reaction products are typically zeolites such as hydroxysodalite, zeolite-P, zeolite-Y, Na-chabazite and faujasite [46,47]. In these systems, curing temperature and type/concentration of alkali activators control reaction kinetics[55].

The conventional method proposed by Davidovits for alkali activation of aluminosilicates involved the reaction of fully dehydroxylated kaolinite clays (metakaolin) under strongly alkaline conditions[49,56]. Dehydroxylation of kaolinite clay at 800°C was recommended for production of metakaolin. However, one of the main advantages of these alternative binders is energy savings associated with production and thus thermal activation to such temperatures negates eco-friendliness of product. This suggests that the use of un-dehydroxylated clays in alkali activation reactions (without compromising the properties of the products) would be beneficial in the production of low embodied energy products). Prior work by Glukhovsky[57] and Berg[58] have demonstrated the feasibility of alkali activation of un-dehydroxylated kaolinitic clays with NaOH at 140-170°C resulting in the transformation of about 30-50% kaolinite to hydroxysodalite which strongly bound other mineral particles in the formation of high strength building materials. Thermal dehydroxylation results in loss of structural water; destruction of crystal structure and conversion of octahedral aluminium to a mixture of 4,5 and 6 fold coordination. Mechano-chemical treatment with sufficient energy has also been reported to disrupt crystal structure of kaolinitic clays rendering them more reactive to the alkali activation process[59]. But, the pretreatment process still requires a considerable amount of energy input which may not present a significant advantage over thermal activation[60]. With 2:1 layer lattice aluminosilicates, high energy milling has also been reported to partially destroy crystal structure and convert 6-cordinated alumina to 4 and 5-cordinated[61]. In comparison with 1:1 aluminosilicate clays, it is much more difficult to increase the reactivity of 2:1 clays due to the protection of the aluminium in the octahedral layer by the repeating silica sheets[60]. Hence, for alkali activation mechanism to be a low-environmental impact method for soil stabilization, there is a need to explore alternative synthesis routes.

2.4 Evaluation of Binding Mechanisms

Given the variable nature of precursors and synthesis conditions, various analytical techniques have been used to evaluate the nature of alkali activated binders[62]. Amongst these techniques, morphological characterizing using scanning electron microscopy (SEM), functional group identification using Fourier transform infrared (FTIR) and phase identification using X-ray diffraction were the key tools used to evaluate extent of alkali activation in this study. A brief description of these techniques is presented in this section.

2.4.1 Morphological Characterisation

The most widely used tool for morphological characterization of alkali activated binders is scanning electron microscopy (SEM). Morphological characterization is performed to analyse the microstructure in order to elucidate the mechanism of strength gain and ascertain the structure of the final product. The SEM is a type of electron microscope which images sample surfaces by scanning via a high energy beam of electrons in raster scan pattern. The electrons interact with the atoms within the sample producing signals that contain information about the sample's surface topography and composition. The types of signals produced by an SEM include secondary electrons, back-scattered electrons, characteristic X-rays etc. In the most standard detection mode, SEM can produce very high resolution images of a sample surface revealing details within 1-5 nm size. Morphological characterization allows for the detection of new phases and units and confirms the degree of alkali activation as indicated by the presence of residual particles from precursor material. Generally, low porosity and high density fine grained structure correspond to high strength alkali activated materials[63].

2.4.2 Functional Group Identification

Fourier Transform infrared (FTIR) is one of the key spectroscopic techniques used in the analysis of alkali activated binders[62]. Using observed molecular bond vibrations at various infrared frequencies, chemical bonds within a material can be identified through infrared absorption spectrum. In addition, FTIR spectroscopy can also be used to provide information on the transition of vibrations arising from small structural changes[64]. With alkali activated clays,

it can be used to evaluate the connectivity within Si-O-(Si,Al) frameworks through shifts in the peak associated with asymmetric stretch of that bond[65,66]. Following alkali activation of aluminosilicates, Si-O-Si and Al-O-Si asymmetric stretching (950-1200cm^{-1}) shifts to lower wave numbers[67,68].

2.4.3 Phase Identification

In the study of clay minerals, XRD analysis is one of the most powerful methods used to provide information about basic crystal dimensions, chemical composition, crystallite size and stacking sequences. With alkali activation, XRD is very useful for the detection of structural changes in order to detect any significant modification in its mineralogical structure. With complete alkali activation, main reaction product is an amorphous gel which appears as a diffuse halo peak on XRD spectra at about 27-30º 2θ [69,70]. Secondary products such as zeolites are crystalline and typically appear as new peaks in the XRD spectra[71,72].

2.4.4 Water Immersion

In this study, a simple water immersion technique was selected to evaluate level of binding obtained due to alkali activation of natural aluminosilicates within the soil. Although this is not a standard method, it was selected as a quick initial assessment of binder development on the basis that unstabilised moulded earth completely disintegrates when totally immersed in water. This implies for a sample to remain stable in water, it must possess sufficient binding to withstand hydrostatic pressures developed under full immersion. According to Davidovits[49,70], bricks produced from the geopolymerisation of kaolinitic clays produced a 3D structure that was water stable with NaO content from as low as 3%. Hence, the water sensitivity test was conducted to serve as an indicator of the viability of this mechanism for the stabilisation of clay minerals particularly at low alkali concentrations.

2.5 Fibre Reinforced Earth-based Building Materials

Earthen matrices generally possess low flexural strength and energy absorption capacities. To remedy this drawback, fibres have been used to improve mechanical properties in earth-based matrices leading to the development of robust composite materials. By definition, fibre reinforced earth-based composite comprises of a soil matrix containing randomly distributed

fibres which provide an improvement in the mechanical behavior of the soil composite[73]. Historically, natural fibres have been used to reinforce soil. However, short synthetic fibre soil composites have received increasing attention in recent times owing to the global drive towards sustainability in the built environment.

2.5.1 Natural fibres

Presently, there has been a great deal of interest on natural fibres for soils reinforcement and various fibre types have been applied as reinforcements in earthen matrices. These fibres have shown huge potential as reinforcements in cementitious materials[74]. Several investigations have been conducted on the addition of lingo-cellulosic fibres in earth matrices with promising results. Typical natural fibres used as reinforcement in earthen construction and their features are presented in Table 2.1.

Table 2:1 Typical natural fibres used as reinforcements in earth-based composites and characteristic features

Fibre type	**Diameter (mm)**	**Density (g/cm^3)**	**Tensile Strength (MPa)**	**Source**
Straw	1-4	2.05	--	[5,75–81]
Coconut coir	0.18-1.01	0.81	228	[82–85]
Sisal	0.02-0.4	1.2-1.45	560	[82,86–88]
Jute	08-1	1.46	216-225	[89,90]
Bagasse	0.31-1.19	0.57	62	[83]
Oil palm fruit	0.19-0.82	0.77	141	[83]
Grewia Optivia	0.03	--	15.35	[91]
Pinux Roxburghii	0.48	--	11.15	[91]
Hibiscus Cannibus	0.13	1.04	--	[92]
Banana	0.04-0.142	1.35	115-274	[89,93]
Phormium Tenax	--	--	--	[94]
Date Palm	--	--	--	[95]
Cassava peel	--	--	--	[96]
Pig hair	0.16	--	99.2	[97]
Wool	--	--	--	[12,98]

2.5.2 Synthetic Fibres

The concept of reinforcing earth-based composite with synthetic fibres has recently attracted increasing attention[73]. However, relative to natural fibres, it is still a new technique in earth-

based construction. Table 2 presents synthetic fibres that have been typically used as reinforcement of earth-based composites.

Table 2:2 Typical synthetic fibres used as reinforcements in earth-based composites

Fibre type	**Diameter (mm)**	**Density (g/cm^3)**	**Tensile Strength (MPa)**	**Source**
Polypropylene	0.15-0.031	0.91-1.16	310-350	[89,99–102]
Polyester	0.03-0.04	1.35	400-600	[103]
Polyethylene	0.4-0.8	0.92	100-620	[104]
Glass[89]	0.05	2.7	330-414	[89]

2.6 Rheological Characterisation of Fresh Fibre Reinforced Earth Paste for Extrusion Moulding

In materials science and engineering, the performance associated with materials is intimately related to its composition and structure; and the structure is largely dependent on synthesis and processing[105]. Processing plays a significant role on fibre dispersion and orientation with attendant effect on composite performance. Compression moulding has largely been the most common processing technique for the production of unfired earth building materials. To improve the performance of earthen composites without losing their advantages and also to enhance manufacturing efficiency, there is a need to investigate alternative and particularly continuous manufacturing processes. The advantages of extrusion technique make it a strong candidate which satisfies these criteria. It has been traditionally used in the forming of green bodies prior to firing in the production of fired bricks, roof tiles etc. Studies by Maskell et al.[25,34,106] have shown that it can be satisfactorily used with in the production of stabilized earth-based building product without the firing component. Furthermore, extrusion has shown great potential in the production of fibre reinforced cementitious composites with superior mechanical performance and durability[107–109]. These studies have shown extruded products with low porosity and good interfacial bond are developed under high shear and compressive stress.

Rheological tests of the fresh earthen mixtures are important to identify the adequate composition and to select criteria for optimum use in extrusion process However, extrusion of fibre reinforced earth pastes has not been extensively studied. Particularly, studies on the

constitutive behaviour of fresh fibre reinforced earthen pastes has not been extensively researched.

A successful extrusion process is highly dependent on the rheology of the paste which is a function of the paste bulk flow properties as well as the interfacial flow behavior between the bulk materials and the equipment wall[109–112]. The ram extrusion has been used extensively in the characterization of the rheology of paste like materials.[113] The set –up is presented in Figure 2.4.

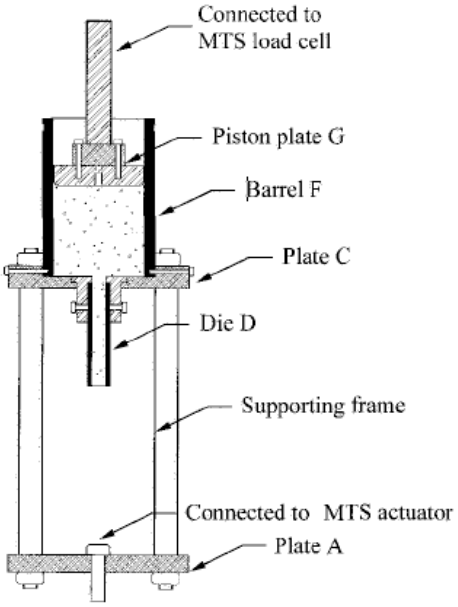

Figure 2:5 Ram Extrusion Set up [114]

The classical Benbow-bridgwater model is an empirical model which describes the ram extrusion process based on the equation[110].

$$P = P_{ent} + P_{land} = 2\ln\left(\frac{D_o}{D}\right)(\sigma_0 + \alpha V) + \frac{4L}{D}(\tau_0 + \beta V)$$

where P is the extrusion pressure, α _is a velocity-dependent factor at the die entry, β _is the velocity-dependent factor at the die land, σ_0 is the paste bulk yield value, τ_0 is the characteristic initial wall shear stress of the paste, D_0 and D are the diameters of the barrel and of the die, respectively, L is the die-land length and V is the extrudate velocity.

2.7 Physical Properties of Fibre Reinforced Earth-Based Composites

Physical properties refer to properties that are dependent on the physics of the material including density, water absorption, porosity, shrinkage, thermal expansion etc. Most studies on earth-based composites focus on density and water absorption as these tests are relatively simple to conduct in the field and may be used to imply mechanical properties without actual tests. A brief description on density and water absorption is presented.

2.7.1 Density

Density is typically used as an indication of the degree of compactness of earth blocks. It is largely dependent of soil/fibre properties, moisture content during moulding and moulding energy[115]. Various studies have related the densities of earthen building materials to compressive strength showing that compressive strength consistently increases with density[116]. The density of stabilized earth blocks has been reported to fall within the range of 1500-2000kg/m^3 [115].

2.7.2 Water Absorption

Low resistance to detrimental effects of moisture is one of the major drawbacks of earthen construction as it affects overall performance of the building products particularly with respect to durability. The water absorption value gives an indication of the presence and significance of voids[96,117] and by inference, the durability of the building material. Water absorption capacity is inversely related to density; with increased density, porosity is reduced and water absorption capacity reduces.

2.8 Mechanical Properties of Fibre Reinforced Composites

2.8.1 Compressive Strength test

Significant attention has been paid to laboratory evaluation of compressive strength as it represents the most important parameter for the description of load bearing parameters for earth blocks. According to Morel et al.[118] typical compressed earth blocks have compressive strengths in the range of 2-3 MPa. There is presently no consensus on the appropriate procedure for the evaluation of the unconfined compressive strength of unfired earth[119]. Testing procedures are often based on those used for concrete or fired bricks. According to Walker [120],

moisture content at testing plays a significant influence on mechanical strength and it's important to standardize moisture contents before testing. Soil inherently possesses sufficient stiffness to resist axial loads in the dry state. Hence, true test of any binding or reinforcing mechanism can only be evaluated in the fully saturated state. As a result, mechanical properties of the test pieces are evaluated under two pre-conditions: oven dry condition and fully saturated condition (total immersion in water for 24hrs). Although authors have argued that testing in the saturated condition is considered inappropriate for unfired earth [121] , achieving water stable units indicates the application of unfired earth may be subsequently be expanded to uncontrolled moisture exposure conditions. In this regard, researchers have evaluated compressive strength in the fully saturated condition and have recommended a minimum compressive strength of 1 MPa[25].

With fibre reinforced composites, inclusion of fibres initially increases the bond between particles as they possess greater tensile strength relative to the surrounding soil matrix and therefore impart improved cohesion and strength to the composite[122,123]. This effect peaks at a particular fibre dosage as increasing fibre content begins to break up the soil resulting in a weakening of the soil-fibre composite[75,92]. On the other hand, other studies [80,96,124] showed a positive increase in compressive strength with increasing fibre content. This may suggest that peak fibre content had not been exploited in these studies. Generally, improvement in compressive strengths with fibre reinforcements have been minimal indicating that the main contributor to compressive strength in fibre reinforced soils is the soil matrix[14].

2.8.2 Flexural strength test

Determination of flexural characteristics is not a common test on unfired earth as earthen units are typically employed compression. However, according to Walker[120], the assessment of this property gives a quick field assessment of the compressive properties of unfired earth-based on an empirical relationship between flexure and compressive strength. For cement-stabilised earth blocks, it is reported that the modulus of rupture shall equal at least one-sixth of the corresponding compressive strength[120]. Typical compressed earth blocks have flexural strengths in the range of 0.5-2 MPa[12]. With respect to fibre reinforcements, effect of fibre dosage on flexural strength follows the same trend with compressive strength where flexural strength increases with fibre dosage up to a maximum value. Whereas, improvement in flexural

strength is minimal with fibre reinforcement, failure is more gradual and ductility of materials is greatly enhanced[75,122]. This is attributed to fibres bridging across cracks and shielding the crack tip. Fibres introduce toughness and increased energy absorption of the earthen matrices. These have implications when composites are applied in bending. In addition, fibres act by bridging growing cracks in the post-crack region. Resistance to crack propagation, which is typically the purpose underlying fracture toughness characteristics, has not always been the subject of scientific interest.

2.8.3 Fracture Resistance

Traditionally, the use of earth-based composites (in the form of rammed earth, adobe bricks, stabilised earth blocks etc.) has typically been applied in load bearing/non load bearing masonry structures where requirement has largely been controlled by the compressive strength of these building materials. Consequently, great attention has been paid to the evaluation of compressive strength of earth-based composites, whereas very limited research has focused on fracture properties of earthen construction materials. However, insight on the fracture behaviour of earthen composites may expand the applications of earth-based construction to structural components where fracture/crack resistance and not necessarily strength is the critical structural parameter such as panels, roof tiles etc. Furthermore, if buildings are likely to encounter lateral loads due to wind or earthquake loading, there is the need for fracture mechanics analyses to better understand conditions that give rise to crack initiation and propagation in earth-based composites.

Fracture of brittle materials was first elucidated by studies by Griffith (1921) where an energy balance concept was used to describe conditions for crack growth such that for a crack to grow in a brittle material, there must be a balance between the increase in surface energy due to crack extension and a corresponding decrease in the potential energy of the system. This led to the development of Linear Elastic Fracture Mechanics (LEFM) which assumes limited plasticity effects ahead of the crack tip as the crack advances. This concept describes the stress intensity factor which is the driving force for crack resistance. Hence, crack will only grow when this value is equal to a critical value referred to as the fracture toughness of the material. Based on

dimensional constraints and direction of loading, this may be described as a material property. K_{1C} describes the critical stress intensity for the crack to grow under mode 1 loading (tearing mode). This test requires certain conditions for the specimen dimensions and quantifies the maximum load to grow the crack.

However, it has been argued that critical stress intensity factor defines toughness of nominally brittle materials and maybe insufficient for the characterization of quasi-brittle materials such as rock and concrete. The presence of discontinuities and pre-existing micro cracks causes highly localized areas of relative weakness[125]. This may lead to microcracking ahead of the crack tip which introduces inelastic behaviour in this region. This suggests that LEFM may not apply if significant degree of inelasticity occurs ahead of the crack tip. Furthermore, in fibre reinforced composites, fibre bridging occurs behind the crack tip forming a fibre bridging zone. This makes the application of LEFM more questionable to fibre reinforced composites. Prior work by Lenci[126] assumed that unfired earth maybe sufficiently brittle and experimentally determined fracture properties under monotonic and cyclic loading using LEFM. Studies by Mustapha et al. [81] demonstrated significant improvement in fracture toughness of earth-based materials as a result of fibre reinforcement using LEFM. Wang et al.[127] determined limit of crack depth to specimen width of 0.3-0.6 for fracture toughness testing of soils using LEFM. Prior work by Lenci[126] evaluated fracture properties of unfired dry earth subjected to monotonic and cyclic loads under 3pts bending. Orazio[128] investigated the fracture toughness of clay fired bricks and related K_{IC} to porosity parameters. Main toughening mechanisms include crack deflection (in the case of heterogenous microstructural features; varying grain sizes, porosities and fibres), fibre debonding and pull out, crack bridging by fibres and microcrack toughening.

2.8.4 Resistance curve behavior

Resistance curves can quantify fracture resistance of a wide range of material behaviour ranging from linear elastic materials, plastic elastic materials to time-dependent (creep) material behaviour[129]. However, very limited research has focused on R-curve behaviour for fracture resistance of earth-based composites. Resistance curve behaviour requires toughening mechanisms which increase with crack extension. Fibre reinforcements have the potential to toughen the composites by crack bridging or fibre pullout mechanisms which give rise to crack tip shielding and wake processes and are responsible for the improved fracture toughness[130]. It has also been argued that a single parameter is not sufficient to adequately characterize the

fracture properties of cementitious materials and that these materials exhibit an R-Curve behaviour i.e increasing stress intensity factor with crack growth which is a material property.

2.8.5 Grid Nanoindentation for Micro-mechanical Characterisation of Earth-based composites

Nanoindentation is a widely used technique to evaluate the elastic modulus and hardness of bulk homogenous materials. Earth-based materials, like many other natural composites, exhibit heterogenous features over a wide range of length scales. Advancement in instrumented indentation allows for the measurement of mechanical properties of these heterogeneities at the appropriate length scales through grid nanoindentation[131]. A combination of grid nano-indentation and statistical convolution techniques allows for both quantitative and qualitative data on the mechanical properties in the material[131,132]. This technique has been successfully used to characterize calcium silicate hydrates in cementitious materials[133,134], hydroxyapatite in bone[133], clay agglomerates in geomaterials[133,135] and alkali activated materials[136–139].

Considering heterogeneous materials to be composed of multiple phases of different mechanical properties and characterized by a length scale D. If the indentation depth is much larger than the characteristic size of individual phases i.e. $h \gg D$, then the properties extracted from the indentation experiment are representative of the average properties of the composite material. On the other hand, if maximum indentation depth $h \ll D$, then a single indentation experiment gives information on either of the phases present in the composite. This suggests that if a large number of tests are carried out on a grid of appropriate spacing, the probability of encountering different phases during indentation is dependent of the area occupied by each phase[131].

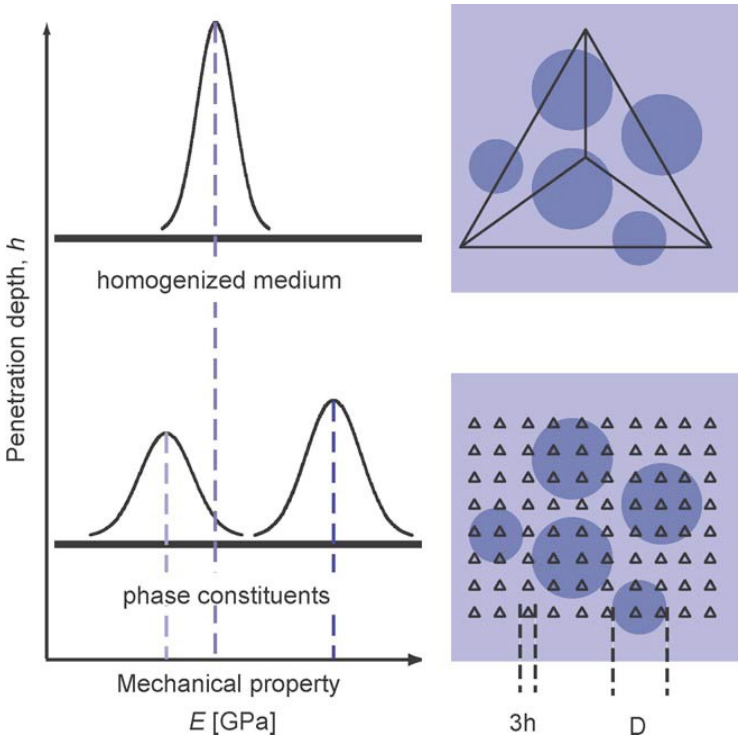

Figure 2:6 Schematic representation of grid indentation technique for homogeneous materials [131]

Following grid indentation, individual phase properties can be determined by statistical deconvolutions applied to histograms of mechanical properties. Experimental probability density function (PDF) can be computed as

$$p_i^{\exp} = \frac{f_i^{\exp}}{N^{\exp}} \cdot \frac{1}{b} \qquad \text{(i)}$$

where p_i^{exp} = experimental PDF, f_i^{exp} = frequency of values, N^{exp} = effective indentation experiments and b = bin size. Deconvolution of M phases involves finding $j = 1,2,3\ldots M$ individual PDFs related to a single material phase. Assuming a normal distribution, PDF for a single phase can be written as

$$p_j(x) = \frac{1}{\sqrt{2\pi s_j^2}} \exp \frac{-(x-\mu_j)^2}{2s_j^2} \qquad \text{(ii)}$$

where p_j is the theoretical PDF of the j[th] phase with μ_j and s_j as the mean and standard deviations of the j[th] phase respectively. The overall PDF covering all M phases is then represented by

$$C(x)=\sum_{j=1}^{M} f_j p_j(x) \qquad \text{(iii)}$$

where f_j is the volume fraction of a single phase.

2.9 Micromechanical Modelling of Earth-based Composites

A combination of micro-mechanical models have been used to study phenomena that are relevant to the strengthening and toughening of composites with fiber and interfacial geometries[140]. These include applications of continuum theory, shear lag models, molecular dynamics and atomistic simulations of the structure and chemistry of interfaces and layers within nano-composite structures. However, there are relatively few studies that involve the application of micromechanical continuum theories and atomistic models to the prediction of the mechanical properties of composite structures that are relevant to sustainable housing. A brief description is presented on some of these models.

2.9.1 Rule of Mixture theory

The simple rule of mixture theory can be used to estimate mechanical and physical properties of composites along different directions[130]. For continuous and aligned fibre reinforced composites (Fig 2.6a), the rule of mixture equations predicts the upper bound of the elastic modulus (corresponding to the longitudinal direction) according to the following expression

$$E_c = E_m V_m + E_f V_f ;$$

and a lower bound (corresponding to the transverse direction) according to

$$E_c = \frac{E_m E_f}{V_m E_f + V_f E_m} ;$$

where E_c, E_m and E_f are the respective Young's moduli of the composite, matrix and fibre; V_m and V_f are respective volume fractions of matrix and fibre;

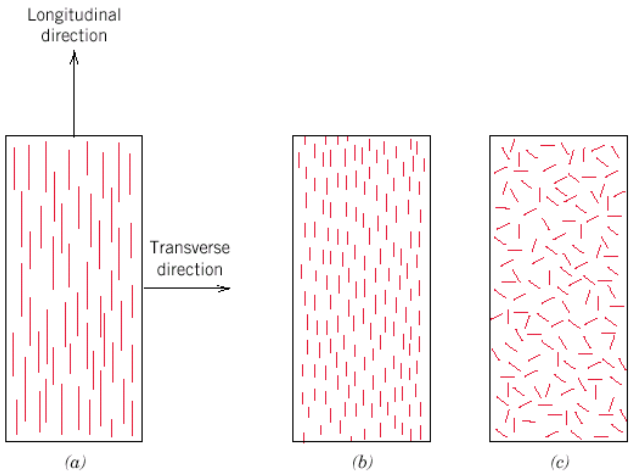

Figure 2:7 Schematic representation of (a) continuous and aligned (b) discontinuous and aligned and (c) discontinuous and randomly oriented fibre reinforced composites[105]

With discontinuous fibres, a fibre length efficiency factor¿¿) is applied whilst a fibre orientation efficiency¿¿) is applied for randomly oriented fibres.

2.9.2 Shear Lag

The shear lag model predicts mechanical properties of composites reinforced with discontinuous fibres. The model is based on the assumption that the applied on the composite is transferred from the matrix to the fibres via shear[130]. Based on repeatable unit cells the following expressions have been derived for the estimation of the composite Young's moduli and strength:

$$\frac{E_c}{E_m} = V_m + V_f\left(\frac{E_f}{E_m}\right)\left[1 - \frac{\tanh(x)}{x}\right] \quad ; \qquad \frac{\sigma_c}{\sigma_m} = 0.5\,V_f\left(2 + \frac{l}{d}\right) + (1 - V_f)$$

$$\text{where } x = \frac{l}{d}\left[(1+\upsilon_m)\frac{E_f}{E_m}\ln(V_f)^{-1/2}\right]^{-1/2}$$

and E_c, E_m and E_f are the respective Young's moduli of the composite, matrix and fibre; V_m and V_f are the respective volume fractions of matrix and fibre; and σ_c, σ_m and σ_f are the respective

flexural strengths of the composite, matrix and fibre; $\frac{l}{d}$ is the fibre aspect ratio and υ_m is Poisson's ratio of the matrix.

2.9.3 Crack Bridging Models

Toughening contribution due to crack bridging by the different fibres has been modeled using crack bridging models to predict the resistance curve behaviour for the different composites. Bridging models based on an idealized elastic-plastic spring model was proposed by Budiansky et al.[141] has been used by various studies [81,142–144] to study toughening due to small scale bridging (SSB).

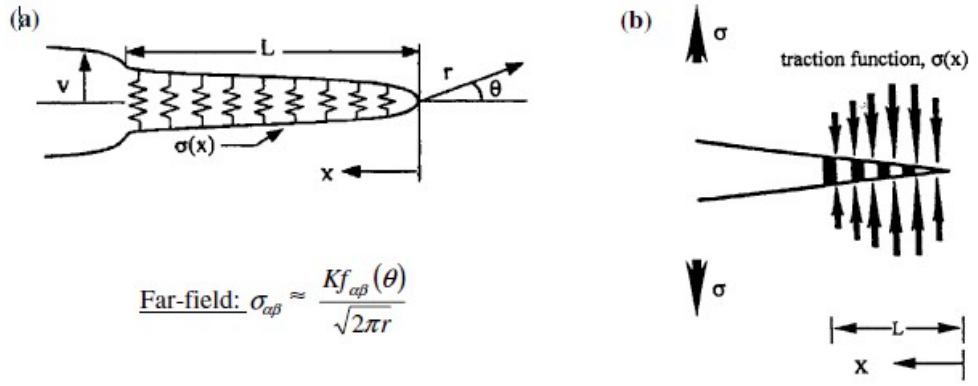

Figure 2:8 Schematic illustrations of crack bridging models (a) Spring model and (b) weighted distribution of traction [143]

For SSB conditions, the bridge length corresponds to values below 0.5mm and the ductile phase toughening contribution to fracture toughness may be expressed as

$$\Delta K_{SSB} = \sqrt{\frac{2}{\pi} \alpha V_f \int_0^L \frac{\sigma_y}{\sqrt{x}} dx}$$

where ΔK_{SSB} is toughening due to SSB, α is the constraint/triaxiality factor, V_f is the volume fraction of the fibres, L is the length of bridging ligament, σ_y is the uniaxial yield stress and x corresponds to the distance from the crack tip.

For large scale bridging (LSB) conditions i.e. bridge lengths exceeding 0.5mm, the toughening due to ligament bridging[145] has been used and is given by

$$\Delta K_{LSB} = V_f \int_0^L \alpha \sigma_y h(a,x)\, dx$$

where ΔK_{LSB} is toughening due to LSB, and *h(a,x)* is the weighting function given by Fett and Munz[146] as

$$h(a,x) = \sqrt{\frac{2}{\pi a}\frac{1}{\sqrt{1-\frac{x}{a}}}\left(1+\sum_{(v,u)}\frac{A_{v,u}\left(\frac{a}{W}\right)}{\left(1-\frac{a}{W}\right)}\left(1-\frac{x}{a}\right)^{v+1}\right)}$$

where the coefficients $A_{v,u}$ for and SENB specimen can be found in Fett and Munz[146].

Prior work by Mustapha et al.[81] used resistance curve experiments to evaluate the toughening contribution of straw fibre in cement stabilised earthen blocks at different fibre volume contents. Their studies showed these can crack bridging models compared satisfactory with experimental values.

2.10 Summary

This chapter reviews the concept of earth as a building material, noting its unique properties as well as drawbacks. The various binding mechanisms that have been used to improve mechanical properties as well as resilience to moisture have been discussed with emphasis on novel binding systems such as alkali activation. Various fibre reinforcements (natural and synthetic) which have been used in earth-based composites have also been discussed alongside modification in mechanical properties such as compressive strength, flexural strength and fracture resistance. The chapter also introduces extrusion moulding as a viable processing option for this class of materials.

It is important to note that fibre-matrix interfacial characteristics control the overall composite behavior. However, these areas have not been investigated fully. Hence, further studies are needed to elucidate these characteristics for the different binder-reinforcement conditions in

order to tailor the design of these class of materials. Studies on fibre-cement composites have demonstrated deleterious effects of alkaline matrix ($Ca(OH)_2$ present in the pores) on the durability of natural fibres [147]. This raises questions as to durability of natural fibres used as reinforcements in alkali activated earth-based composites. Consequently, there is a need for studies which give insights on deterioration mechanisms associated with this class of materials as it controls overall durability performance of these composites. Long term interactions between fibre and alkaline matrix need to be evaluated via accelerated ageing tests to determine the practicability of this reinforcing solution.

References

[1] G. Minke, Building with earth: design and technology of a sustainable architecture, Walter de Gruyter, 2012.

[2] B. Berge, C. Butters, F. Henley, Chapter 8 - Soil materials, in: B. Berge, C. Butters, F.B.T.-T.E. of B.M. (Second E. Henley (Eds.), Architectural Press, Oxford, 2009: pp. 119–138. doi:https://doi.org/10.1016/B978-1-85617-537-1.00008-1.

[3] F. Pacheco-Torgal, S. Jalali, Earth construction: Lessons from the past for future eco-efficient construction, Constr. Build. Mater. 29 (2012) 512–519. doi:10.1016/j.conbuildmat.2011.10.054.

[4] F. Pacheco-Torgal, S. Jalali, Earth construction: Lessons from the past for future eco-efficient construction, Constr. Build. Mater. 29 (2012) 512–519. doi:10.1016/j.conbuildmat.2011.10.054.

[5] H. Binici, O. Aksogan, T. Shah, Investigation of fibre reinforced mud brick as a building material, Constr. Build. Mater. 19 (2005) 313–318. doi:10.1016/j.conbuildmat.2004.07.013.

[6] E. Quagliarini, S. Lenci, The influence of natural stabilizers and natural fibres on the mechanical properties of ancient Roman adobe bricks, J. Cult. Herit. 11 (2010) 309–314. doi:10.1016/j.culher.2009.11.012.

[7] M. Lawrence, A. Heath, P. Walker, Mortars for thin unfired clay masonry walls, in: Proc. LEHM 5th Int. Conf. Build. with Earth, Koblenz, Ger., 2008: pp. 9–12.

[8] J.K. Mitchell, K. Soga, Fundamentals of soil behavior., John Wiley & Sons Ltd, Chichester, 2005.

[9] V. Rigassi, Compressed earth blocks: Manual of production, Dtsch. Zent. Fur Entwicklungstechnologien-GATE. (1995).

[10] P. Koorevaar, G. Menelik, C.B.T.-D. in S.S. Dirksen, eds., 3 Static Equilibria in Soils, in: Elem. Soil Phys., Elsevier, 1983: pp. 63–114. doi:https://doi.org/10.1016/S0166-2481(08)70050-3.

[11] B.C.S. Chittoori, A.J. Puppala, T. Wejrungsikul, L.R. Hoyos, Experimental studies on stabilized clays at various leaching cycles, J. Geotech. Geoenvironmental Eng. 139 (2013) 1665–1675.

[12] C. Galán-Marín, C. Rivera-Gómez, J. Petric, Clay-based composite stabilized with natural polymer and fibre, Constr. Build. Mater. 24 (2010) 1462–1468.

doi:10.1016/j.conbuildmat.2010.01.008.
[13] D.N. Little, Evaluation of structural properties of lime stabilized soils and aggregates, National Lime Association, 1998.
[14] H. Danso, B. Martinson, M. Ali, C. Mant, Performance characteristics of enhanced soil blocks: A quantitative review, Build. Res. Inf. 43 (2015) 253–262. doi:10.1080/09613218.2014.933293.
[15] C. Meyer, The greening of the concrete industry, Cem. Concr. Compos. 31 (2009) 601–605. doi:https://doi.org/10.1016/j.cemconcomp.2008.12.010.
[16] M.S. Imbabi, C. Carrigan, S. McKenna, Trends and developments in green cement and concrete technology, Int. J. Sustain. Built Environ. 1 (2012) 194–216. doi:https://doi.org/10.1016/j.ijsbe.2013.05.001.
[17] C.D.F. Rogers, S. Glendinning, C.C. Holt, Slope stabilization using lime piles—a case study, Proc. Inst. Civ. Eng. - Gr. Improv. 4 (2000) 165–176. doi:10.1680/grim.2000.4.4.165.
[18] K.M.A. Hossain, Development of stabilised soils for construction applications, Proc. Inst. Civ. Eng. - Gr. Improv. 163 (2010) 173–185. doi:10.1680/grim.2010.163.3.173.
[19] S. Jegandan, M. Liska, A.A.-M. Osman, A. Al-Tabbaa, Sustainable binders for soil stabilisation, Proc. Inst. Civ. Eng. - Gr. Improv. 163 (2010) 53–61. doi:10.1680/grim.2010.163.1.53.
[20] P.H. Y., G.G. S., G. Nizar, Soil Stabilization Using Basic Oxygen Steel Slag Fines, J. Mater. Civ. Eng. 18 (2006) 229–240. doi:10.1061/(ASCE)0899-1561(2006)18:2(229).
[21] X. Li, Shrinkage cracking of soils and cementitiously-stabilized soils: mechanisms and modeling, (2014).
[22] P.-C. Aïtcin, 3 - Portland cement, in: P.-C. Aïtcin, R.J.B.T.-S. and T. of C.A. Flatt (Eds.), Woodhead Publishing, 2016: pp. 27–51. doi:https://doi.org/10.1016/B978-0-08-100693-1.00003-5.
[23] S. Horpibulsuk, C. Phetchuay, A. Chinkulkijniwat, A. Cholaphatsorn, Strength development in silty clay stabilized with calcium carbide residue and fly ash, Soils Found. 53 (2013) 477–486. doi:https://doi.org/10.1016/j.sandf.2013.06.001.
[24] C.N. Cesar, F. Diego, F. Lucas, H.K. Salvagni, Key Parameters for Strength Control of Artificially Cemented Soils, J. Geotech. Geoenvironmental Eng. 133 (2007) 197–205. doi:10.1061/(ASCE)1090-0241(2007)133:2(197).
[25] D. Maskell, A. Heath, P. Walker, Inorganic stabilisation methods for extruded earth masonry units, Constr. Build. Mater. 71 (2014) 602–609. doi:10.1016/j.conbuildmat.2014.08.094.
[26] A. Behnood, Soil and clay stabilization with calcium- and non-calcium-based additives: A state-of-the-art review of challenges, approaches and techniques, Transp. Geotech. 17 (2018) 14–32. doi:https://doi.org/10.1016/j.trgeo.2018.08.002.
[27] J.K. Mitchell, K. Soga, Soil Formation, Fundam. Soil Behhavior. (2005) 5–33.
[28] H.L. Bohn, R.A. Myer, G.A. O'Connor, Soil chemistry, John Wiley & Sons, 2002.
[29] F.G. Bell, Stabilisation and treatment of clay soils with lime. Part 1-basic principles, Gr. Eng. 21 (1988).
[30] F.G. Bell, Lime stabilization of clay minerals and soils, Eng. Geol. 42 (1996) 223–237. doi:10.1016/0013-7952(96)00028-2.
[31] J.L. Eades, R.E. Grim, Reaction of hydrated lime with pure clay minerals in soil stabilization, Highw. Res. Board Bull. (1960).

[32] T. Zhang, X. Yue, Y. Deng, D. Zhang, S. Liu, Mechanical behaviour and micro-structure of cement-stabilised marine clay with a metakaolin agent, Constr. Build. Mater. 73 (2014) 51–57. doi:https://doi.org/10.1016/j.conbuildmat.2014.09.041.
[33] Z. Wu, Y. Deng, S. Liu, Q. Liu, Y. Chen, F. Zha, Strength and micro-structure evolution of compacted soils modified by admixtures of cement and metakaolin, Appl. Clay Sci. 127–128 (2016) 44–51. doi:https://doi.org/10.1016/j.clay.2016.03.040.
[34] D. Maskell, A. Heath, P. Walker, Use of metakaolin with stabilised extruded earth masonry units, Constr. Build. Mater. 78 (2015) 172–180. doi:10.1016/j.conbuildmat.2015.01.041.
[35] S. Horpibulsuk, R. Rachan, A. Chinkulkijniwat, Y. Raksachon, A. Suddeepong, Analysis of strength development in cement-stabilized silty clay from microstructural considerations, Constr. Build. Mater. 24 (2010) 2011–2021. doi:https://doi.org/10.1016/j.conbuildmat.2010.03.011.
[36] S. Kolias, V. Kasselouri-Rigopoulou, A. Karahalios, Stabilisation of clayey soils with high calcium fly ash and cement, Cem. Concr. Compos. 27 (2005) 301–313. doi:https://doi.org/10.1016/j.cemconcomp.2004.02.019.
[37] A. Kavak, G. Bilgen, O. Capar, Using ground granulated blast furnace slag with seawater as soil additives in lime-clay stabilization, in: Test. Specif. Recycl. Mater. Sustain. Geotech. Constr., ASTM International, 2012.
[38] A.K. Sabat, Stabilization of expansive soil using waste ceramic dust, Electron. J. Geotech. Eng. 17 (2012).
[39] E.A. Basha, R. Hashim, H.B. Mahmud, A.S. Muntohar, Stabilization of residual soil with rice husk ash and cement, Constr. Build. Mater. 19 (2005) 448–453. doi:https://doi.org/10.1016/j.conbuildmat.2004.08.001.
[40] S. Pourakbar, A. Asadi, B.B.K. Huat, M.H. Fasihnikoutalab, Stabilization of clayey soil using ultrafine palm oil fuel ash (POFA) and cement, Transp. Geotech. 3 (2015) 24–35. doi:https://doi.org/10.1016/j.trgeo.2015.01.002.
[41] K. Nakarai, T. Yoshida, Effect of carbonation on strength development of cement-treated Toyoura silica sand, Soils Found. 55 (2015) 857–865. doi:https://doi.org/10.1016/j.sandf.2015.06.016.
[42] S. Haas, H.-J. Ritter, Soil improvement with quicklime – long-time behaviour and carbonation, Road Mater. Pavement Des. 20 (2019) 1941–1951. doi:10.1080/14680629.2018.1474793.
[43] J.L. Provis, J.S.J. Van Deventer, Alkali avtivated materials, 2014. doi:10.1007/978-94-007-7672-2.
[44] W.M. Kriven, 5.9 Geopolymer-Based Composites BT - Comprehensive Composite Materials II, in: Elsevier, Oxford, 2018: pp. 269–280. doi:https://doi.org/10.1016/B978-0-12-803581-8.09995-1.
[45] I. Garcia-Lodeiro, A. Palomo, A. Fernández-Jiménez, 2 - An overview of the chemistry of alkali-activated cement-based binders, in: F. Pacheco-Torgal, J.A. Labrincha, C. Leonelli, A. Palomo, P.B.T.-H. of A.-A.C. Chindaprasirt Mortars and Concretes (Eds.), Woodhead Publishing, Oxford, 2015: pp. 19–47. doi:https://doi.org/10.1533/9781782422884.1.19.
[46] A. Palomo, M.T. Blanco-Varela, M.L. Granizo, F. Puertas, T. Vazquez, M.W. Grutzeck, Chemical stability of cementitious materials based on metakaolin, Cem. Concr. Res. 29 (1999) 997–1004. doi:10.1016/S0008-8846(99)00074-5.
[47] P. Duxson, A. Fernández-Jiménez, J.L. Provis, G.C. Lukey, A. Palomo, J.S.J. Van

Deventer, Geopolymer technology: The current state of the art, J. Mater. Sci. 42 (2007) 2917–2933. doi:10.1007/s10853-006-0637-z.
[48] J.L. Provis, J.S.J. Van Deventer, Geopolymers : structure, processing, properties and industrial applications, 2009. http://www.sciencedirect.com/science/book/9781845694494.
[49] J. Davidovits, C. James, Low Temperature Geopolymeric Setting (LTGS) and Archaeometry, Geopolymer ’88. 1 (1988) 69–78.
[50] V.D. Glukhovsky, Ancient, modern and future concretes, in: Proc. First Int. Conf. Alkaline Cem. Concr., Kiev, Ukraine, 1994: pp. 1–9.
[51] P. Duxson, J.L. Provis, G.C. Lukey, F. Separovic, J.S.J. Van Deventer, 29Si NMR study of structural ordering in aluminosilicate geopolymer gels, Langmuir. 21 (2005) 3028–3036. doi:10.1021/la047336x.
[52] L. Weng, K. Sagoe-Crentsil, Dissolution processes, hydrolysis and condensation reactions during geopolymer synthesis: Part I—Low Si/Al ratio systems, J. Mater. Sci. 42 (2007) 2997–3006.
[53] J.L. Provis, S.L. Yong, P. Duxson, 5 - Nanostructure/microstructure of metakaolin geopolymers, in: J.L. Provis, J.S.J.B.T.-G. van Deventer (Eds.), Woodhead Publ. Ser. Civ. Struct. Eng., Woodhead Publishing, 2009: pp. 72–88. doi:https://doi.org/10.1533/9781845696382.1.72.
[54] A. Palomo, S. Alonso, A. Fernandez Jiménez, I. Sobrados, J. Sanz, Alkaline activation of fly ashes: NMR study of the reaction products, J. Am. Ceram. Soc. 87 (2004) 1141–1145.
[55] M. Criado, A. Palomo, A. Fernández-Jiménez, Alkali activation of fly ashes. Part 1: Effect of curing conditions on the carbonation of the reaction products, Fuel. 84 (2005) 2048–2054. doi:https://doi.org/10.1016/j.fuel.2005.03.030.
[56] J. Davidovits, Geopolymers - Inorganic polymeric new materials, J. Therm. Anal. 37 (1991) 1633–1656. doi:10.1007/BF01912193.
[57] V.D. Glukhovsky, Soil silicates (Gruntosilikaty), USSR Kiev Budivelnik Publ. (1959).
[58] L.G. Berg, B.A. Demidenko, V.A. Remiznikova, M.S. Nizamov, Unfired finishing building materials based on kaolin, Stroit. Mater. 10 (1970) 22.
[59] K.J.D. MacKenzie, D.R.M. Brew, R.A. Fletcher, R. Vagana, Formation of aluminosilicate geopolymers from 1: 1 layer-lattice minerals pre-treated by various methods: a comparative study, J. Mater. Sci. 42 (2007) 4667–4674.
[60] K.J.D. Mackenzie, 14 - Utilisation of non-thermally activated clays in the production of geopolymers, in: J.L. Provis, J.S.J.B.T.-G. van Deventer (Eds.), Woodhead Publ. Ser. Civ. Struct. Eng., Woodhead Publishing, 2009: pp. 294–314. doi:https://doi.org/10.1533/9781845696382.2.294.
[61] P.J. Sánchez-Soto, J.L. Pérez-Rodríguez, I. Sobrados, J. Sanz, Influence of grinding in pyrophyllite− mullite thermal transformation assessed by 29Si and 27Al MAS NMR spectroscopies, Chem. Mater. 9 (1997) 677–684.
[62] J.L. Provis, A. Palomo, C. Shi, Advances in understanding alkali-activated materials, Cem. Concr. Res. 78 (2015) 110–125. doi:10.1016/j.cemconres.2015.04.013.
[63] M. Steveson, K. Sagoe-Crentsil, Relationships between composition, structure and strength of inorganic polymers, J. Mater. Sci. 40 (2005) 2023–2036.
[64] Y.M. Liew, C.Y. Heah, A.B. Mohd Mustafa, H. Kamarudin, Structure and properties of clay-based geopolymer cements: A review, Prog. Mater. Sci. 83 (2016) 595–629. doi:10.1016/j.pmatsci.2016.08.002.

[65] A. Fernández-Jiménez, A. Palomo, Composition and microstructure of alkali activated fly ash binder: Effect of the activator, Cem. Concr. Res. 35 (2005) 1984–1992. doi:https://doi.org/10.1016/j.cemconres.2005.03.003.
[66] C.A. Rees, J.L. Provis, G.C. Lukey, J.S.J. van Deventer, In Situ ATR-FTIR Study of the Early Stages of Fly Ash Geopolymer Gel Formation, Langmuir. 23 (2007) 9076–9082. doi:10.1021/la701185g.
[67] A. Marsh, A. Heath, P. Patureau, M. Evernden, P. Walker, Alkali activation behaviour of un-calcined montmorillonite and illite clay minerals, Appl. Clay Sci. 166 (2018) 250–261. doi:https://doi.org/10.1016/j.clay.2018.09.011.
[68] S.O. Sore, A. Messan, E. Prud'homme, G. Escadeillas, F. Tsobnang, Synthesis and characterization of geopolymer binders based on local materials from Burkina Faso – Metakaolin and rice husk ash, Constr. Build. Mater. 124 (2016) 301–311. doi:https://doi.org/10.1016/j.conbuildmat.2016.07.102.
[69] I. Lecomte, M. Liégeois, A. Rulmont, R. Cloots, F. Maseri, Synthesis and characterization of new inorganic polymeric composites based on kaolin or white clay and on ground-granulated blast furnace slag, J. Mater. Res. 18 (2003) 2571–2579. doi:DOI: 10.1557/JMR.2003.0360.
[70] J. Davidovits, Geopolymer : chemistry and applications, Institut Geopolymere, Saint-Quentin, 2011.
[71] A.D. Hounsi, G.L. Lecomte-Nana, G. Djétéli, P. Blanchart, Kaolin-based geopolymers: Effect of mechanical activation and curing process, Constr. Build. Mater. 42 (2013) 105–113. doi:10.1016/j.conbuildmat.2012.12.069.
[72] I. Aldabsheh, H. Khoury, J. Wastiels, H. Rahier, Dissolution behavior of Jordanian clay-rich materials in alkaline solutions for alkali activation purpose. Part I, Appl. Clay Sci. 115 (2015) 238–247. doi:10.1016/j.clay.2015.08.004.
[73] S.M. Hejazi, M. Sheikhzadeh, S.M. Abtahi, A. Zadhoush, A simple review of soil reinforcement by using natural and synthetic fibers, Constr. Build. Mater. 30 (2012) 100–116. doi:10.1016/j.conbuildmat.2011.11.045.
[74] H. Savastano, S.F. Santos, J. Fiorelli, V. Agopyan, Sustainable use of vegetable fibres and particles in civil construction, Second Edi, Elsevier Ltd., 2016. doi:10.1016/B978-0-08-100370-1.00019-6.
[75] M. Bouhicha, F. Aouissi, S. Kenai, Performance of composite soil reinforced with barley straw, Cem. Concr. Compos. 27 (2005) 617–621. doi:10.1016/j.cemconcomp.2004.09.013.
[76] Ş. Yetgin, Ö. ÇAVDAR, A. Çavdar, The effects of the fiber contents on the mechanic properties of the adobes, Constr. Build. Mater. 22 (2008) 222–227. doi:10.1016/j.conbuildmat.2006.08.022.
[77] F. Clementi, S. Lenci, T. Sadowski, Fracture characteristics of unfired earth, (2008) 193–198. doi:10.1007/s10704-008-9239-x.
[78] I. Alam, A. Naseer, A.A. Shah, Economical stabilization of clay for earth buildings construction in rainy and flood prone areas, Constr. Build. Mater. 77 (2015) 154–159. doi:10.1016/j.conbuildmat.2014.12.046.
[79] F. Parisi, D. Asprone, L. Fenu, A. Prota, Experimental characterization of Italian composite adobe bricks reinforced with straw fibers, Compos. Struct. 122 (2015) 300–307. doi:10.1016/j.compstruct.2014.11.060.
[80] Q. Piattoni, E. Quagliarini, S. Lenci, Experimental analysis and modelling of the

mechanical behaviour of earthen bricks, Constr. Build. Mater. 25 (2011) 2067–2075. doi:10.1016/j.conbuildmat.2010.11.039.
[81] K. Mustapha, E. Annan, S.T. Azeko, M.G. Zebaze Kana, W.O. Soboyejo, Strength and fracture toughness of earth-based natural fiber-reinforced composites, J. Compos. Mater. 50 (2016) 1145–1160. doi:10.1177/0021998315589769.
[82] K. Ghavami, R.D. Toledo Filho, N.P. Barbosa, Behaviour of composite soil reinforced with natural fibres, Cem. Concr. Compos. 21 (1999) 39–48. doi:10.1016/S0958-9465(98)00033-X.
[83] H. Danso, D.B. Martinson, M. Ali, J.B. Williams, Physical , mechanical and durability properties of soil building blocks reinforced with natural fibres, Constr. {&} Build. Mater. 101 (2015) 797–809. doi:10.1016/j.conbuildmat.2015.10.069.
[84] J. Khedari, P. Watsanasathaporn, J. Hirunlabh, Development of fibre-based soil-cement block with low thermal conductivity, Cem. Concr. Compos. 27 (2005) 111–116. doi:10.1016/j.cemconcomp.2004.02.042.
[85] E. Obonyo, Developing enhanced, ligno-cellulosic fibre reinforcement for low-cost, cementitious, construction materials, Archit. Eng. Des. Manag. 8 (2012) 30–41. doi:10.1080/17452007.2011.613216.
[86] A. Mesbah, J.-C. Morel, P. Walker, K. Ghavami, Development of a Direct Tensile Test for Compacted Earth Blocks Reinforced with Natural Fibers, J. Mater. Civ. Eng. 16 (2004) 95–98. doi:10.1061/(ASCE)0899-1561(2004)16:1(95).
[87] R. Mattone, Sisal fibre reinforced soil with cement or cactus pulp in bahareque technique, Cem. Concr. Compos. 27 (2005) 611–616. doi:10.1016/j.cemconcomp.2004.09.016.
[88] J.-C. Morel, K. Ghavami, A. Mesbah, Theoretical and Experimental Analysis of Composite Soil Blocks Reinforced with Sisal Fibres Subjected to Shear by, Mason. Int. 13 (2000) 54–62.
[89] E.R. Sujatha, S.S. Devi, Reinforced soil blocks : Viable option for low cost building units, Constr. Build. Mater. 189 (2018) 1124–1133. doi:10.1016/j.conbuildmat.2018.09.077.
[90] M.S. Islam, K. Iwashita, Earthquake resistance of adobe reinforced by low cost traditional materials, J. Nat. Disaster Sci. 32 (2010) 1–21.
[91] V. Sharma, H.K. Vinayak, B.M. Marwaha, Enhancing compressive strength of soil using natural fibers, Constr. Build. Mater. 93 (2015) 943–949. doi:10.1016/j.conbuildmat.2015.05.065.
[92] Y. Millogo, J.C. Morel, J.E. Aubert, K. Ghavami, Experimental analysis of Pressed Adobe Blocks reinforced with Hibiscus cannabinus fibers, Constr. Build. Mater. 52 (2014) 71–78. doi:10.1016/j.conbuildmat.2013.10.094.
[93] M. Mostafa, N. Uddin, Experimental analysis of Compressed Earth Block (CEB) with banana fibers resisting flexural and compression forces, Case Stud. Constr. Mater. 5 (2016) 53–63. doi:10.1016/j.cscm.2016.07.001.
[94] M. Segetin, K. Jayaraman, X. Xu, Harakeke reinforcement of soil-cement building materials: Manufacturability and properties, Build. Environ. 42 (2007) 3066–3079. doi:10.1016/j.buildenv.2006.07.033.
[95] B. Taallah, A. Guettala, The mechanical and physical properties of compressed earth block stabilized with lime and filled with untreated and alkali-treated date palm fibers, Constr. Build. Mater. 104 (2016) 52–62. doi:10.1016/j.conbuildmat.2015.12.007.
[96] M.C.N. Villamizar, V.S. Araque, C.A.R. Reyes, R.S. Silva, Effect of the addition of coal-ash and cassava peels on the engineering properties of compressed earth blocks, Constr.

Build. Mater. 36 (2012) 276–286. doi:10.1016/j.conbuildmat.2012.04.056.
[97] G. Araya-letelier, J. Concha-riedel, F.C. Antico, C. Valdés, G. Cáceres, Influence of natural fiber dosage and length on adobe mixes damage-mechanical behavior, Constr. Build. Mater. 174 (2018) 645–655. doi:10.1016/j.conbuildmat.2018.04.151.
[98] F. Aymerich, L. Fenu, P. Meloni, Effect of reinforcing wool fibres on fracture and energy absorption properties of an earthen material, Constr. Build. Mater. 27 (2012) 66–72. doi:10.1016/j.conbuildmat.2011.08.008.
[99] G. Araya-Letelier, J. Concha-Riedel, F.C. Antico, C. Sandoval, Experimental mechanical-damage assessment of earthen mixes reinforced with micro polypropylene fibers, Constr. Build. Mater. 198 (2019) 762–776. doi:https://doi.org/10.1016/j.conbuildmat.2018.11.261.
[100] A. Pekrioglu Balkis, The effects of waste marble dust and polypropylene fiber contents on mechanical properties of gypsum stabilized earthen, Constr. Build. Mater. 134 (2017) 556–562. doi:10.1016/j.conbuildmat.2016.12.172.
[101] P. Donkor, E. Obonyo, Earthen construction materials: Assessing the feasibility of improving strength and deformability of compressed earth blocks using polypropylene fibers, Mater. Des. 83 (2015) 813–819. doi:10.1016/j.matdes.2015.06.017.
[102] C. Tang, B. Shi, W. Gao, F. Chen, Y. Cai, Strength and mechanical behavior of short polypropylene fiber reinforced and cement stabilized clayey soil, Geotext. Geomembranes. 25 (2007) 194–202. doi:10.1016/j.geotexmem.2006.11.002.
[103] A. Kumar, B.S. Walia, J. Mohan, Compressive strength of fiber reinforced highly compressible clay, Constr. Build. Mater. 20 (2006) 1063–1068. doi:https://doi.org/10.1016/j.conbuildmat.2005.02.027.
[104] S. Khaled, M. Mehedy, Tensile Strength and Toughness of Soil–Cement–Fly-Ash Composite Reinforced with Recycled High-Density Polyethylene Strips, J. Mater. Civ. Eng. 14 (2002) 177–184. doi:10.1061/(ASCE)0899-1561(2002)14:2(177).
[105] W.D. Callister, D.G. Rethwisch, Materials science and engineering: an introduction, John wiley & sons New York, 2007.
[106] D. Maskell, A. Heath, P. Walker, Laboratory scale testing of extruded earth masonry units, Mater. Des. 45 (2013) 359–364. doi:10.1016/j.matdes.2012.09.008.
[107] K.G. Kuder, S.P. Shah, Processing of high-performance fiber-reinforced cement-based composites, Constr. Build. Mater. 24 (2010) 181–186. doi:10.1016/j.conbuildmat.2007.06.018.
[108] X. Zhou, Z. Li, Characterization of rheology of fresh fiber reinforced cementitious composites through ram extrusion, Mater. Struct. Constr. 38 (2005) 17–24. doi:10.1617/14064.
[109] R.S. Teixeira, S.F. Santos, G.H.D. Tonoli, A.L. Christoforo, H.S. Jr, F.A.R. Lahr, Extrudable cement-based composites reinforced with curauá (Ananas erectifolius) and polypropylene fibers ., (n.d.).
[110] J.J. Benbow, E.W. Oxley, J. Bridgwater, The extrusion mechanics of pastes-the influence of paste formulation on extrusion parameters, Chem. Eng. Sci. 42 (1987) 2151–2162. doi:10.1016/0009-2509(87)85036-4.
[111] S. Srinivasan, D. Deford, P.S. Shah, The use of extrusion rheometry in the development of extrudate fibre-reinforced cement composites, Concr. Sci. Eng. 1 (1999) 26–36.
[112] X. Zhou, Characterization of rheology of fresh fiber reinforced cementitious composites through ram extrusion, Mater. Struct. 38 (2004) 17–24. doi:10.1617/14064.
[113] R.N. Das, C.D. Madhusoodana, K. Okada, Rheological studies on cordierite honeycomb

extrusion, J. Eur. Ceram. Soc. 22 (2002) 2893–2900.
[114] X. Zhou, Z. Li, Numerical simulation of ram extrusion in short-fiber-reinforced fresh cementitious composites, J. Mech. Mater. Struct. 4 (2010) 1755–1769. doi:10.2140/jomms.2009.4.1755.
[115] F.V. Riza, I.A. Rahman, A.M.A. Zaidi, Possibility of lime as a stabilizer in compressed earth brick (CEB), Int. J. Adv. Sci. Eng. Inf. Technol. 1 (2011) 582–585.
[116] H. Guillaud, Characterization of earthen materials, Terra Lit. Rev. (2008) 21.
[117] A. Guettala, B. Mezghiche, R. Chebili, H. Houari, Durability of lime stabilised earth blocks, in: Challenges Concr. Constr. Vol. 5, Sustain. Concr. Constr., 2002: pp. 645–654. doi:10.1680/scc.31777.0064.
[118] J.C. Morel, A. Pkla, P. Walker, Compressive strength testing of compressed earth blocks, Constr. Build. Mater. 21 (2007) 303–309. doi:10.1016/j.conbuildmat.2005.08.021.
[119] J.E. Aubert, P. Maillard, J.C. Morel, M. Al Rafii, Towards a simple compressive strength test for earth bricks ?, (2015). doi:10.1617/s11527-015-0601-y.
[120] P.J. Walker, Strength and Erosion Characteristics of Earth Blocks and Earth Block Masonry, J. Mater. Civ. Eng. 16 (2004) 497–506. doi:10.1061/(ASCE)0899-1561(2004)16:5(497).
[121] J. Tingle, R. Santoni, Stabilization of Clay Soils with Nontraditional Additives, Transp. Res. Rec. J. Transp. Res. Board. 1819 (2003) 72–84. doi:10.3141/1819b-10.
[122] Y. Cai, B. Shi, C.W.W. Ng, C. Tang, Effect of polypropylene fibre and lime admixture on engineering properties of clayey soil, Eng. Geol. 87 (2006) 230–240.
[123] Y. Millogo, J.-C. Morel, J.-E. Aubert, K. Ghavami, Experimental analysis of Pressed Adobe Blocks reinforced with Hibiscus cannabinus fibers, Constr. Build. Mater. 52 (2014) 71–78.
[124] I. Demir, An investigation on the production of construction brick with processed waste tea, Build. Environ. 41 (2006) 1274–1278. doi:10.1016/J.BUILDENV.2005.05.004.
[125] S. Mindess, The Fracture Process Zone in Concrete BT - Toughening Mechanisms in Quasi-Brittle Materials, in: S.P. Shah (Ed.), Springer Netherlands, Dordrecht, 1991: pp. 271–286. doi:10.1007/978-94-011-3388-3_17.
[126] S. Lenci, F. Clementi, T. Sadowski, Experimental determination of the fracture properties of unfired dry earth, Eng. Fract. Mech. 87 (2012) 62–72. doi:10.1016/j.engfracmech.2012.03.005.
[127] J.-J. Wang, S.-Y. Huang, J.-F. Hu, Limit of crack depth in KIC testing for a clay, Eng. Fract. Mech. 164 (2016) 19–23. doi:https://doi.org/10.1016/j.engfracmech.2016.08.006.
[128] M. D'Orazio, S. Lenci, L. Graziani, Relationship between fracture toughness and porosity of clay brick panels used in ventilated façades: Initial investigation, Eng. Fract. Mech. 116 (2014) 108–121. doi:10.1016/j.engfracmech.2013.12.003.
[129] T.L. Anderson, T.L. Anderson, Fracture mechanics: fundamentals and applications, CRC press, 2005.
[130] W. Soboyejo, Mechanical Properties of Engineered Materials, CRC Press, 2002.
[131] G. Constantinides, K.S. Ravi Chandran, F.-J. Ulm, K.J. Van Vliet, Grid indentation analysis of composite microstructure and mechanics: Principles and validation, Mater. Sci. Eng. A. 430 (2006) 189–202. doi:https://doi.org/10.1016/j.msea.2006.05.125.
[132] G. Constantinides, F.-J. Ulm, K. Van Vliet, On the use of nanoindentation for cementitious materials, Mater. Struct. 36 (2003) 191–196. doi:10.1007/BF02479557.
[133] F. Ulm, M. Vandamme, C. Bobko, J.A. Ortega, Statistical Indentation Techniques for

Hydrated Nanocomposites: Concrete, Bone, and Shale, 2692 (2007). doi:10.1111/j.1551-2916.2007.02012.x.
[134] L. Sorelli, G. Constantinides, F. Ulm, F. Toutlemonde, Cement and Concrete Research The nano-mechanical signature of Ultra High Performance Concrete by statistical nanoindentation techniques, Cem. Concr. Res. 38 (2008) 1447–1456. doi:10.1016/j.cemconres.2008.09.002.
[135] D. Hou, G. Zhang, R.R. Pant, J.S. Shen, M. Liu, H. Luo, Nanoindentation Characterization of a Ternary Clay-Based Composite Used in Ancient, (n.d.) 1–14. doi:10.3390/ma9110866.
[136] H. Lee, V. Vimonsatit, P. Chindaprasirt, Mechanical and micromechanical properties of alkali activated fly-ash cement based on nano-indentation, Constr. Build. Mater. 107 (2016) 95–102. doi:https://doi.org/10.1016/j.conbuildmat.2015.12.013.
[137] M. Zhang, M. Zhao, G. Zhang, T. El-Korchi, M. Tao, A multiscale investigation of reaction kinetics, phase formation, and mechanical properties of metakaolin geopolymers, Cem. Concr. Compos. 78 (2017) 21–32. doi:10.1016/j.cemconcomp.2016.12.010.
[138] J. Němeček, V. Šmilauer, L. Kopecký, Nanoindentation characteristics of alkali-activated aluminosilicate materials, Cem. Concr. Compos. 33 (2011) 163–170. doi:https://doi.org/10.1016/j.cemconcomp.2010.10.005.
[139] Y. Ma, G. Ye, J. Hu, Micro-mechanical properties of alkali-activated fly ash evaluated by nanoindentation, 147 (2017) 407–416. doi:10.1016/j.conbuildmat.2017.04.176.
[140] P.K. Valavala, G.M. Odegard, Modeling techniques for determination of mechanical properties of polymer nanocomposites, Rev. Adv. Mater. Sci. 9 (2005) e44.
[141] B. Budiansky, J.C. Amazigo, A.G. Evans, Small-scale crack bridging and the fracture toughness of particulate-reinforced ceramics, J. Mech. Phys. Solids. 36 (1988) 167–187. doi:https://doi.org/10.1016/S0022-5096(98)90003-5.
[142] T. Tan, S.F. dos Santos, H. Savastano, W.O. Soboyejo, Fracture and resistance-curve behavior in hybrid natural fiber and polypropylene fiber reinforced composites, J. Mater. Sci. 47 (2012) 2864–2874.
[143] H. Jr Savastano, A. Turner, C. Mercer, W.O. Soboyejo, Mechanical behavior of cement-based materials reinforced with sisal fibers, J. Mater. Sci. 41 (2006) 6938–6948. doi:10.1007/s10853-006-0218-1.
[144] H. Savastano, S.F. Santos, M. Radonjic, W.O. Soboyejo, Fracture and fatigue of natural fiber-reinforced cementitious composites, Cem. Concr. Compos. 31 (2009) 232–243. doi:10.1016/j.cemconcomp.2009.02.006.
[145] D.R. Bloyer, R.O. Ritchie, K.T. Venkateswara Rao, Fracture toughness and R-Curve behavior of laminated brittle-matrix composites, Metall. Mater. Trans. A. 29 (1998) 2483–2496. doi:10.1007/s11661-998-0220-0.
[146] T. Fett, D. Munz, Stress lntensity Factors and Weight Functions for One-dimensional Cracks Kernforschungszentrum Karlsruhe, (1994).
[147] H.E. Gram, P. Nimityongskul, Durability of natural fibres in cement-based roofing sheets, J. Ferrocem. 17 (1987) 328–334.

3.0 Chapter Three: Synthesis of Alkali Activated Binders using in situ Aluminosilicates in Extruded Earth-Based Building Materials

This chapter focuses on the synthesis-property relationship of extruded earth-based building products which harnesses the alkali activation of in situ aluminosilicates within soils as binding mechanism.

3.1 Introduction

Owing to the global thrust towards environmental sustainability, studies on earthen construction have witnessed a resurgence in recent decades as a result of its eco-friendly indices relative to contemporary construction materials [1]. For instance, it has been reported that unfired clay bricks require only 14% of the embodied energy required for the production of fired bricks and 25% of the energy required for the production of lightweight concrete [2]. In addition, earthen construction possesses excellent thermal and moisture buffering properties [3] which reduce the heating and cooling loads required in buildings [4]. Despite these advantages, the major drawback of building with earth has been its sensitivity to water resulting in a lower durability. This has been attributed to strong attraction of water to soil mineral surfaces particularly clay minerals [5]. Traditional methods of stabilisation have focused on the use of additives such as lime and cement or kiln firing. More recent efforts have focused on alternative additives to encourage a more widespread use of earthen construction; biopolymers [6–8]; and other pozzolans such as Coal ash [9]; Metakaolin [10]; Lime activated GGBS [11]; Agricultural by-products -Rice husk ash/bagasse ash [12]. Studies have demonstrated that with adequate stabilisation, extruded earth building units may be produced using similar procedure for the production of fired earth bricks/tiles without the energy intensive kiln firing process [13, 14]

Previous work by Davidovits [15] proposed the Low Temperature Geopolymeric Setting (LTGS) as a stabilization mechanism for the production of high mechanical strength and water stable building units at drying temperatures of 50-250°C. The authors reported that kaolinite mineral in clay/lateritic soils can be transformed into a three dimensional compound producing water stable building blocks with satisfactory mechanical properties using the geopolymer technology. However, results from Maskell et al. [16] demonstrated that the LTGS was ineffective for the stabilisation of a predominantly silty soil containing kaolinite under varying NaOH conditions. Whereas Alkali Activated Materials (AAMs) refer to the broadest classification comprising any binder system derived from the reaction of any aluminosilicate solid and alkali metal source[17], geopolymers are a subset of AAMs where

the binder phase is sourced exclusively from aluminosilicates with highly coordinated products [18]. Presently, extensive studies have demonstrated the improved properties of AAC's and AAC based concretes relative to Portland cement concrete. However, very little work has been conducted to harness this technology for the improvement of earthen masonry given that the major composition of earth are aluminosilicates.

Authors have argued that given the variable mineralogical composition of soils, it is not possible to know if alkali activation would provide a sufficient mechanism for the stabilisation of soils [16]. However, Xu and van Deventer [19] demonstrated that a wide number of clay minerals can be used as source materials for alkali activation. They emphasized the need to optimise the concentration of alkaline solution for each mineral type as each aluminosilicate demonstrated varying dissolution rates. In alkali activation, the key is to identifying the most significant variables that are required for the reaction to occur and according to Duxson et al. [20], these include the source materials and processing conditions. Nonetheless, giving the availability of earth in various parts of the world and its potential to provide sustainable construction materials, the presence of aluminosilicates in earth triggers interest as to whether alkali activation can be harnessed for the production of building units. Slaty et al. [21] demonstrated alkali activation of kaolinitic clays using NaOH with mass ratios of 8-20% to produce composites with satisfactory mechanical properties both in the dry and saturated condition. The use of high concentration alkali hydroxide solutions may lead to safety and occupational health and safety concerns particularly in factories. Also, the addition of high alkaline concentrations may negate the benefits of unfired earth as a sustainable construction material.

The objective of this study was to explore the role of alkali activation as a viable stabilisation mechanism for production of unfired earthen building units. Studies have shown that high molarity concentration of alkaline solution favour the dissolution of clay minerals and consequently yield materials with improved mechanical properties [22]. However, with a goal to attain minimal environmental and cost impact, effect of curing temperature on alkali activated samples produced with low alkali concentration was evaluated in this study. The experimental methodology involved characterising the soil to identify the mineralogical composition, producing specimens using the extrusion technique, evaluating the mechanical and physical properties, further characterization using X-ray Diffraction and Scanning Electron Microscopy and Electron Dispersive X-ray Spectroscopy; to determine the feasibility of this mechanism for the development of robust and eco-friendly construction materials. Commercialisation of alkali activation technology is advancing in various parts of

the world and the adoption of this technology may be useful in replacing the energy intensive kiln firing process adopted in the production of building bricks and roof tiles. Typical clay soil used for the production of fired roof tiles in Sao Paulo, Brazil was used.

3.2 Materials and Method

The soil used for this study was supplied by Top Telha Ceramic Tile Company, Leme and sourced from Brazilian quarries in the State of Sao Paulo, Brazil. The soils are typical source materials used for the production of fired roof tiles. Characterization was carried out by Scanning Electron Microscopy with chemical analysis by Energy Dispersive X-ray Spectroscopy (EDX). Fig 3.1 shows the Back Scatter Electron image of the as-received samples showing wide variation of particle sizes. Particles are predominantly irregular shaped and with smaller sized particles agglomerating over larger particles. Particles range in diameter from as high as 0.4mm to a few micrometers.

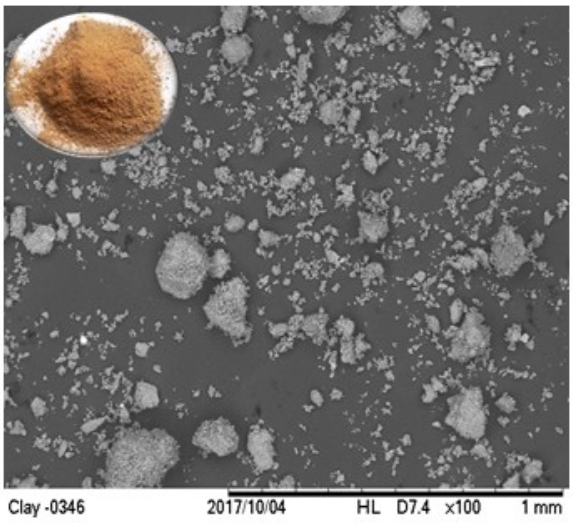

Figure 3:9 SEM-BSE Image of Soil

As-received soil was used without any form of mechanical pre-treatment even though it was assumed that the larger sized particles would not contribute to the reaction due to their low specific surface. They were retained to provide dimensional stability to the samples.

Sodium Hydroxide used was of caustic soda pellets with 97% purity whilst sodium silicate used was in the powder form and were both supplied by Dinamica Quimica Contemporanea Ltd, Brazil. The chemical composition of sodium silicate powder comprised 18% $Na_2O$and 63% SiO_2. In the preparation sequence, sodium hydroxide pellets and sodium silicate powder

were dissolved into the required amount of water and the solution allowed to cool for 24 hours given the exothermic nature of the dissolution. The experimental methodology adopted in this study was largely based on studies conducted by Maskell et al. [23] [13] [14] on stabilisation of unfired extruded earth bricks. This method of production closely represents the industrial production of extruded fired bricks (without the kiln firing process) to allow for easy adoption of innovative processes in already existing factories. In their studies, they have shown that the optimum moisture for extrusion moulding is typically within the range of the plastic limit of the soil as extrusion at moisture contents lower than the plastic limit result in notable surface cracking [13]. Hence, a moisture content corresponding to the plastic limit of the soil was adopted. The mixture was homogenised in a high energy intensive Eirich mixer (capacity 10l) for 5mins at high speed. The mixture was transferred to a Gelenski MVIG-05 laboratory extruder operating at a linear speed of approximately 4mm/s. Cylindrical samples were extruded with diameter 40mm for axial compression tests whilst plates of 200mm×50mm×15mm were produced for flexural tests. (Figure 3.2)

Figure 3:10 Extrusion Process

3.2.1 Optimisation of Processing Conditions

According to Davidovits [15, 22], the quantity of alkaline activator added to the argillaceous material determines the level of crosslinking resulting in the formation of water stable units. Although a wide range of materials can serve as precursors, phase composition determines its reactivity and thus the degree of dissolution[24]. This has necessitated the de-hydroxylation

of clay minerals to break down the crystalline structure. As the starting clay, was not thermally activated, a strong alkaline solution would be required for the reactions to proceed. Alternatively, the source materials would have required mechanical attrition to obtain finer sized particles. However, the objective of the study was to develop a sustainable building material with minimal cost and environmental impact. Hence, as-received soil was used for the study without any form of pre-treatment. Previous studies showed that the minimum sodium hydroxide content required to achieve water stable units was 3% NaOH content by dry weight of soil[22]. As a result, this minimum stabilisation content was adopted to ensure that the building units had minimal environmental impact. With the adopted moisture content corresponding to the plastic limit of the soil (25%), this would yield a 3M NaOH solution which corresponds to the lower bound molarity typically used in alkali activation. In addition, sodium silicate was included in the activator solution as it is commonly used to hasten the reaction by providing readily available Si in the reaction. Studies have shown that a sodium hydroxide to sodium silicate ratio of 0.22-025 yields optimum results [25] . As a result, a mass ratio of sodium hydroxide to sodium silicate of 0.25 was adopted in this study.

The curing regime was varied to ascertain if the alkali activation process would be accelerated through an initial elevated curing temperature as well as additional curing at room temperature. A set of specimens were cured at room temperature (24°C±2) and RH of 60% for varying duration of 7 and 15 days. Another set of specimens were cured initially at elevated temperatures (60 and 105°C) for 5hrs and left in the laboratory at room temperature of 24C±2 and RH of 60% and tested after 7 and 15 days. Studies have shown that optimum curing temperature is a function of NaOH concentration with lower optimum curing temperature corresponding to low NaOH concentration [26].

Table 3:3 Material Composition

Material	%
Clay	100
Water/Solid ratio	25
Sodium Hydroxide	3.0
Sodium Silicate	0.75

3.2.2 Stability in water

Due to the moisture sensitivity of earth as a result of the presence of clay minerals, studies have shown that a good indication of stabilisation of earth for construction is an assessment of its stability in water[27, 28]. According to Davidovits [22], bricks produced from the

geopolymerisation of kaolinitic clays produced a 3-D structure that was water stable with Na_2O content from as low as 3%. Hence, the water sensitivity test was conducted to serve as an indicator of the viability of this mechanism for the stabilisation of clay minerals particularly at low alkali concentrations. The water stability was assessed by full immersion of samples in de-ionised water at room temperature (24±3) for 24hrs. The mass of the absorbed water was measured and expressed as a percentage of the weight of the dry mass of the sample. The samples were tested at 3, 7 and 15 days to determine the water stability. Treated and untreated samples subjected to the various curing conditions were also, immersed in water for 24hrs and evaluated by physical assessment.

3.2.3 Mechanical and Physical Characterization

A minimum of 5 specimens each were subjected to physical and mechanical tests. Physical characterization comprised evaluation of water absorption, bulk density and apparent void volume according to BS EN 772-4:1998. Mechanical characterization was carried out under axial compression and four points bending using a Universal Testing Machine (Emic DL-30000 model) equipped with a 1kN load cell. The tests were performed until the decrease in load carrying capacity dropped to 5% of the maximum load.

There is presently no consensus on the appropriate procedure for the evaluation of the unconfined compressive strength of unfired earth[29]. Testing procedures are often based on those used for concrete or fired bricks. Unconfined compressive strength was evaluated using procedure adopted in [23] which is a modification of BS EN 772-1:2000. According to [28], moisture content at testing plays a significant influence on mechanical strength and it's important to standardize moisture contents before testing. As a result, mechanical properties of the test pieces were evaluated under two pre-conditions: oven dry condition (60°C for 24hrs) and fully saturated condition (total immersion in water for 24hrs). Although authors have argued that testing in the saturated condition is considered inappropriate for unfired earth [30], we attempted to evaluate under this condition to ascertain the degree of stabilisation obtained through alkali activation. Achieving water stable units would also indicate the application of unfired earth may subsequently be expanded to uncontrolled moisture exposure conditions. Cylindrical samples were tested in axial compression at an aspect ratio of 2 to minimise effect of platen restraints. The specimens were sufficiently flat and tested in uncapped manner as studies have shown that there is no significant variation associated with capping small scale specimens [23]

3.2.4 Scanning Electron Microscope (SEM) Analysis

Scanning Electron Microscopy was performed to analyse the microstructure in order to elucidate the mechanism of strength gain and ascertain the structure of the final product. Scanning electron microscopy (SEM) was used with a Back-Scatter Electron (BSE) image detector, operated at 15 kV accelerating voltage, for visualization of the microstructure on the surface. The images were captured with a Hitachi Tabletop Microscope TM3000; magnifications used ranged between x500 and x3000. The preparation of specimens for the BSE detector was accomplished with impregnation using epoxy resin. BSE samples were manually polished in a Struers TegraPol-11 machine using silicon carbide abrasive paper with sequential grit sizes 320, 600, 1000 for 6 min, using alcohol as lubricant. A final polishing was carried out using in turn 6, 3, 1 µm diamond polishing compound for 6 min with each size.

3.2.5 X-ray Diffraction Analysis

X-Ray Diffraction (XRD) was performed using a Rigaku MiniFlex 600 with range 10-70° (2θ) with a rate of 0.02°/min and Cu Kα to identify crystalline phases in materials. XRD spectra of samples cured at varying temperatures were analysed and compared with the starting material in order to detect any significant modification in its mineralogical structure.

3.2.6 FTIR Spectra Analysis

FTIR spectra were acquired using a Bruker Alpha-p IR spectrophotometer operating in absorbance mode. The IR spectra were acquired between 400 and 4000 cm-1 (resolution of 4cm-1). Each sample was pulverised and mixed with dry KBr powder. The acquisition began with the deposition of about 50 mg of sample onto a diamond substrate. The spectra were then obtained after 12 scans. The device was driven by Spectrum software for acquisition and data processing.

3.3 Results and Discussion

3.3.1 Source Materials Characterization

. The particle size distribution showed 68% of particles finer than 75µm with a liquid limit and plasticity index of 42.5% and 17.69% respectively, based on which the soil was classified as CL (inorganic clays of low plasticity). These are predominantly silt sized which is typical for soils used for fired roof tiles or bricks.[31] The Atterberg limits of the soils plot above the A-line of the plasticity chart classifying the soils as clayey soils. These properties do not fit the criteria required for ideal soils for cement stabilisation; suitable soils should be generally coarse grained soils with low clay fractions with P.I of between 5 and 15% as soils with

higher values are characterised by low compressive strengths, inadequate durability and excessive drying shrinkage[27]. Suitable stabilisation mechanisms would be the energy intensive kiln firing process. The elemental composition of the soil expressed in oxides presented in Table 3.2 show Silica and Alumina as the major components of the soil at 70.39% and 13.31% respectively. The mineralogical characterisation of the initial clay soil showed the soil contained predominantly muscovite. Quartz and sanidine were also detected with trace amounts of hematite.

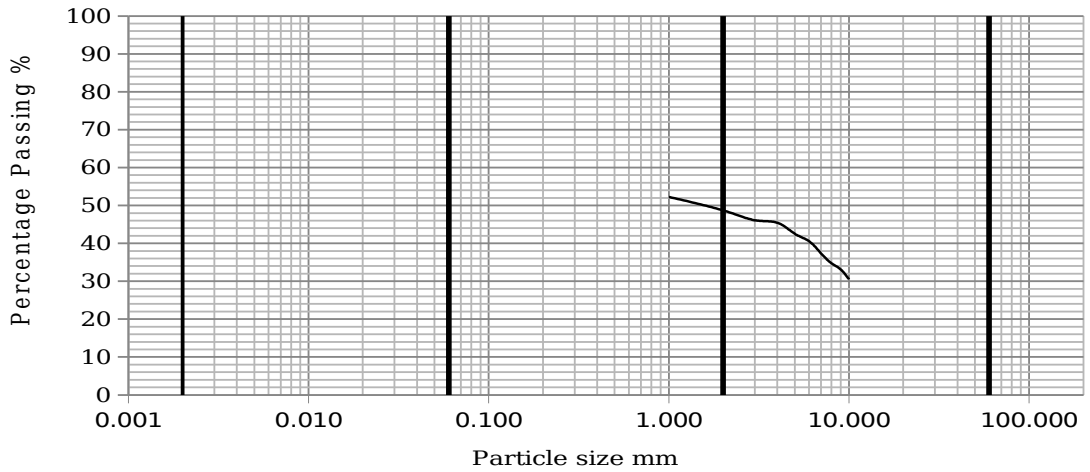

Figure 3:11 Particle Size Distribution

Table 3:4 Elemental composition of soil

Element	SiO_2	Al_2O_3	Fe_2O_3	TiO_2	CaO	MgO	K_2O	Na_2O	MnO	P_2O_5
%	70.39	13.31	4.09	0.55	0.14	1.68	4.97	0.16	0.13	0.07

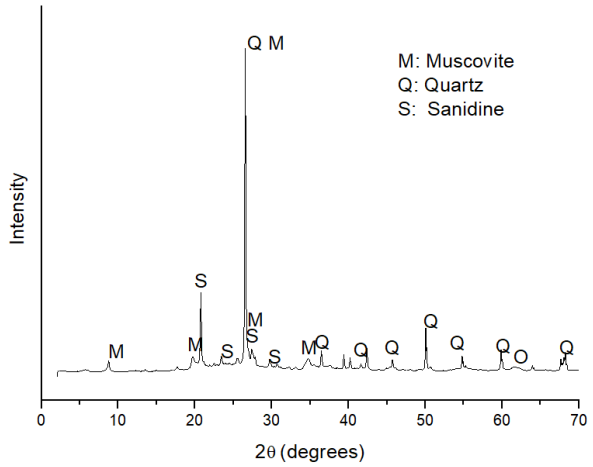

Figure 3:12 XRD Spectra of Soil

In theory, any material composed of silica and aluminium can be alkali activated This has been verified by studies by Xu and van Deventer[19] who studied the alkali activation of 16 natural aluminosilicate materials. Their results confirm the reactivity of a wide range of aluminosilicate including illite which is an interlayer-deficient mica. This suggests that the main reactive aluminosilicate mineral present in the soil would be muscovite which belongs to the mica family. It is a 2:1 dioctahedral phylosilicate mineral predominantly found in sedimentary and metamorphic rocks [32] and is one of the main rock forming minerals found in granites, pegmatites and schists. According to Davidovits[15], most clay minerals react with alkali to form a ceramic setting of type polysialate (Si-O-Al-O) or poly(sialate-siloxo) Si-O-Al-O-Si-O at drying temperatures (50-200°C) to form zeolites of either sodalite, natrolite, analcime or kaoliphitic phases depending on the silica to alumina ratio. Kaolinite has been predominantly used as the aluminosilicate source particularly in geopolymerisation. It is therefore interesting to know whether muscovite present in the soil can provide requisite alumina and silica sources to provide sufficient binding in the production of building units. Literature is scarce with regards to behaviour of micaceous minerals in the presence of alkaline solution. However studies by [33] have shown that the behaviour of muscovite is similar to smectite group of clays given the similarities in their structures.

3.3.2 Water Stability

Typically, unfired earth tends to disintegrate upon direct contact with water, limiting their use to internal controlled walling systems. However, as mentioned earlier, we adopted the water sensitivity test as an indicator of durability of the stabilised units when exposed to flooding conditions. Also, Seco et al. [34] correlated water absorption behaviour of stabilised earth

blocks to outdoor exposure over time and reported water absorption to be a satisfactory indicator of durability of earth blocks.

(a) **(b)** **(c)**

Figure 3:13 Water stability of samples cured at different initial curing temperatures (a) room temp (b) 60˚C (c) 105˚C

All untreated specimens, irrespective of curing conditions disintegrated within minutes of total immersion in water. This is typical for unstabilised clays and has been reported extensively. Figure 3.5 presents behaviour of alkali activated specimens following immersion in water. As can be observed in the figure, samples cured at room temperature and initial curing temperature of 60˚C showed high sensitivity to water. Whereas untreated samples disintegrated immediately in water, failure of samples cured at room temperature was characterised by a delamination of outer surface followed by complete disintegration of samples. Also, samples cured at 60˚C disintegrated initially by the formation of multiple crack patterns on the surface before complete disintegration. The nature of failure of these samples compared to the untreated samples suggests that some reaction took place particularly at the surfaces of the samples but was insufficient to produce binding to withstand internal pore pressures development during water immersion. However, only samples cured at 105˚C were stable in water and retained sufficient stability to allow for mechanical testing. This behaviour is contrary to alkali activation of kaolinitic minerals where curing at low temperatures produces sufficient binding to attain water stable units even at low alkaline solutions[22]. However, studies by Kuwahara [33] have shown that the activation energy required for the dissolution of muscovite is higher than that required for kaolinite. This may explain why a higher temperature was required to achieve water stable

units. This suggests that curing temperature is a critical variable in the optimisation of micaceous earthen building units using low alkali concentrations.

3.3.3 Physical Properties

Water absorption, density and apparent porosity were determined using the water displacement method. Since samples cured at room temperature and 60˚C were not water stable, only samples cured at 105˚C could be tested. Results from the physical tests reveal an average water absorption of 22% with a bulk density of 1.66g/cm^3 and apparent void volume of 36.6%. The average water absorption just satisfies the maximum specification according to ASTM standards for fired bricks under moderate weathering conditions which is 22% for building and facing bricks. Similar high water absorptions have been reported in cement stabilisation of fine grained soils [35] and this has been related to clay content. The water absorption value obtained in this study may be attributed to the predominantly fine grained nature of the soil which resulted in increased soil suction as a result of smaller pore spaces. Similar densities have been reported in cement stabilisation of predominantly silty soils[36]. The absorption capacity of stabilised earth gives an indication of the presence and significance of voids[37] . The average void volume of 36.6% suggests that about one-third of the samples comprises of voids. This high apparent porosity is indicative of a low packing density and contact among particles. This could be attributed to the soil grading as well as production method adopted. Studies have shown that manufacturing process determine mechanical performances of unfired earth [38]. It is possible that a lower moulding moisture content (for instance, the optimum moisture content) of the soil would have resulted in a better packing density. However, the requirements of extrusion moulding for soils in the plastic state govern the moisture content that can be used. Given, the linear relationship between porosity and strength of unfired earth [35] it is expected that extrusion of samples on the dry side of the plastic limit may yield samples with improved mechanical properties. However, it is important to note that high porosities and low density in earthen construction induces low thermal conductivities in the building units [39] which is significant in passive design of buildings.

3.3.4 Compressive Strength

Figure 3.6 presents testing configuration and failure modes observed with the specimens. Failure was characterized by the formation of near vertical surface cracks and exfoliation of the lateral sides in all cases. This would indicate the compressive stresses resulted in inelastic

deformations to the specimens causing the lateral sides to exfoliate and fall off. The samples demonstrated some considerable cracking and deformation before failure. Despite the loss of the sides, the central core was still intact.

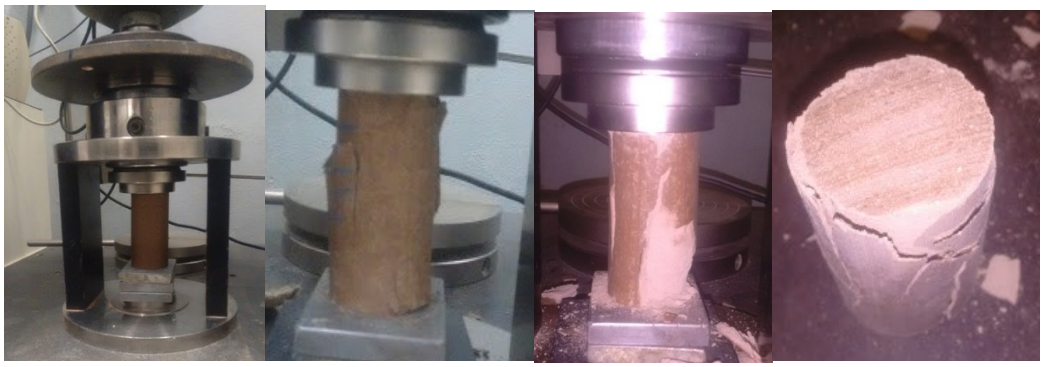

Figure 3:14 Failure patterns of specimens

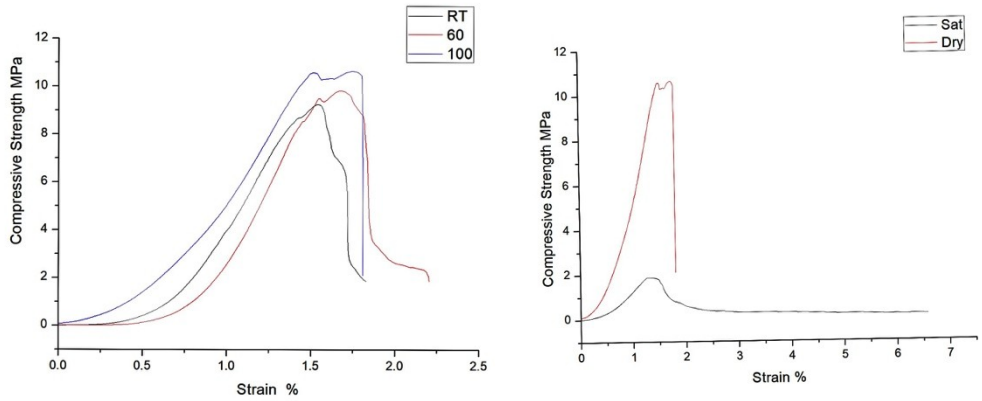

Figure 3:15 Characteristic Compression Stress-strain curves

Effect of Initial curing temperature

The characteristic stress-strain curves obtained are presented in Figure 3.7. It can be observed that curves comprises of three distinct stages. An initial consolidation stage which is characterised by increasing strain at a constant stress. At this stage, it is assumed that the soil grains are being redistributed and gradually filling the voids that exist in the microstructure. In the second stage, a pseudo-linear section is activated up to peak failure. At the peak stress, samples did not fail immediately: instead they were subjected to significant deformation before structural collapse. Attainment of peak stress in all cases is observed to begin at a

strain corresponding to 1.5%. The post-peak performance is characterised by almost brittle failure with little or no deformation. This behaviour deviates slightly from typical response of cylindrical unfired earth specimens as reported in some studies [40]. However peak stresses are considerably higher than average values typically achieved with unfired earth. Maskell et al. [13] defined a minimum strength requirement of 2.9MPa for unfired earth walling unit in the dry condition. Results obtained demonstrate potential of alkali activation as a suitable binding mechanism for fine grained soils.

At room temperature curing, average peak stress obtained after 7days was about 9MPa. Initial curing at elevated temperatures (60˚C and 105˚C) for 5hrs, resulted in average compressive strength of about 10 MPa and 11MPa respectively indicating that in the dry condition, influence of elevated initial curing temperature may not be detected in preconditioned samples. The preconditioning of bricks which comprised of drying at 60˚C for 24hrs helped the moisture content to reach equilibrium thereby resulting in relatively stable compressive strengths. Clays possess an inherent axial compressive strength that is lost in the presence of moisture [27] and this was confirmed in this study as will be discussed in the following section. Notwithstanding, these results are comparable to values obtained in alkali activation of other clay minerals; Slaty et al. obtained compressive strength of 12MPa at 8% NaOH addition to kaolinitic soils whilst at 3% Davidovits obtained 15MPa for curing at 85˚C. In comparison with fired bricks, compressive strength did not meet the minimum ASTM specification for fired bricks under moderate weathering conditions of 17.2 MPa, and this may be attributed to the high porosity observed with the samples. Hence, it is expected that increased packing density may result in significantly improved mechanical properties.

Evaluation of compressive strength should be taken in the saturated condition to determine the ‘least’ strength to give the lower bound performance of earth blocks [27]. Despite satisfactory compressive strengths obtained in the oven dry condition, only samples cured initially at 105˚C could be tested in the saturated condition. This then signifies the importance of initial curing temperature to the alkali activation process. Hence, a true test of stabilisation of clay particles should be evaluated using the saturated compressive strength since the inherent strength of dry clay may present a misleading resistance to compression. Despite the improved oven dry compressive strength observed with alkali activated samples cured at room temp and 105˚C, all samples disintegrated in water when subjected to total immersion for 24hrs indicating that insufficient reaction had taken place and binding was not sufficient to withstand hydrostatic forces. Figure 3.7b presents stress-strain characteristics of samples with initial curing temp of 105˚C and tested in the dry and saturated condition. In contrast to

the dry condition, post peak performance of samples tested in the saturated condition exhibits almost ductile failure with strains exceeding 6%.

In the saturated condition, the compressive strength dropped by 83% to 1.82MPa for samples tested after 7 days. This suggests that the residual strength observed in the saturated condition can be solely attributed to alkali activation of a fraction of the clays. The large drop observed may be attributed to the absorption of water by the unreacted clay minerals [41] as well as development of pore water pressures within the fine grains [27]. This reduction in strength has been reported in various studies where wet strength to dry strength ratio of 20-55% have been recorded for cement stabilised earth masonry [36][35] and 30% in geopolymer stabilised kaolinitic soils [22]. The large amount of unreacted minerals may be attributed to the low alkaline concentration used in the study. However, average values of 1MPa have been established as minimum compressive strength in the saturated condition for unfired earth [13] and values obtained in this study exceed this minimum specification.

Effect of curing condition

Given the low reactivity of uncalcined clay minerals, studies have reported that additional curing at room temperature allows for continued dissolution of minerals resulting in improved mechanical properties [22]. Additional curing at room temperature did not reveal significant change in compressive strength for all samples as can be observed in Figure 3.8. According to Oelkers et al. [42], dissolution of silica and alumina species in muscovite is relatively fast at the initial stage but subsequently reduces as it reaches a steady state of solution concentration. This would suggest that compressive strength stabilises at an early age unlike other clay minerals following the attainment of steady state concentration of species. Also, additional curing of samples in room temperature from 7 to 15 days of samples cured below 60˚C did not improve their water stability as samples disintegrated after extended curing.

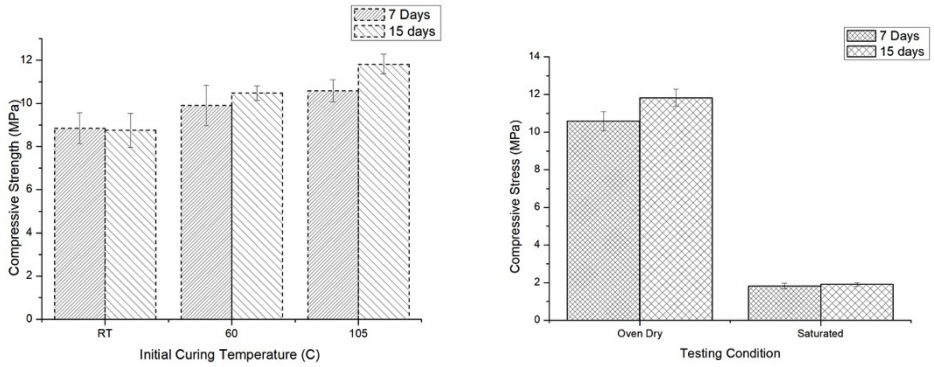

Figure 3:16 Effect of additional curing at room temperature on compressive strengths

The results indicate that initial curing temperature is a critical variable compared to elongated curing at room temperature in alkali activation of micaceous minerals.

3.3.5 Flexural Strength

Determination of flexural characteristics is not a common test on unfired earth as earthen units are typically employed in compression. However, according to Walker [27, 28], the assessment of this property gives a quick field assessment of the compressive properties of unfired earth-based on an empirical relationship between flexure and compressive strength. For cement-stabilised earth blocks, it is reported that the modulus of rupture shall equal at least one-sixth of the corresponding compressive strength [27]. Flexural strength was evaluated in four point bending in both oven dry condition and saturated condition for samples with initial curing temperature of cured 105˚C to evaluate if alkali activated specimens may be applied in bending.

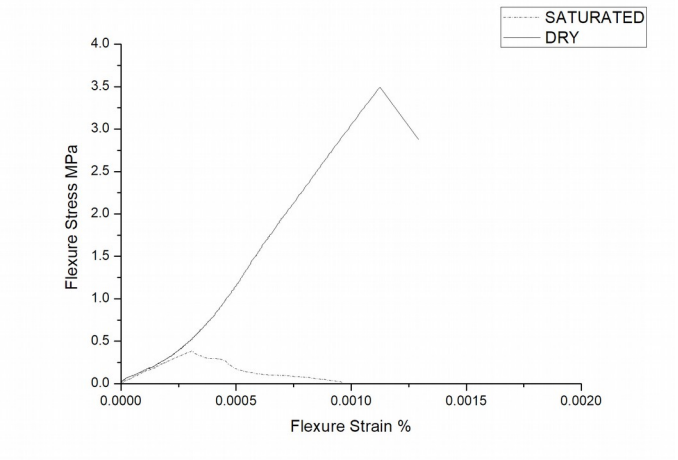

Figure 3:17 Characteristic Flexure Stress-Strain curves

Average flexural strength of 3.5MPa was observed in the oven dry condition and 0.4 MPa in the saturated condition. Typical values obtained for unfired earth range from 0.5 to 2MPa [43, 44]. As was observed with the compressive strength, a 70% drop in the MOR is also observed in the saturated condition. Failure mode of the samples under four points bending was through the development of a tensile crack at mid span. In the oven dry condition, the MOR corresponds to one-third of the compressive strength in the oven dry condition and one-fifth in the saturated condition. This is an agreement with proposed specification and indicates that this indirect assessment of compressive strength of cement stabilised earth blocks may also be applied to alkali activated earth blocks. Variation coefficients in all cases are reasonably low which indicated consistency of results.

3.3.6 XRD Analysis

Figure 3.10 shows the XRD spectra of the starting clay and alkali activated samples cured at room temperature and elevated temperatures of 60˚C and 105˚C for 5hrs and analysed after 14days. The spectra of the starting clay showed crystalline peak characteristic of muscovite, quartz and sanidine. The original crystalline phases identified with the starting materials remained after alkali activation confirming the presence of residual unreacted clay minerals in the mixture. This explains the significant water absorption of immersed samples which resulted in significant drop in mechanical properties in the saturated condition. However, it also suggests that alkali activated blocks would maintain hygroscopic and moisture buffering properties which is typically associated with earth construction.

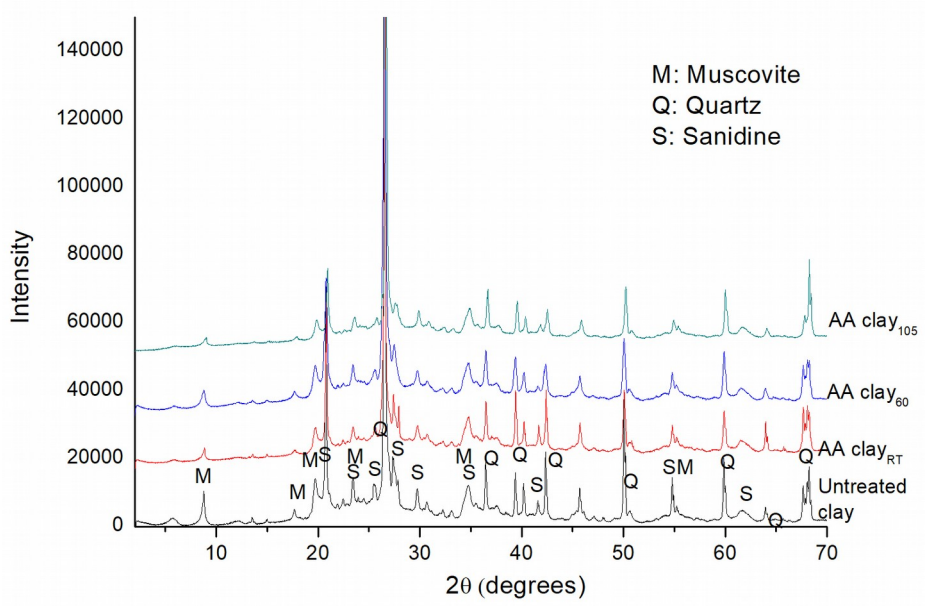

Figure 3:18 XRD spectra of starting clay and alkali activated clay at different curing temperatures

As shown in the XRD spectra, quartz mineral largely remains unreactive in the alkali activation process. There was an observed reduction in intensity of muscovite with alkali activation. This suggests that reactions took place between these minerals and the alkaline solution resulting in a dis-organisation of structure of the crystalline phase. Similar reduction in peak intensity after alkaline treatment of natural clay minerals has been reported in other studies [45, 46] According to Kuwahara [47], dissolution of muscovite minerals takes place primarily at the edge surfaces of with little to no reaction taking place at the basal surfaces. This would explain weak interactions observed. A comparison of the spectra of samples cured at varying temperature shows the peaks tend to lose intensity with increase in curing temperature. This suggests that the dissolution of muscovite increased with increase in curing temperature. This is in agreement with studies which have reported dissolution of muscovite in alkaline conditions to increase with increase in temperature [33] Curing temperature is a critical variable particularly with the low reactivity of the starting clay as higher temperatures deliver more energy to dissolve alumina and silica species. [24] This suggests that elevated initial curing temperature is critical to allow significant reaction to provide sufficient binding in micaceous minerals. This is in contrast to geopolymer formation, where reactions proceed at room temperature and elevated curing is restricted to a maximum of 90˚C as higher temperatures cause a break down the binding gel phase.

Analysis of the spectra further revealed that no new crystalline or amorphous phases were formed with alkali activation. The main reaction products of alkali activation of Ca-free aluminosilicate systems are typically sodium aluminosilicate hydrates (N-A-S-H) which exhibit long and medium range disorder making it appear amorphous in XRD spectra.[22] and has been reported extensively. Other studies have mentioned the presence of zeolitic phases as secondary products of alkali activation of kaolin and other clay minerals. [22][18, 48, 49] [50]. These products of alkali activation were not observed from the XRD spectra in this study. Absence of new peaks has also been reported in other studies [51, 52]. The absence of new peaks observed in this study is expected given the low concentration of alkaline solution as well as low reactivity of precursors used. Other authors have also discovered peaks corresponding to natrite, trona, nahcolite, etc. which are formed as a result of reaction of excess NaOH in the pores with CO_2. The low concentration alkali activator solution adopted may explain the absence of these compounds.

3.3.7 SEM-EDX Characterization

Back scatter scanning electron micrographs at various magnifications are presented in Figure 3.11. The micrographs show a heterogenous microstructure comprising of a binder phase surrounding particles of varying sizes. At 100X magnification, it can be observed that there is a gradation in microstructure from the surface of samples inwards from the top surfaces to a depth of 300-400 μm revealing a compact microstructure relative to the lower strata. This may be attributed to the evaporation of water during the curing process resulting in concentration gradients and thus difference in reactivity of the clay minerals. Also, liquid phase migration which is typically observed during extrusion moulding [53] may also result in concentration gradients within the samples with higher concentrations at the surface relative to the interior parts. Consequently, higher dissolution rates at the surface relative to the interior parts would result in graded microstructure as observed. Because the same pattern is observed irrespective of curing condition, it is assumed that the latter (liquid phase migration) takes place prior to curing is responsible for this stratification. This further explains the delamination of outer surfaces observed during failure.

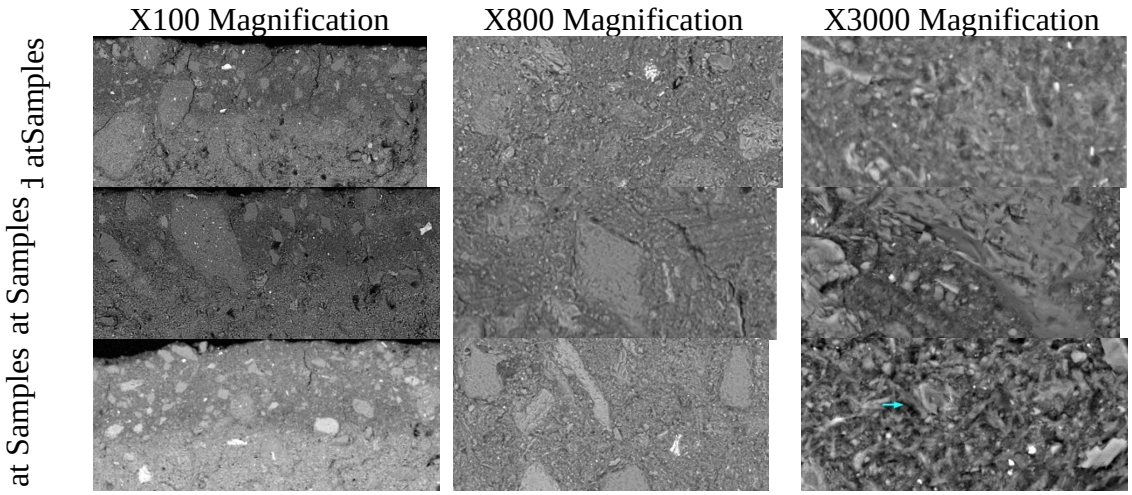

Figure 3:19 SEM BSE images at varying magnifications for samples cured at different temperatures

An analysis of the microstructure of samples cured at room temperature reveal a porous structure comprising of voids as well as linear cracks surrounding larger sized particles. This explains the lack of water stability of these specimens as high pore pressures developed would compromise the integrity of these samples. At elevated initial curing temperatures, the voids and linear cracks tend to disappear with increasing temperature. At higher magnification (3000X), fibrous crystals appear randomly throughout the microstructure with a length range of about 3μm in samples cured at room temperature and appear to increase in

diameter with increase in initial curing temperature. The formation of secondary products have reported extensively in various studies as the binding mechanism obtained in alkali activation. However, these new products were not identified in the X-ray spectra. According to Rees et al. [54], samples with the same Na/Al ratio may have XRD patterns with the same location of peaks but varying intensities. Alternatively, the possibility of the production of amorphous reactant products could also explain the absence of new peaks in the XRD spectra.

EDX analysis was conducted to further elucidate the elemental composition of the alkali activated clay as well as illustrate elemental distribution to show where elemental combinations and variations exist. Figure 11 shows BSE images with combined map distribution of major elements as well as single elemental maps below. The maps confirms the presence of the following elements in the system; Silicon, Aluminium, Potassium, Magnesium, Sodium, Iron and Titanium. Muscovite polymorph identified through XRD analysis had the formula $Al_{2.726}Ca_{0.011}Fe_{0.03}K_{0.776}Mg_{0.02}Na_{0.181}O_{11}Si_{3.15}Ti_{0.02}$. The distribution of these elements in the maps shows muscovite to be dominant mineral comprising finer particles. The spatial distribution of these elements also suggest muscovite mineral to be the main reactant in the alkali activation process. From the adjoining image overlays to the left of each BSE image, larger sized particles can be identified by the predominant elemental composition. For instance, quartz particles are easily identifiable as the silica dense portions of the maps whereas, orthoclase particles can also be identified by the potassium dense portions. The unreacted quartz and orthoclase particles are surrounded by a binder phase and is presumably a reaction product of muscovite associated with alkali activation.

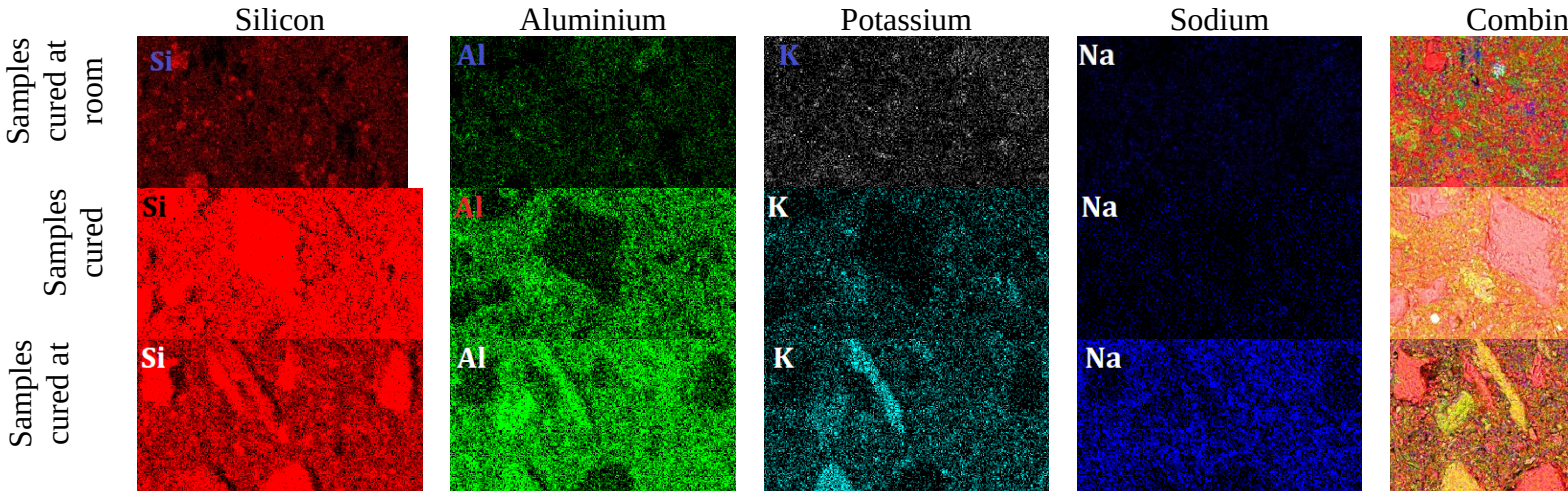

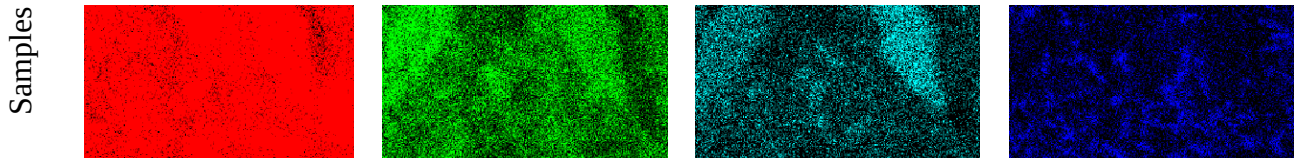

Figure 3:20 EDX analysis of Microstructure

As presented in Figure 3.12, EDX analysis of these structures reveal a difference in the spatial distribution of elements at varying curing temperatures. At room temp curing, the various elements can be distinguished from the combined overlays and this distinction disappears with increase in curing temperature. At higher temperatures, we see a progressively homogenous distribution of elements where individual elements in the binder are not clearly distinguished. This suggests the formation of new products. Silicon elemental maps reveal a silicon rich system distributed throughout the system confirming silica to be the dominant element as obtained from XRF analysis. Single elemental maps show an increase in intensity of spatial distribution of elements with increase in temperature. Since the only variable was the curing temperature, we can assume that the increase in temperature favoured the dissolution of reactive species and contributed to formation of new products [55]. The increase in temperature reduces the activation energy thereby promoting higher rate of dissolution of minerals leading to improved mechanical properties [33]. Also, other authors have suggested an increase in alkalinity derived from loss of water at higher curing temperatures may also lead to a higher dissolution of minerals [56].

There are scarce published results on the products of alkali activation of muscovite minerals compared to other clay minerals, as a result the products were not readily identified. Pacheco-torgal et al. demonstrated the possibility of using a tungsten mine waste containing muscovite and quartz for the production of alkali activated binders [57–59]. However the starting material was dehydroxylated and hence significant comparison cannot be made. However, closer magnification of samples cured at 105˚C revealed the elemental composition of fibrous precipitates observed from the SEM images to contain sodium, silicon, aluminium and potassium which may presumably be analogous to sodium aluminosilicate hydrates which are typical products of alkali activation of clay minerals. But the absence of new peaks in the XRD spectra may suggest that the reaction products where of an amorphous nature. As can be observed from the sodium elemental distribution, these precipitates are distinct from the surrounding unreacted muscovite minerals and we may conclude are responsible for the improved binding observed at this temperature.

3.3.8 FTIR Characterization

In order to further characterise newly formed phases observed from SEM/EDX analysis, Figure 3.14 presents FTIR spectra of pure muscovite mineral and alkali activated samples cured at 105˚C only. FTIR spectrum of muscovite mineral is dominated by a Si-O-Al band at 975 cm^{-1}.

On the other hand, dominant band in the activated soil is broader with a higher intensity and is located at a higher wavenumber (1031 cm^{-1}). Studies by Prud'homme et al.[60] have shown that total displacement of main band during the formation of geopolymers is approximately 40 cm^{-1} to a position which corresponds to 940 cm^{-1} . This is attributed to asymmetric stretching of Si-O-Si and Si-O-(Al) vibration bonds [25, 61, 62]. However, larger main band displacement (56 cm^{-1}) observed in this study can be attributed to the formation of aluminosilicate gels with Na [60]. Due to the low reactivity of the precursors as well as low alkalinity of solutions, weak concentration of Si and Al species in the system would inhibit the polycondensation reaction and consequently, network formation[60]. This explains the absence of new peaks or characteristic geopolymer 'hump' in the XRD spectra. This also confirms structural alteration of muscovite as observed with XRD spectra. Similar behaviour has been reported with alkali activation of uncalcined illite [63]. The stretching vibration absorption peaks of O-H and H-O-OH can be observed at 3447 and 1636 cm^{-1} and confirm the presence of chemically bound water([61]) in the uncalcined soil. FTIR spectra also shows slight carbonate bands associated with atmospheric carbonation of unconsumed NaOH in the system. These carbonates are typically associated with low reactive precursors such as natural clays[63]. Evidence confirms results from XRD which indicate no significant amount of carbonates were formed due to low molarity of alkali activators used.

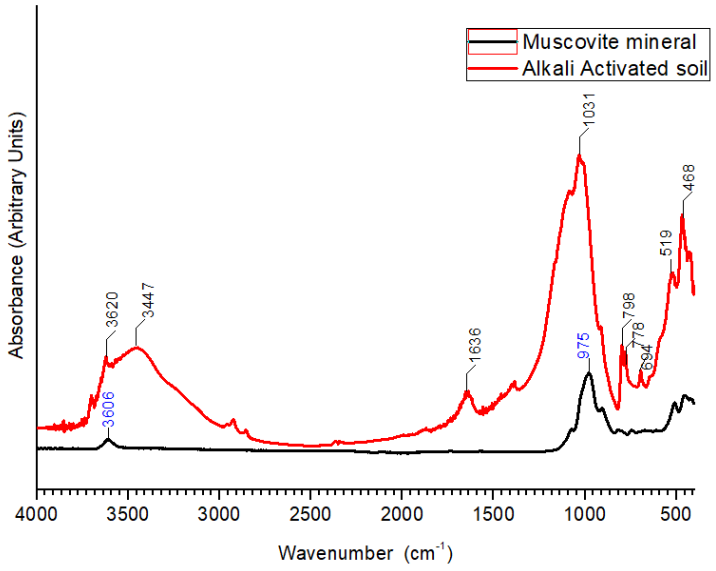

Figure 3.14 FTIR Spectra of alkali activated sample (cured at 105˚C) and pure muscovite mineral

3.3.9 Environmental Impact Analysis

An analysis of embodied energy was conducted to evaluate the environmental impact analysis of the process. This was ultimately compared to that associated with the production of fired bricks. A full life cycle analysis is beyond the scope of this paper. However, embodied energy analysis provides an indication of the overall environmental impact of building materials. In terms of manufacturing processes, the embodied energy associated with the production of fired bricks for a wall thickness of 100mm is 535.5MJ/m^2 compared to extrusion of unfired earth which requires 77.6MJ/m^2 [64] However, loss of strength with increase in moisture content limits the application of unfired earth to controlled environments. According to Maskell [65], the inclusion of chemical additives to unfired earth has a detrimental effect on embodied energies and global warming potentials. It has been reported that sodium hydroxide and sodium silicate have embodied energies of 23MJ/m^2 and 16MJ/m^2 respectively [64]. Based on these estimates, Table 3.3 presents embodied energy associated with the use of alkali activators and thermal curing for the production of a wall with thickness of 100mm.

Table 3:5 Analysis of Embodied energies associated with production

	Quantity (% by dry weight of soil)	Embodied energy (MJ/m^2)
Sodium Hydroxide	3.0	182.8
Sodium Silicate	0.75	31.8
Heat curing		6.8 [66]
Extrusion Process		77 [65]
Total		**298.9**

The production of source materials (alkali activators) is the most energy intensive component of the production process. Hence, a smaller energy footprint may be obtained by locating a source of alkalinity form natural sources (such as wood ash/rice husk ash) to serve as substitutes. Nonetheless, the results show that despite the use of energy intensive alkali activators, building materials with lower embodied energy compared to fired bricks, are achievable with alkali activation.

3.4 Summary/Conclusions

This study explored the feasbility of producing sustainable building materials from natural aluminosilicate minerals present in soil using low concentration alkali activator solutions. Small scale samples were produced using extrusion moulding and subjected to different curing regimes to ascertain the effect of initial curing temperature as well as curing duration on the alkali activation and consequent strength development in uncalcined muscovite based soils. Literature is scarce on the alkali activation of the natural muscovites; this study has provided some insight on behaviour of such minerals in low concentration alkali activator solutions.

The results reveal alkali activation of these clays to be a satisfactory mechanism for the stabilisation of these soils and was evident in the impressive mechanical properties obtained in the dry state relative to other stabilisation mechanisms. These materials may be suitable for load-bearing masonry applications. However, in the saturated condition, sufficient binding for the production of water stable units was achieved only at elevated initial curing temperatures of 105˚C for 5hrs revealing the temperature dependence of the process. This suggests that the scope of application of building units may be expanded to moisture susceptible environments with proper optimisation.

Analysis of XRD spectra reveal unreacted clay minerals after alkali activation. However, the presence of this residual clays suggest that the alkali activated clays may retain hygroscopic and moisture buffering properties which is associated with earthen construction thereby enhancing the thermal efficiency of the building. Further studies would need to be conducted to clearly establish the porosity-thermal conductivity behaviour of alkali activated clays.

Porous and graded microstructure reveal limitations associated with extrusion moulding and suggest that optimisation of moisture content during moulding will result in enhanced packing density and consequently improved mechanical and physical properties.

SEM-EDX/FTIR analysis reveal the formation of phases which are presumably Na-aluminosilicates formed as a result of a dissolution of muscovite and are responsible for the binding observed. The variation of the formation of binders with increasing curing temperature further confirm the need of higher temperatures to facilitate the dissolution of alumina and silica species from natural aluminosilicates.

References

1. Pacheco-Torgal F, Jalali S (2012) Earth construction: Lessons from the past for future eco-efficient construction. Constr Build Mater 29:512–519. https://doi.org/10.1016/j.conbuildmat.2011.10.054
2. Morton T (2006) Feat of clay Moves to develop UK production of unfired clay bricks are driven by the growing demand for sustainable construction materials to. 2–3
3. McGregor F, Heath A, Fodde E, Shea A (2014) Conditions affecting the moisture buffering measurement performed on compressed earth blocks. Build Environ 75:11–18. https://doi.org/10.1016/j.buildenv.2014.01.009
4. Rode C, Grau K (2008) Moisture buffering and its consequence in whole building hygrothermal modeling. J Build Phys 31:333–360. https://doi.org/10.1177/1744259108088960
5. Mitchell JK, Soga K (2005) Fundamentals of soil behavior. John Wiley & Sons Ltd, Chichester
6. Nakamatsu J, Kim S, Ayarza J, et al. (2017) Eco-friendly modification of earthen construction with carrageenan: Water durability and mechanical assessment. Constr Build Mater 139:193–202. https://doi.org/10.1016/j.conbuildmat.2017.02.062
7. Dove CA, Bradley FF, Patwardhan S V. (2016) Seaweed biopolymers as additives for unfired clay bricks. Mater Struct Constr 49:4463–4482. https://doi.org/10.1617/s11527-016-0801-0
8. Galán-Marín C, Rivera-Gómez C, Petric J (2010) Clay-based composite stabilized with natural polymer and fibre. Constr Build Mater 24:1462–1468. https://doi.org/10.1016/j.conbuildmat.2010.01.008
9. Villamizar MCN, Araque VS, Reyes CAR, Silva RS (2012) Effect of the addition of coal-ash and cassava peels on the engineering properties of compressed earth blocks. Constr Build Mater 36:276–286. https://doi.org/10.1016/j.conbuildmat.2012.04.056
10. Maskell D, Heath A, Walker P (2015) Use of metakaolin with stabilised extruded earth masonry units. Constr Build Mater 78:172–180. https://doi.org/10.1016/j.conbuildmat.2015.01.041
11. Oti JE, Kinuthia JM, Robinson RB (2014) The development of unfired clay building material using Brick Dust Waste and Mercia mudstone clay. Appl Clay Sci 102:148–154. https://doi.org/10.1016/j.clay.2014.09.031
12. Lima SA, Varum H, Sales A, Neto VF (2012) Analysis of the mechanical properties of compressed earth block masonry using the sugarcane bagasse ash. Constr Build Mater 35:829–837. https://doi.org/10.1016/j.conbuildmat.2012.04.127
13. Maskell D, Heath A, Walker P (2014) Inorganic stabilisation methods for extruded earth masonry units. Constr Build Mater 71:602–609. https://doi.org/10.1016/j.conbuildmat.2014.08.094
14. Maskell D, Heath A, Walker P (2016) Appropriate structural unfired earth masonry units. Proc Inst Civ Eng - Constr Mater 169:261–270. https://doi.org/10.1680/jcoma.15.00034
15. Davidovits J, James C (1988) Low Temperature Geopolymeric Setting (LTGS) and Archaeometry. Geopolymer ’88 1:69–78
16. Maskell D, Heath A, Walker P (2014) Geopolymer Stabilisation of Unfired Earth Masonry Units. Key Eng Mater 600:175–185. https://doi.org/10.4028/www.scientific.net/KEM.600.175
17. Shi C, Roy D, Krivenko P (2006) Alkali-activated cements and concretes. CRC press

18. Duxson P, Provis JL, Lukey GC, et al. (2005) 29Si NMR study of structural ordering in aluminosilicate geopolymer gels. Langmuir 21:3028–3036. https://doi.org/10.1021/la047336x
19. Xu H, Van Deventer JSJ (2000) The geopolymerisation of alumino-silicate minerals. Int J Miner Process 59:247–266. https://doi.org/10.1016/S0301-7516(99)00074-5
20. Duxson P, Fernández-Jiménez A, Provis JL, et al. (2007) Geopolymer technology: The current state of the art. J Mater Sci 42:2917–2933. https://doi.org/10.1007/s10853-006-0637-z
21. Slaty F, Khoury H, Wastiels J, Rahier H (2013) Characterization of alkali activated kaolinitic clay. Appl Clay Sci 75–76:120–125. https://doi.org/10.1016/j.clay.2013.02.005
22. Davidovits J (2011) Geopolymer : chemistry and applications. Institut Geopolymere, Saint-Quentin
23. Maskell D, Heath A, Walker P (2013) Laboratory scale testing of extruded earth masonry units. Mater Des 45:359–364. https://doi.org/10.1016/j.matdes.2012.09.008
24. Ahmari S, Zhang L (2014) The properties and durability of mine tailings-based geopolymeric masonry blocks. Elsevier Ltd
25. Hounsi AD, Lecomte-Nana GL, Djétéli G, Blanchart P (2013) Kaolin-based geopolymers: Effect of mechanical activation and curing process. Constr Build Mater 42:105–113. https://doi.org/10.1016/j.conbuildmat.2012.12.069
26. Ahmari S, Zhang L, Zhang J (2012) Effects of activator type/concentration and curing temperature on alkali-activated binder based on copper mine tailings. J Mater Sci 47:5933–5945. https://doi.org/10.1007/s10853-012-6497-9
27. Walker PJ (1995) Strength, durability and shrinkage characteristics of cement stabilised soil blocks. Cem Concr Compos 17:301–310. https://doi.org/10.1016/0958-9465(95)00019-9
28. Walker PJ (2004) Strength and Erosion Characteristics of Earth Blocks and Earth Block Masonry. J Mater Civ Eng 16:497–506. https://doi.org/10.1061/(ASCE)0899-1561(2004)16:5(497)
29. Aubert JE, Maillard P, Morel JC, Rafii M Al (2015) Towards a simple compressive strength test for earth bricks ? https://doi.org/10.1617/s11527-015-0601-y
30. Tingle J, Santoni R (2003) Stabilization of Clay Soils with Nontraditional Additives. Transp Res Rec J Transp Res Board 1819:72–84. https://doi.org/10.3141/1819b-10
31. Heath A, Walker P, Lawrence M (2009) Compressive strength of extruded unfired clay masonry units. 105–112. https://doi.org/10.1680/coma.2009.162
32. Velde B (1965) Experimental Determination Of Muscovite Polymorph Stabilities B . Vorno , Geophysical Laboratory , Carnegi , e Institution of abundant constituents of sedimentary and metamorphic rocks . These micas are also frequent but less abundant in plutonic igneous. 50:
33. Kuwahara Y (2008) In situ observations of muscovite dissolution under alkaline conditions at 25-50 C by AFM with an air/fluid heater system. Am Mineral 93:1028–1033. https://doi.org/10.2138/am.2008.2688
34. Seco A, Urmeneta P, Prieto E, et al. (2017) Estimated and real durability of unfired clay bricks: Determining factors and representativeness of the laboratory tests. Constr Build Mater 131:600–605. https://doi.org/10.1016/j.conbuildmat.2016.11.107
35. Latha B V, Reddy Venkatarama VM (2013) Influence of soil grading on the characteristics of cement stabilised soil compacts. https://doi.org/10.1617/s11527-013-

0142-1
36. Ojo EB, Matawal DS, Isah AK (2016) Statistical Analysis of the Effect of Mineralogical Composition on the Qualities of Compressed Stabilized Earth Blocks. 28:. https://doi.org/10.1061/(ASCE)MT.1943-5533.0001609
37. Guettala A, Houari H, Mezghiche B, Chebili R (2002) Durability of Lime Stabilized Earth Blocks. Courr du Savoir 2:61–66. https://doi.org/10.1680/scc.31777.0064
38. Kouakou CH, Morel JC (2009) Strength and elasto-plastic properties of non-industrial building materials manufactured with clay as a natural binder. Appl Clay Sci 44:27–34. https://doi.org/https://doi.org/10.1016/j.clay.2008.12.019
39. Bidoung JC, Pliya P, Meukam P, et al. (2016) Behaviour of clay bricks from small-scale production units after high temperature exposure. Mater Struct 49:4991–5006. https://doi.org/10.1617/s11527-016-0838-0
40. Ben Ayed H, Limam O, Aidi M, Jelidi A (2016) Experimental and numerical study of Interlocking Stabilized Earth Blocks mechanical behavior. J Build Eng 7:207–216. https://doi.org/10.1016/j.jobe.2016.06.012
41. Reddy VB V, Kumar PP (2009) Role of clay content and moisture on characteristics of cement stabilised rammed earth
42. Oelkers EH, Schott J, Gauthier JM, Herrero-Roncal T (2008) An experimental study of the dissolution mechanism and rates of muscovite. Geochim Cosmochim Acta 72:4948–4961. https://doi.org/10.1016/j.gca.2008.01.040
43. Galán-Marín C, Rivera-Gómez C, Petric J (2010) Clay-based composite stabilized with natural polymer and fibre. Constr Build Mater 24:1462–1468. https://doi.org/10.1016/j.conbuildmat.2010.01.008
44. Morel JC, Pkla A, Walker P (2007) Compressive strength testing of compressed earth blocks. Constr Build Mater 21:303–309. https://doi.org/10.1016/j.conbuildmat.2005.08.021
45. Elert K, Sebastián E, Valverde I, Rodriguez-navarro C (2008) Alkaline treatment of clay minerals from the Alhambra Formation : Implications for the conservation of earthen architecture. 39:122–132. https://doi.org/10.1016/j.clay.2007.05.003
46. Cristelo N, Glendinning S, Fernandes L, Pinto AT (2012) Effect of calcium content on soil stabilisation with alkaline activation. Constr Build Mater 29:167–174. https://doi.org/10.1016/j.conbuildmat.2011.10.049
47. Kuwahara Y (2006) In-situ AFM study of smectite dissolution under alkaline conditions at room temperature. Am Mineral 91:1142–1149. https://doi.org/10.2138/am.2006.2078
48. Heah CY, Kamarudin H, Mustafa Al Bakri AM, et al. (2012) Study on solids-to-liquid and alkaline activator ratios on kaolin-based geopolymers. Constr Build Mater 35:912–922. https://doi.org/10.1016/j.conbuildmat.2012.04.102
49. Patel MJ, Blackburn S, Wilson DI (2017) Modelling of paste ram extrusion subject to liquid phase migration and wall friction. Chem Eng Sci 172:487–502. https://doi.org/10.1016/j.ces.2017.07.001
50. Criado M, Fernández-Jiménez A, de la Torre AG, et al. (2007) An XRD study of the effect of the SiO2/Na2O ratio on the alkali activation of fly ash. Cem Concr Res 37:671–679. https://doi.org/10.1016/j.cemconres.2007.01.013
51. Bernal SA, Provis JL, Walkley B, et al. (2013) Gel nanostructure in alkali-activated binders based on slag and fly ash, and effects of accelerated carbonation. Cem Concr Res 53:127–144. https://doi.org/10.1016/j.cemconres.2013.06.007

52. Palomo A, Grutzeck MW, Blanco MT (1999) Alkali-activated fly ashes: A cement for the future. Cem Concr Res 29:1323–1329. https://doi.org/https://doi.org/10.1016/S0008-8846(98)00243-9
53. Mascia S, Patel MJ, Rough SL, et al. (2006) Liquid phase migration in the extrusion and squeezing of microcrystalline cellulose pastes. Eur J Pharm Sci 29:22–34. https://doi.org/10.1016/j.ejps.2006.04.011
54. Rees CA, Provis JL, Lukey GC, van Deventer JSJ (2008) The mechanism of geopolymer gel formation investigated through seeded nucleation. Colloids Surfaces A Physicochem Eng Asp 318:97–105. https://doi.org/10.1016/j.colsurfa.2007.12.019
55. Heah CY, Kamarudin H, Mustafa Al Bakri AM, et al. (2011) Effect of curing profile on kaolin-based geopolymers. Phys Procedia 22:305–311. https://doi.org/10.1016/j.phpro.2011.11.048
56. Temuujin J, van Riessen A, Williams R (2009) Influence of calcium compounds on the mechanical properties of fly ash geopolymer pastes. J Hazard Mater 167:82–88. https://doi.org/https://doi.org/10.1016/j.jhazmat.2008.12.121
57. Pacheco-Torgal F, Castro-Gomes J, Jalali S (2009) Tungsten mine waste geopolymeric binder: Preliminary hydration products investigations. Constr Build Mater 23:200–209. https://doi.org/10.1016/j.conbuildmat.2008.01.003
58. Pacheco-Torgal F, Castro-Gomes JP, Jalali S (2008) Investigations of tungsten mine waste geopolymeric binder: Strength and microstructure. Constr Build Mater 22:2212–2219. https://doi.org/10.1016/j.conbuildmat.2007.08.003
59. Pacheco-Torgal F, Abdollahnejad Z, Camões AF, et al. (2012) Durability of alkali-activated binders: A clear advantage over Portland cement or an unproven issue? Constr Build Mater 30:400–405. https://doi.org/10.1016/j.conbuildmat.2011.12.017
60. Prud'homme E, Autef A, Essaidi N, et al. (2013) Defining existence domains in geopolymers through their physicochemical properties. Appl Clay Sci 73:26–34. https://doi.org/https://doi.org/10.1016/j.clay.2012.10.013
61. Li N, Shi C, Wang Q, et al. (2017) Composition design and performance of alkali-activated cements. Mater Struct Constr 50:1–11. https://doi.org/10.1617/s11527-017-1048-0
62. Sore SO, Messan A, Prud'homme E, et al. (2016) Synthesis and characterization of geopolymer binders based on local materials from Burkina Faso ??? Metakaolin and rice husk ash. Constr Build Mater 124:301–311. https://doi.org/10.1016/j.conbuildmat.2016.07.102
63. Marsh A, Heath A, Patureau P, et al. (2018) Alkali activation behaviour of un-calcined montmorillonite and illite clay minerals. Appl Clay Sci 166:250–261. https://doi.org/https://doi.org/10.1016/j.clay.2018.09.011
64. Frischknecht R, Jungbluth N, Althaus H-J, et al. (2005) The ecoinvent Database: Overview and Methodological Framework (7 pp). Int J Life Cycle Assess 10:3–9. https://doi.org/10.1065/lca2004.10.181.1
65. Maskell D, Heath A, Walker P (2014) Comparing the Environmental Impact of Stabilisers for Unfired Earth Construction. Key Eng Mater 600:132–143. https://doi.org/10.2966/scrip.
66. Manjunatha LR, Anvekar SR, Sagari SS, Archana K (2014) An Economic and Embodied Energy Comparison of Geo- polymer , Blended Cement and Traditional Concretes. 2:63–69

4.0 Chapter 4: Rheological Characterisation of Fibre Reinforced Alkali Activated Earth-based Composites

This chapter studies the effects of different fibre reinforcements and volume composition on rheological properties. Inclusion of varying fibres modifies the rheology of the fresh paste in different ways with attendant effect on extrusion pressures, which has implications from a process control point of view.

4.1 Introduction

Compression moulding has largely been the most common processing technique for the production of unfired earth building materials. To improve the performance of earthen composites without losing their advantages and also to enhance manufacturing efficiency, there is a need to investigate alternative and particularly continuous manufacturing processes. Extrusion process is a well-established process in the fired brick industry used for continuous forming of products and has been reported to impart distinct physical and mechanical properties. Studies by Maskell et al.[1] have demonstrated the manufacturing process of fired bricks (excluding the energy intensive firing process) may also be suitable for the production of unfired earthen building units. Furthermore, various studies on fibre-reinforced cementitious products have demonstrated high performance of composites produced using extrusion process [2–4]). Extrusion process involves forcing a highly viscous dough-like plastic/pseudo-plastic mixture through a shaped die. The rheology needs to be controlled to prevent defects such as surface or edge tearing, lamination and voids which reduce performance of the extruded material[2].

Successful development of extruded fibre reinforced composites requires the initial testing to determine rheology and establish compositional dependence on extrusion parameters. The ram rheometer has been reported as a good method to calibrate the rheology of fresh fibre-reinforced cementitious pastes[2,3,6] and fibre reinforced ceramic pastes[7]. However, there is scarce literature on the rheological behaviour of fibre reinforced earth composites. A wide range of natural and synthetic fibres have been used as reinforcements to improve mechanical performance of earthen composites. However, it is not clear how these fibres would modify the rheology of the fresh soil pastes during the extrusion process. An understanding of these modifications is critical for the selection of suitable processing parameters. Extrusion parameters

such as throughput, pressure, force and power requirement are highly dependent on the rheological properties and, hence, the material parameters of the fresh pastes[5].

This current research contributes to this field by an experimental study on the rheology of fibre reinforced earth-based composites to establish the relationship between fibre type/content on processing viz-a-viz extrudability. The results of this work would be useful in selecting appropriate fibre type and content from a process control point of view. Studies like this are encouraged to promote the use of this technology particularly for the development of robust earth-based building materials. Very few studies have paid attention to effect of fibre reinforcements on the overall rheological behaviour of fresh fibre reinforced earth pastes. In this paper, the effects of fibre additions on the rheological behaviour of paste and the relationships between the fibre dosages on extrudate velocity are investigated. This current research contributes to this field by an experimental study on the rheology of fibre reinforced earth composites to characterise the effect of fibre reinforcement type and dosage on the bulk and interfacial rheology in order to establish the relationship between fibre type/content and extrudability. The specific objective of the study was to evaluate the effect of fibre type (sisal, eucalyptus pulp and polypropylene) and fibre dosage (0, 0.25, 1.0 and 2.0 wt.%) on rheological properties of fresh alkali activated earth-based paste using ram extrusion.

4.2 Materials and Methods

4.2.1 Materials

Paste formulations comprised of a three component system; a solid phase split into powder and reinforcement phases as well as a liquid phase. Powder phase comprised of a typical soil used for the production of roof tiles and was supplied Top Telha Ceramic Tile Company, Leme São Paulo State, and sourced from Brazillian quarries. Particle size distribution of the soil (Table 4.1) was determined by mechanical sieving and hydrometer sedimentation in accordance with BS 1377:2. Atterberg limits were also determined in accordance with BS 1377:2 and show liquid limit and plastic limit of soil to be 42.5% and 24.9% respectively.

Table 4:6 Properties of Soil

Characteristics	***%***
Atterberg Limits	
Liquid Limit	42.5
Plastic Limit	24.9
Linear Shrinkage	9.18
Particle Size Distribution	
Sand	35
Silt	33
Clay	32

Effect of three different fibres as reinforcement phases was evaluated in this study;

- Sisal (*Agave sisalana*) fibres are a promising reinforcement and have been used in various composites as a result of its low cost, low density, high specific strength and ready availability [8]. Sisal fibres used in this study were extracted from the waste of baler twine cordage and was donated by the Association for the Sustainable Development of the Sisal Producing Region, Valente, Bahia State, Brazil. Microscopic morphological characterization was performed and range of diameter was determined.
- Eucalyptus pulp fibre was chosen because it is inexpensive, abundantly available and free of lignin. Studies have demonstrated the benefits of eucalyptus pulps as reinforcement of cementitious materials [9,10]. Unbleached Eucalyptus cellulosic pulp produced in Sao Paulo Brazil was used in this study.
- Polypropylene fibre is the most widely used synthetic fibre used as reinforcement for soil [11] and was selected for the basis of comparison. Polypropylene fibre produced by Saint-Gobain, Brazil was used in this study. These fibres are monofilaments with circular section and their surfaces are very smooth.

Table 4.2 presents a summary of properties of fibres expressed as average values ± standard deviation. Based on dimensions, sisal and pulp possess similar aspect ratios whilst polypropylene has an aspect ratio which is an order of magnitude higher than the ligno-cellulosic fibres. Density of the fibres was obtained using a Quantachrome Instruments Multipycnometer. Using these dimensions, the number of reinforcing filaments in a unitary volume (1 cm^3) of fibre content was computed and is presented in Table 4.2.

Table 4:7 Properties of Fibres

Characteristic	Fibre Type		
	Sisal	Eucalyptus Pulp	Polypropylene
Average Fibre length (mm)	10 ± 0.3	0.7 ± 0.01	10 ± 0.01
Equivalent Diameter (μm)	190 ± 55	12 ± 0.1	12 ± 0.01
Density (g/cm^3)	1.420 ± 0.003	1.62 ± 0.02	0.91 ± 0.002
Aspect ratio	52	58	833
No of filaments in 1 cm^3	3.5E+03	1.3E+07	4.4E+05

Binding mechanism adopted in this study was via alkali activation of natural aluminosilicates present within the soil. As a result, liquid phase composition comprised of alkali activator solutions only. Typically, processing aids are used to control the rheology of the fresh ceramic pastes. In this study, the feasibility of using alkali activator solutions only as liquid phase was evaluated in a bid to minimise processing costs. Alkaline activator used in this study was a solution of sodium hydroxide and sodium silicate. NaOH pellets with 97% purity and sodium silicate powder was used and both chemicals were supplied by Dinâmica Química Contemporânea Ltd, Brazil. The mass ratio of sodium hydroxide/soil and sodium silicate/soil was 3% and 0.75%, respectively.

4.2.2 Paste preparation

The paste was obtained by mixing alkali activator solution with the soil in a mass ratio (i.e soil moisture content) of 25% which corresponds to the plastic limit of the soil. This was selected based on findings from Maskell et al.[1] where extrusion of soil pastes was more effective if soil was in a plastic state. In the preparation sequence, soil and fibre were mixed in the dry state using a Hobart planetary mixer at low speed for 5 mins. The soil-fibre mixture was homogenised with the alkali activator solution at a higher speed to provide enough shear to break down agglomerates generated during the wet-mixing stage in accordance with procedures in Teixeira et al. [3].

4.2.3 Ram Extruder

In this study, ram extrusion was adopted based on similar rheology studies on fibre reinforced cementitious pastes [2–4,6] and ceramic pastes [7,12]. This approach has been adopted because it

yields information on the die entry as well as the parallel flow region of the extrusion system, and is thus preferred for these studies.

The set-up of ram extruder is shown in Figure 4.1.

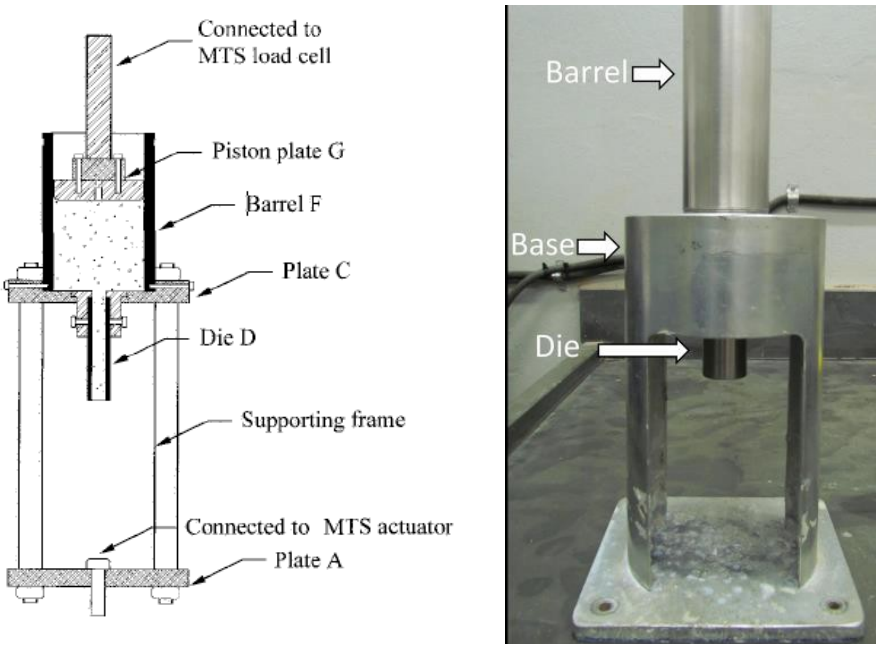

Figure 4:21Schematic representation and set-up of Ram Extruder

The extrusion of ceramic pastes can be mathematically described using the Benbow-Bridgwater model which describes extrusion pressures as a function of flow properties of the material, extrusion rate and geometrical details of the extruder[12,13]. The paste flows from a barrel with a larger diameter D_o into a die land with a smaller diameter D and a length L with a mean die land extrudate velocity V under the driving piston. By assuming plastic deformation in the die entry and plug flow in the die land and neglecting pressure drop at the die exit, the model predicts the total extrusion pressure as the summation of die entry pressure drop (P_{ent}) and die land pressure drop (P_{land}). P_{ent} describes the work done to deform the paste in the die entry region and die land pressure drop (P_{land}) which accounts for the work to overcome the friction (simple shear) in the die land. The model describes convergent flow to be governed by a yield mechanism whilst the plug flow in the die land by wall resistance.

Based on these mechanisms, extrusion pressure is given as

$$P = P_{ent} + P_{land} = 2\ln\left(\frac{D_o}{D}\right)\left(\sigma_0 + \alpha V^m\right) + \frac{4L}{D}\left(\tau_0 + \beta V^n\right) \quad \text{(i)}$$

where P is the extrusion pressure, α is a velocity-dependent factor at the die entry, β is the velocity-dependent factor at the die land, σ_0 is the paste bulk yield value, τ_0 is the characteristic initial wall shear stress of the paste, D_0 and D are the diameters of the barrel and of the die, respectively, L is the die-land length and V is the extrudate velocity with *m* and *n* as extrudate velocity exponents. In this study, the exponents *m* and *n* are taken as 1 i.e., the extrusion pressure-velocity relationship is taken as linear, which was confirmed in the study and thus the equation is reduced to a simple four-parameter model.

$$P = P_{ent} + P_{land} = 2\ln\left(\frac{D_o}{D}\right)\left(\sigma_0 + \alpha V\right) + \frac{4L}{D}\left(\tau_0 + \beta V\right) \quad \text{(ii)}$$

The extrusion was performed using a specially constructed ram extruder fitted to a 50kN load cell on a material testing system, EMIC 30000. Ram extruder comprised of rigid barrel with inner diameter of 38.1 mm and capillary dies of diameter 12.7 mm and varying lengths. Lumps of pastes were placed in the barrel and tamped down several time with a metal rod to remove large air bubbles. A barrel with a large amount of paste enables performing several tests for a fixed die length but different extrudate velocities within one operation thus enhancing the accuracy and consistency of experimental data[12]. Extrusion pressures were measured for dies of different lengths (12.7mm, 50.8mm & 101.6mm) corresponding to length to diameter ratios (L/D) of 1, 4 and 8. For each test, the extrusion pressures was recorded as function of time and ram displacement at a series of ram velocities of 0.05mm/s, 0.08mm/s, 1.2mm/s and 1.8mm/s corresponding to extrudate velocities of 5.9 mm/s, 8.9 mm/13.3 mm/s and 20mm/s respectively for each die land length. For each speed, the average pressure was taken and the data was plotted against L/D.

4.3 Results

4.3.1 Paste Extrusion pressures

Figure 4.2 presents plots of extrusion profiles showing the evolution of extrusion pressure with ram displacement at maximum fibre content (2 wt.%) for the various die land lengths. The initial stage of the extrusion profile of the plain soil paste shows an approximately linear increase in pressure with ram displacement as the piston enters and fills the die region. The pressure reaches maximum when steady state is achieved and corresponds to the emergence of extrudate from the die exit. Subsequently, pressure then decreases gradually as the paste-wall interfacial contact area in the barrel decreases. The quasi-stable nature of extrusion profiles following emergence of extrudate confirms homogeneous distribution of liquid phase and the absence of liquid phase migration (L.P.M). With fibre inclusion, there is an observed deviation from the initial linear profile attributed to an initial consolidation of fibre-soil paste before the onset of flow in the die land.

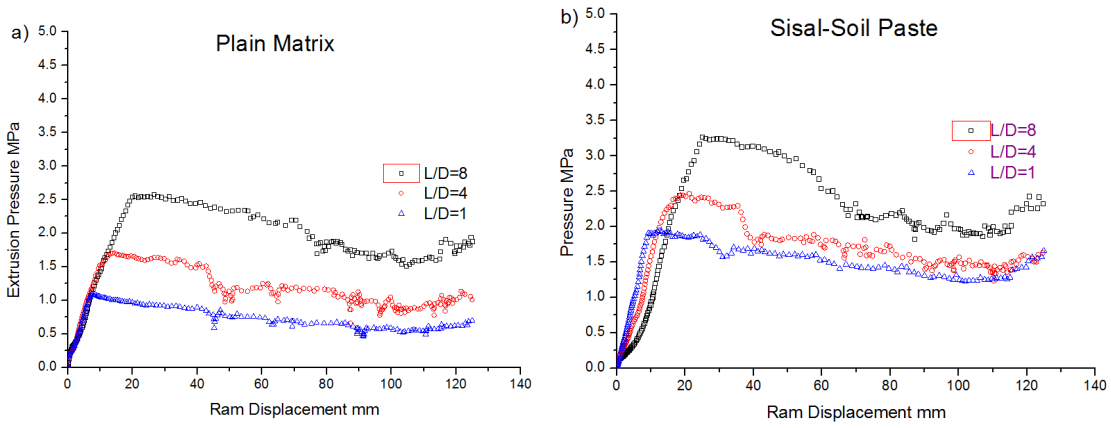

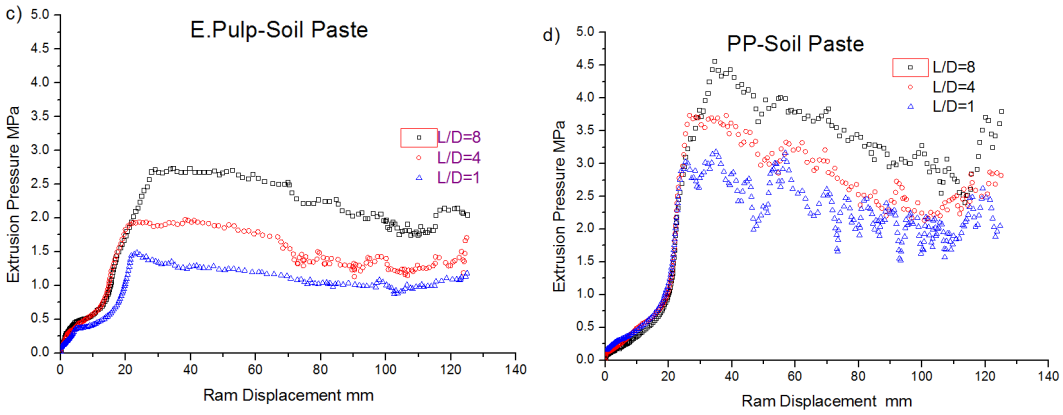

Figure 4:22 Extrusion pressures as a function of ram displacement for different pastes (a) plain soil (b) sisal-soil paste (c) E.pulp-soil paste (d) polypropylene-soil paste

The extrusion pressure gives an indication of the stiffness of semi-solid pastes as a higher pressure is required to extrude a stiffer paste. The addition of high aspect ratio polypropylene fibres (*l/d = 833*) results in thickening of the paste over and above that brought about by the addition of a similar dosage of sisal and pulp fibres with lower aspect ratios (*l/d ≈ 55*). Consequently, incorporation of polypropylene fibres results in about 80% increase in extrusion pressure over the plain soil paste whereas eucalyptus pulp or sisal increases the extrusion pressure by 10% and 30% respectively. Pressure generally increases with the degree that the particles deviate from spherical shapes [7]. In addition, significant fluctuation observed with extrusion profiles for polypropylene-soil pastes give an indication of the stability of paste flow during extrusion. These pressure fluctuations are associated with local paste inhomogeneities [14].

The profiles indicate that at equivalent fibre contents, polypropylene fibres make the paste stiffer whereas pulp makes the paste softer and by comparison easier to extrude. From a manufacturing cost point of view, these observations indicate that short sisal and pulp fibres are best suited for extruded soil-fibre pastes as they do not significantly alter extrusion pressures of plain soil pastes and fibre content can be varied over a considerable range without unduly affecting pastes extrusion behaviour. Extrusion pressures are in good agreement with results associated with common ceramic pastes[12,15]. Formulations containing polypropylene may require further

optimisation with rheology modifiers and super-plasticisers to lower extrusion pressures and minimise wear/abrasion of the extruder and accessories.

(a) (b) (c)

Figure 4:23 Extruded samples: a) sisal-soil b) E.pulp-soil and c) polypropylene-soil

4.3.2 Prediction of Extrusion Pressures

The four-parameter Benbow-Bridgwater model was used to predict the relationship between pressure and extrudate velocity for various fibre dosages. Changes of total extrusion pressures for pastes with various fibre contents as a function of extrudate velocity are shown in Fig. 4.4. The plots show an overall satisfactory agreement between measured and predicted extrusion pressures for all pastes. Relationship between pressure and extrudate velocity is satisfactorily linear at low extrudate velocities. At higher extrudate velocities, (>13 mm/s), relationship begins to deviate from linearity indicating that the 4-parameter model is only valid at low extrusion velocities. However, these low extrusion speeds correspond to typical extrusion speeds used in practice confirming that the 4-parameter model provides a good description of rheological

behaviour of fibre reinforced soil pastes for extruded earth-based building products.

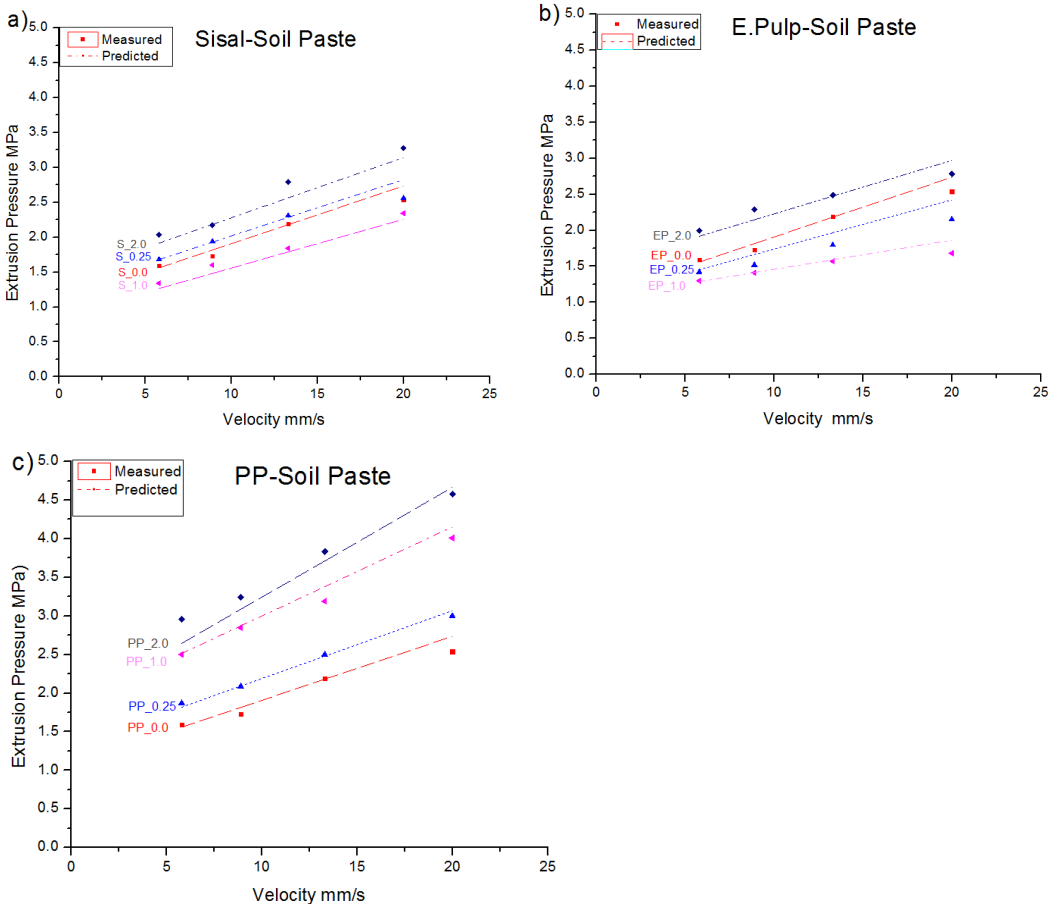

Figure 4:24 Variation of total extrusion pressures for pastes with various fibre contents as function of extrudate velocity (L/D=8)

4.3.3 Effect of fibre type

Figure 4.5 presents contribution of pressure drop in the die entry and die land to the overall extrusion pressures as a function of fibre volume fraction at different extrusion velocities. Introduction of fibres into the fresh paste resulted in two inverse effects: increase in the die entry pressure drop with a corresponding decrease in the die land pressure drop. This counteracting effect can be explained by (i) increased fibre-matrix interaction in the barrel with fibre addition

which increased paste viscosity resulting in higher pressure drop in the die entry region (ii) decreased wall slip as a result of the presence of longitudinally oriented fibres along the wall bulk extrudate interface in the die land with attendant reduction in the die land wall resistance[4,16]. For pastes with sisal and pulp, the reduction in die land shear strength was more significant below 1 wt.%. As the fibre content increases, these two effects counteract each other as the increased viscosity of the paste reduces the effect on wall slip in the die land

When comparing effect of different fibres, it can be seen that an incorporation of polypropylene fibres to the fresh paste leads to a higher drop in the die entry pressure relative to the ligno-cellulosic counterparts. Ductile polypropylene fibres easily tangles making it difficult to be aligned resulting in a greater die entry pressure, while stiffer sisal fibres tend to be aligned during extrusion process which reduces extrusion pressure. On the other hand, pulp slightly modified viscosity due to dimensional similarity with soil particles. Shorter length of fibres would also require less work to make them flow into the die land from the barrel. Due to higher viscosity imparted by polypropylene fibres, effect of fibres on wall slip in the die land is not as significant as ligno-cellulosic counterparts. This indicates that polypropylene fibres affect the bulk rheological properties in the die entry to a greater extent than the interface rheological properties in the die land. Sisal fibres on the other hand, resulted in the highest reduction in die land pressure drop indicating that sisal fibres modified the interface rheological properties in the die land compared to the other fibres. With pulp fibres, approximately equivalent and opposite effects in the die entry and die land pressures counteract each other and explains low extrusion pressures associated with pulp-soil pastes. With polypropylene-soil pastes, die entry pressure drop demonstrated the highest sensitivity to variation in extrudate velocity relative to sisal and pulp fibre pastes. This suggests that a higher degree of process control during extrusion is required with polypropylene-soil pastes as changes in fibre content are more likely to significantly affect extrusion pressures.

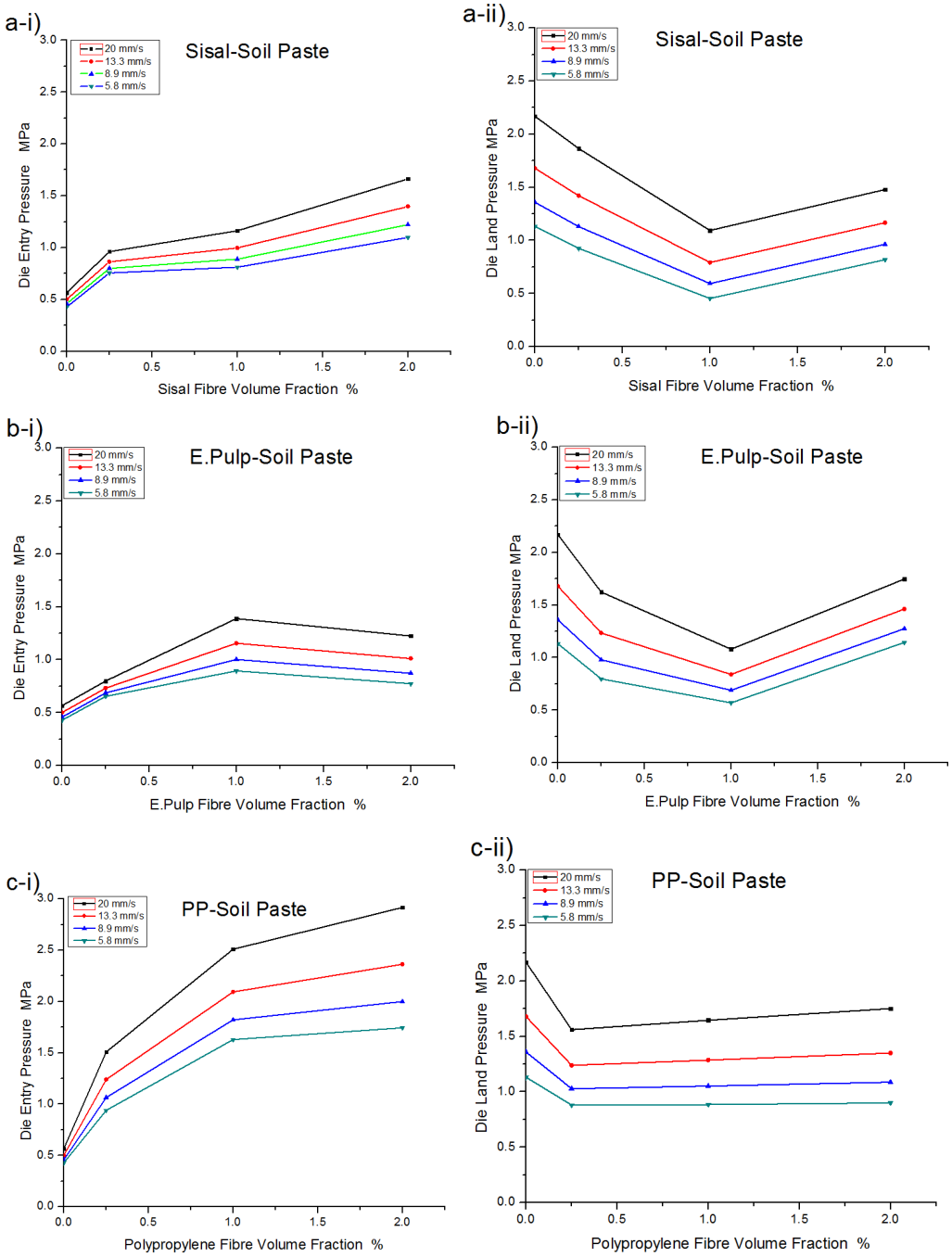

Figure 4:25 Effects of fibre types and velocity on die entry pressure (i) and die land pressures (ii) for different fibres: (a) sisal (b) E.Pulp (c) Polypropylene

4.3.4 Effect of fibre dosages

In the die entry, incorporation of fibres increases the paste viscosity as particles became more close-packed and composite became stiffer with increasing fibre content. Pastes tended to get stiffer with more fibre incorporation as a result of increased fibre interactions between fibres, which formed a larger network structure and increased work to align fibre as they approached die entry[2]. The greater the aspect ratio, the greater the increase in apparent viscosity attributed to fibre-fibre interactions[7]. Consequently, extrusion of polypropylene fibre pastes showed a higher sensitivity to variation in fibre content in the die entry. Pulp and sisal with similar aspect ratios showed approximately similar sensitivity to variation in fibre content. With increase in polypropylene, higher viscosity of paste plus wall slip due to fibre alignment counteracted each other to a certain extent resulting in almost constant die land pressure drop with increase in fibre content.

Incorporation of sisal and pulp fibres gradually increased die entry pressure as a result of increased fibre-matrix interactions but reduced die land pressure due to increased wall-slip. As more fibres were included, the wall slip effect due to fibre alignment increased remarkably which even exceeded the viscosity increasing effect due to fibre matrix interactions up to 1 wt.%. However, further increase in fibre content significantly increased the viscosity due to increase of fibre-matrix interactions, which exceeded viscosity decreasing effect caused by wall slip; increasing the die land wall pressure drop. Increase of viscosity is less significant compared to increase in wall slip attributed to alignment of fibres. Consequently, variation of die land pressure drop showed a higher sensitivity to fibre content. At higher speeds, pressure drop in the die land is higher for all fibre types. Evolution of extrusion pressures of Sisal and E.pulp soil pastes show approximately equivalent trends and may attributed to aspect ratio of fibres. Increased wall slip associated with fibres indicates inclusion of fibres would be beneficial in minimising wear/abrasion of the extruder and accessories.

4.3.5 Benbow-Bridgwater rheology parameters

The rheology parameters derived from the Benbow-Bridgwater model are presented in Table 4.3. It can be seen that static bulk yield stress, σ_0 increased from 169 kPa in the plain soil paste to 395 kPa with sisal fibres, to 268 kPa with pulp fibres and 575 kPa with polypropylene fibres at 2 wt.

%. Increasing the fibre dosage largely enhanced the bulk yield stress. These changes correlate directly with die entry pressures and are thought to be the main reason for trends observed. On the other hand, change in die wall shear stress was not as significant with the incorporation of fibres. Static wall shear stress, τ_0 which is generally considered as the shear yield strength of the thin lubricating layer between the paste and die land wall was significantly low compared to the static bulk yield stress, σ_0. This suggests that extrusion pressures would largely be governed by pressure drop in the die entry and therefore significantly affected by fibre-matrix interactions relative to wall slip. The static wall shear stress decreased with fibre inclusion indicating that fibres introduced significant wall slip. Higher wall slip associated with sisal fibres indicates that larger dimensions of sisal fibres favoured liquid phase migrations through the pores within the solid particles.

The α-value which characterizes the effect of velocities on the paste bulk yield strength describes the dependence of the flow resistance to extrudate velocities in die entry. The wall velocity factor, β represents the dynamic behaviour of the shear stress and shows the velocity dependent properties of the fresh pastes. A higher α and β value indicates an increase in flow resistance to a given increment in extrusion velocities. Higher α values compared to β suggests that convergent flow is the main contributor to pressure drop for all fibre reinforcements. As observed,

Table 4:8Rheological parameters of pastes with different fibres/dosages

		σ_0 kPa	α kPa.s.mm^{-1}	τ_0 kPa	β kPa.s.mm^{-1}
Sisal	0	169	4.42	22	2.28
	0.25	305	6.62	17	2.07
	1	304	11.23	6	1.41
	2	395	18.11	17	1.45
EP	0	169	4.42	22	2.28
	0.25	271	4.64	14	1.82
	1	315	15.87	11	1.10
	2	268	14.47	28	1.33
Polypropylene	0	169	4.42	22	2.28
	0.25	322	18.24	19	1.50
	1	577	28.21	18	1.67
	2	575	37.59	17	1.87

4.4 Conclusion

Rheology has been analysed for a range of soil pastes comprising an alkali activated fresh paste containing different fibres and dosages. This has enabled the effects of fibre addition on the bulk and interfacial rheology behaviour of

earth-based composites to be studied using ram extrusion. Based on this study, the following conclusions can be drawn:

- The Benbow-Bridgwater model has been satisfactorily used to characterise the contribution of parallel and convergent fluxes associated with the incorporation of different fibre reinforcements in an alkali activated earth paste.

- Fresh alkali activated earth-based composites showed Bingham plastic behaviour at low extrusion rates and demonstrated satisfactory extrudability without the need for rheology modifiers.

- Introduction of fibres into the fresh paste resulted in two counteracting effects on the extrusion pressures: increase in die entry pressures due to fibre-matrix interaction in the barrel which increased paste viscosity; and reduction in die land wall resistance due decreased wall slip as a result of the presence of longitudinally oriented fibres along the wall-extrudate interface. However, rheological parameters show that convergent flow in the die entry region is the dominant contributor to extrusion pressures for all fibres studied.

- Fresh pastes incorporating polypropylene fibres showed both greater die entry and die land pressure than that reinforced with sisal fibres of the same fibre length and dosage due to difference in aspect ratio and stiffness. In addition, convergent flows were strongly dependent on fibre content and extrusion velocities. Consequently, polypropylene-soil pastes recorded the highest extrusion pressures at 80% increase relative to the plain soil paste.

- Addition of E.Pulp fibres caused a slight variation in rheological response indicating that rheological behaviour of soil pastes dominates and fibre content can be varied over a considerable range without unduly affecting pastes extrusion behaviour.

- The results of this study have demonstrated the relationship between fibre loading and resultant rheology of fresh alkali activated earth-based pastes. The ram extruder can.

This can be useful in the tailoring of paste formulation for extrusion purposes as well as a tool to aid the design of suitable processing equipment.

References

[1] D. Maskell, A. Heath, P. Walker, Laboratory scale testing of extruded earth masonry units, Mater. Des. 45 (2013) 359–364. doi:10.1016/j.matdes.2012.09.008.

[2] S. Srinivasan, D. Deford, P.S. Shah, The use of extrusion rheometry in the development of extrudate fibre-reinforced cement composites, Concr. Sci. Eng. 1 (1999) 26–36.

[3] R.S. Teixeira, S.F. Santos, A.L. Christoforo, H. Savastano, F.A.R. Lahr, Extrudability of cement-based composites reinforced with curauá (Ananas erectifolius) or polypropylene fibers, Constr. Build. Mater. 205 (2019) 97–110. doi:https://doi.org/10.1016/j.conbuildmat.2019.02.010.

[4] X. Zhou, Z. Li, Characterization of rheology of fresh fiber reinforced cementitious composites through ram extrusion, Mater. Struct. Constr. 38 (2005) 17–24. doi:10.1617/14064.

[5] F. Laenger, Rheology of Ceramic Bodies BT - Extrusion in Ceramics, in: F. Händle (Ed.), Springer Berlin Heidelberg, Berlin, Heidelberg, 2007: pp. 141–159. doi:10.1007/978-3-540-27102-4_7.

[6] K.G. Kuder, S.P. Shah, Processing of high-performance fiber-reinforced cement-based composites, Constr. Build. Mater. 24 (2010) 181–186. doi:10.1016/j.conbuildmat.2007.06.018.

[7] S. Blackburn, H. Böhm, The influence of powder packing on the rheology of fibre-loaded pastes, J. Mater. Sci. 29 (1994) 4157–4166. doi:10.1007/BF00414194.

[8] Y. Li, Y.-W. Mai, L. Ye, Sisal fibre and its composites: a review of recent developments, Compos. Sci. Technol. 60 (2000) 2037–2055. doi:10.1016/S0266-3538(00)00101-9.

[9] H. Savastano, S.F. Santos, M. Radonjic, W.O. Soboyejo, Fracture and fatigue of natural fiber-reinforced cementitious composites, Cem. Concr. Compos. 31 (2009) 232–243. doi:10.1016/j.cemconcomp.2009.02.006.

[10] J.E.M. Ballesteros, S.F. Santos, G. Mármol, H. Savastano, J. Fiorelli, Evaluation of cellulosic pulps treated by hornification as reinforcement of cementitious composites, Constr. Build. Mater. 100 (2015) 83–90. doi:10.1016/j.conbuildmat.2015.09.044.

[11] S.M. Hejazi, M. Sheikhzadeh, S.M. Abtahi, A. Zadhoush, A simple review of soil reinforcement by using natural and synthetic fibers, Constr. Build. Mater. 30 (2012) 100–116. doi:10.1016/j.conbuildmat.2011.11.045.

[12] J.J. Benbow, E.W. Oxley, J. Bridgwater, The extrusion mechanics of pastes—the influence of paste formulation on extrusion parameters, Chem. Eng. Sci. 42 (1987) 2151–2162. doi:https://doi.org/10.1016/0009-2509(87)85036-4.

[13] S. Blackburn, T.A. Lawson, Mullite—Alumina Composites by Extrusion, J. Am. Ceram. Soc. 75 (1992) 953–957. doi:10.1111/j.1151-2916.1992.tb04165.x.

[14] S.L. Rough, D.I. Wilson, J. Bridgwater, A model describing liquid phase migration within an extruding microcrystalline cellulose paste, Chem. Eng. Res. Des. 80 (2002) 701–714. doi:10.1205/026387602320776786.

[15] R. Nath Das, C.D. Madhusoodana, K. Okada, Rheological studies on cordierite honeycomb extrusion, J. Eur. Ceram. Soc. 22 (2002) 2893–2900. doi:10.1016/S0955-

2219(02)00045-6.
[16] K.C.M. Nair, R.P. Kumar, S. Thomas, S.C. Schit, K. Ramamurthy, Rheological behavior of short sisal fiber-reinforced polystyrene composites, Compos. Part A Appl. Sci. Manuf. 31 (2000) 1231–1240. doi:https://doi.org/10.1016/S1359-835X(00)00083-X.

5.0 Chapter Five: Characterisation of Properties of Fibre Reinforced Alkali Activated Earth-based Composites

This chapter focuses on the composition-property relationship of extruded earth-based building products reinforced with different fibres at varying proportions to evaluate the compositional dependence of alkali activated earth-based composites as robust building materials.

5.1 Introduction

During the past four decades, there has been increasing focus on research into Nonconventional Materials and Technologies (NOCMATs) such as lingo-cellulosic fibres, as well as composites reinforced with these fibres, for a wide range of building construction purposes[1]. These studies have been motivated by the high specific strength of ligno-cellulosic fibres and their ready availability particularly in developing countries for the development of low-cost eco-friendly construction materials.[2] Also, the use of traditional earth-based building materials for construction has resurged over the last decades as a result of its availability, good thermal and acoustic properties and lower cost compared to conventional building materials. Historically, ligno-cellulosic fibres have been used to enhance the properties of earthen construction to minimize shrinkage characteristics as well as improved flexural strength/toughness. It is well documented that the presence of ligno-cellulosic fibres in soil matrix enhances ductility of the composite depending on the matrix and the properties of fibre reinforcements [3,4] . Tang et al. [5] results show that inclusion of fibre reinforcement within cemented and uncemented clayey soils improved mechanical properties as well as transformed brittle behavior to ductile behavior. This improvement in ductility was attributed to crack bridging mechanisms. Bouhicha et al. [6] demonstrated improvements in compressive strength and shrinkage characteristics of straw reinforced earth composites. Mustapha et al. [7] demonstrated improved compressive, flexural strengths and fracture toughness with the inclusion of straw in earthen building materials.

Despite the improvement in ductility of fibre reinforced earth-based composites, poor resistance to abrasion, weathering and water erosion of earth, has necessitated the need for the inclusion of binders to improve durability and mechanical performance of earthen construction. Cement has been the most utilized binder but current research focus is now being geared towards the development of alternative binders. Alkali activation of natural clay minerals present in earth can be an alternative mechanism for the stabilization of earth for

building construction purposes. Alkali activation refers to the reaction of solid aluminosilicates under alkaline conditions to produce a hardened binder which is based on a combination of hydrous alkali-aluminosilicate and/or alkali-alkali earth-aluminosilicate phases[8]. Clay minerals are aluminosilicates being composed primarily of alumina and silica. Based on the theory of alkali activation, this mechanism may be adopted for the development of in situ binders by the reaction between clay minerals present in the soil and an alkaline solution which can be harnessed in the development of earth-based construction materials. However, despite this potential, there is scarce literature on the use of alkali activation as binding mechanism in earthen construction.

Most of the studies reported in literature focus on fibre reinforced earthen matrices stabilized with cement and scarce studies have elucidated the effect of alkali-activated matrices on ligno-cellulosic fibres in strength development. The mechanical properties of fiber-reinforced composites depend on the fiber-matrix interface, since the strength of such a composite is obtained by transferring the stress between the fibers and the matrix. [9]For this reason, the interaction of fibres and the alkali activated matrix is expected to play an important role in the behavior of the composites. However, it is not clear how this alkali activated matrix would react and interphase with vegetable fibres which are typically used for reinforcement in earth building materials. This is further complicated by the fact that alkali activation of some uncalcined clay minerals requires curing at elevated temperatures (up to 250 ˚C) which may influence fibre properties.

Studies on fibre-cement composites have demonstrated deleterious effects of alkaline compounds of the matrix (specifically $Ca(OH)_2$ present in the pores) on the reinforcing effect of ligno-cellulosic fibres [10]. The two main mechanisms responsible for degradation of these fibres within alkaline cement based matrices are: (i) dissolution of lignin and hemicellulose in the middle lamellae due to the adsorption of calcium and hydroxyl ions, and (ii) fibre mineralization caused by migration of hydration products onto fibre surface and fibre lumen [11]. However, it should be noted that the alkalinity within the alkali activated soil is expected to reduce with time as it gets used up in the reaction, compared to cement based matrices where alkalinity is based on a reaction product. Nonetheless, this raise questions as to behavior of ligno-cellulosic fibres used as reinforcements in alkali activated earth-based composites. The knowledge of this behavior will allow for the expanded applications of alkali activation as stabilization mechanisms for soil stabilization in applications where toughness and not necessarily strength are required.

This paper reports the results of an experimental investigation aimed at studying the modification in strength and post-crack behavior induced by the inclusion of reinforcing fibres in an earth-based matrix stabilized using alkali activation. A comparative analysis is presented on the effectiveness of the use of ligno-cellulosic fibres and synthetic fibres as reinforcements. Samples were tested in dry and saturated conditions and subjected to flexural loading to compare mechanical response and evaluate the effect of varying fibre contents. Physical tests were also studied and optimum fibre contents evaluated. Presently, sustainable and affordable housing is a topical issue in the building construction sector. The possibility of the mass production of prefabricated robust panels made of earth and plant based fibres has an immediate potential in meeting increasing housing demands in line with targets set by the Sustainable Development Goals (SDGs) particularly in the developing world.

5.2 Materials and Methods

The experimental program was designed taking into cognizance the objective of the study. The materials and characterization techniques are described.

5.2.1 Characterization of Materials

Soil

Soil used in this study was supplied by Top Telha Ceramic Tile Company in Leme, São Paulo State, Brazil. Table 5.1 presents the summary of geotechnical properties of the soil. Particle size distribution of the soil was determined by mechanical sieving and hydrometer sedimentation in accordance with BS 1377:2. Based on the results, the soil is predominantly silt sized with 68% of particles finer than 75 µm, which is typical for soils used for fired roof tiles or bricks [12]. Atterberg limits was determined in accordance with BS 1377:2. and plot above the A-line of the plasticity chart classifying the soils as clayey soils. These properties do not fit the criteria required for ideal soils for cement stabilisation; suitable soils should be generally coarse grained soils with low clay fractions with Plasticity Index of between 5 and 15% as soils with higher values are characterized by low compressive strengths, inadequate durability and excessive drying shrinkage [13]. The elemental composition of the soil expressed in oxides show Silica and Alumina as the major components of the soil at 70.4% and 13.3% respectively. Given the nature of binding mechanism, it was necessary to determine the mineralogical composition of soil to determine nature of clay minerals present in soil. X-Ray Diffraction (XRD) was performed using a Rigaku MiniFlex 600 with range

10-70° (2θ) at a rate of 0.02°/min and showed mineralogical composition to be predominantly muscovite, with traces of quartz and sanidine.

Table 5:9 Properties of Soil

Characteristics	***%***
Atterberg Limits	
Liquid Limit	42.5
Plastic Limit	24.9
Linear Shrinkage	9.18
Particle Size Distribution	
Sand	35
Silt	33
Clay	32
Mineral Content	
Muscovite	52.5
Quartz	32.7
Orthoclase	12.9
Chemical Composition	
SiO_2	70.39
Al_2O_3	13.31
Fe_2O_3	4.09
K_2O	4.97

Alkali Activator Solution

Alkaline activator used in this study was a solution of sodium hydroxide and sodium silicate. Sodium hydroxide (NaOH) powder used was of caustic soda pellets with 97% purity whilst sodium silicate powder was used and both chemicals were produced by Dinâmica Química Contemporânea Ltd, Brazil. The weight ratio of sodium hydroxide/soil and sodium silicate/soil was 3% and 0.75% respectively. These weight ratios correspond to lower bound molarity of alkali activator solution reported in literature [14] and were selected to ensure that building units had minimal environmental impact.

Fibres

Three fibre types were selected (sisal, Eucalyptus pulp and propylene) to evaluate their reinforcing effect on the alkali activated clay matrix. Optical and Scanning Electron Microscopy (SEM) with backscattered electrons (BSE) detector images of each fibre are illustrated in Figure 5.1.

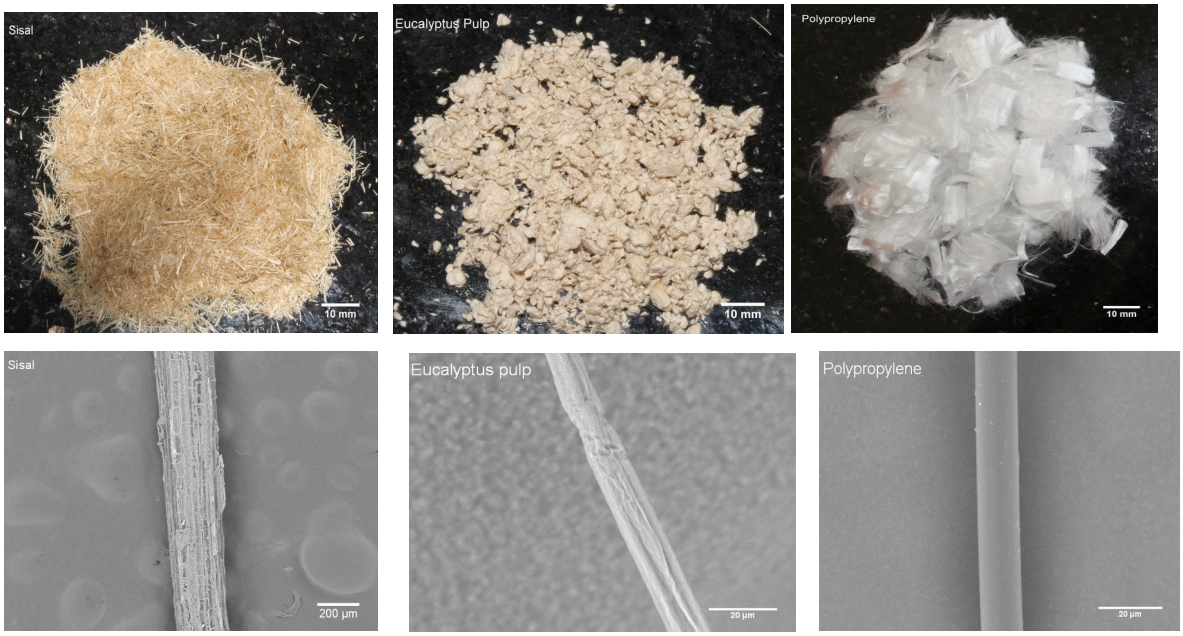

(a) (b) (c)

Figure 5:26 Optical and SEM images of Fibres: (a) Sisal (b) Eucalyptus Pulp and (c) Polypropylene

Sisal (*Agave sisalana*) fibres are a promising reinforcement for use in various composites as a result of its low cost, low density, high specific strength and ready availability [15]. Sisal fibres used in this study were extracted from the waste of baler twine cordage, which was donated by the Association for the Sustainable Development of the Sisal Producing Region, Valente, Bahia State, Brazil. Additional fibre characteristics can be found in previous work [16]. These residual fibres presented a wide range in fibre thickness (100 µm – 250 µm). Fibres were manually cut to average lengths of 10mm. As observed in Fig 5.1a, fibre morphology presents a rough surface with deposits of calcium oxalate [16].

Unbleached hardwood kraft pulp extracted from *Eucalyptus urophylla* was obtained from the paper manufacturing process. Pulping is a delignification process which chemically degrades non-cellulose components of fibres which has been shown to improve their durability in alkaline environment. [17] Studies have demonstrated the benefits of eucalyptus pulps as reinforcement in cementitious materials [18,19] However, literature is scarce on the use of pulp fibres in the reinforcement of earth-based matrices. Unbleached Eucalyptus cellulosic pulp produced in São Paulo, Brazil was used in this study. Additional fibre characteristics can be found in other studies. [20]

Polypropylene fibre is the most widely used synthetic fibre as reinforcement for soil [4] as it as yielded promising results [21]. It possesses good ductility and resistance to alkaline attack

relative to cellulose fibres [17] and was selected in this study for the basis of comparison with the vegetable fibres. Polypropylene fibre produced by Saint-Gobain, Brazil was used in this study. These fibres are monofilaments with approximately circular section with relatively smooth surfaces as presented in Fig 5.1c.

Table 5.2 presents a summary of properties of fibres expressed as average ± standard deviation. Physical attributes of fibres was characterized using optical microscopy. Based on dimensions, sisal and pulp possess similar aspect ratios whilst polypropylene has an aspect ratio which is one order of magnitude higher than the ligno-cellulosic fibres. Density of the fibres was obtained using a Quantachrome Instruments Multipycnometer. Using these dimensions, the number of reinforcing filaments in a unitary volume (1 cm^3) of fibre content was computed and is presented in Table 5.2. As observed, pulp microfibers presented the highest number of filaments for an equivalent volume fraction of fibres. Number of pull-out fibres within a matrix is typically associated with the reinforcing capacity [20]

Table 5:10 Characteristics of Fibres

Characteristic	Fibre Type		
	Sisal	Eucalyptus Pulp	Polypropylene
Average Fibre length (mm)	10 ± 0.3	0.7 ± 0.01	10 ± 0.01
Equivalent Diameter (μm)	190 ± 55	12 ± 0.1	17 ± 0.01
Density (g/cm^3)	1.420 ± 0.003	1.62 ± 0.02	0.91 ± 0.002
Aspect ratio	52	58	588
No of filaments in 1 cm^3	3.5E+03	1.3E+07	4.4E+05

5.2.2 Mixtures and Preparation of specimens

Ten different composites were prepared for this study; a plain unreinforced matrix as well as 9 other composites incorporating 3 volume fractions of fibres (0.5, 1.0 & 2.0 vol.%) for the three different fibres. Unfortunately, high aspect ratio of polypropylene fibres hindered the extrusion of polypropylene reinforced composites at 2% vol. fraction. Table 5.3 presents the material composition for each mix. Given the low number of reinforcing filaments presented by sisal fibres relative to other fibres, fibre contents in this study were set in relation to sisal fibre to maintain equivalent volume reinforcement. Fibre content was computed using soil-fibre mixture only (sum equal to 100%) whilst alkali activation solution was set as a constant percentage relative to dry soil to ensure that soil condition corresponded to plastic state for a workable extrusion.

Table 5:11 Mix Compositions

Composite	Soil (g)	Fibres (g)			Water (g)	Sodium Hydroxide (g)	Sodium Silicate (g)
		Sisal	Eucalyptus Pulp	Polypropylene			
Plain - Matrix	6000	--	--	--	1500	180	45
Sisal-0.5	5970	30	--	--	1493	179	45
Sisal-1.0	5940	60	--	--	1485	178	45
Sisal-2.0	5880	120	--	--	1470	176	44
E.Pulp-0.5	5965	--	35	--	1480	179	45
E.Pulp-1.0	5930	--	70	--	1460	178	44
E.Pulp-2.0	5861	--	139	--	1420	176	44
PP-0.5	5981	--	--	19	1495	179	45
PP-1.0	5963	--	--	37	1491	179	45
PP-2.0	5925	--	--	75	1481	178	44

Alkaline activator solution was produced by dissolving requisite quantities of pellets/powders in deionized water and allowing to cool for 24 h. The paste was obtained by mixing alkali activator solution with the soil in a mass ratio (i.e. soil moisture content) of 25%, which corresponds to the plastic limit of the soil. This was selected based on findings from Maskell et al. [22], where extrusion of soil-based samples was more effective if mixture was in a plastic state. Hence, alkali activator solution for all mixtures was determined as a percent of dry soil only.

In the preparation of unreinforced composites, soil and alkali activator solution were homogenized using a high energy intensive Eirich mixer (capacity 10 L) for 5 min at high speed. Sisal and polypropylene fibre-soil composites were produced by first homogenizing soil and their respective fibres in the dry state for 5 min at high speed before the introduction of the alkali activator solution with additional mixing for 5 min. In the case of the pulp-soil mixture, pulp fibres were dispersed in the alkaline solution using a magnetic stirrer for 10 min before transferring it to the soil and homogenising for 5 min in the mixer. Given the high number of reinforcing filaments in pulp microfibers, adequate dispersion of fibres in liquid is necessary to ensure effective distribution of fibres. In each case, fibres were introduced in varying volume fractions (0, 0.5, 1.0 & 2.0 vol.%). However, as a result of high aspect ratio

of polypropylene fibres relative to the ligno-cellulosic fibres, extrusion of 2.0 vol.% polypropylene was not feasible.

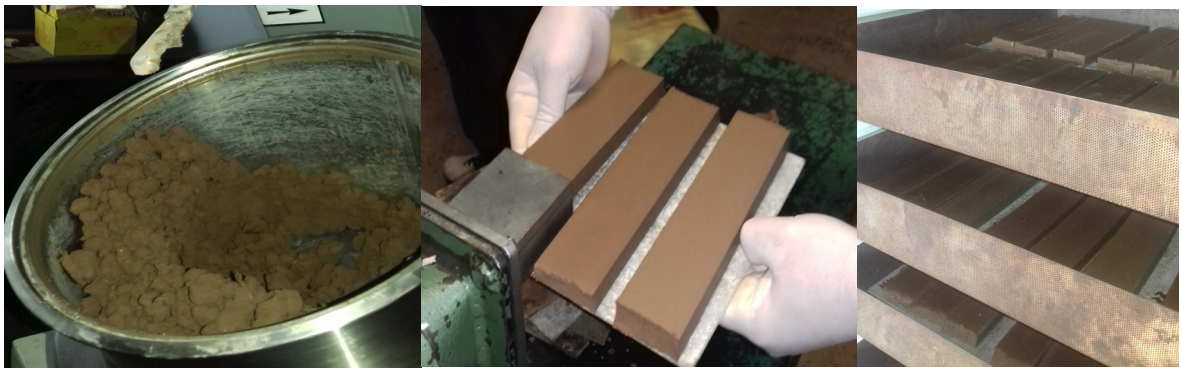

(a) (b) (c)

Figure 5:27 Production process: (a) Mixing (b) Extrusion of specimens (c) Specimen drying in the oven at 105°C

Following homogenization, fibre-soil mixtures were transferred to a laboratory extruder (Gelenski, model MVIG-05) with a cross section die width/height ratio of 3.3 and operating at a linear speed of approximately 4 mm/s. Plates of 200 mm×50 mm×15 mm were produced. Samples were cured initially at elevated temperature of 105°C for 5 h and left in the laboratory at room temperature of (24 ± 2)°C and relative humidity (RH) of 60% and tested after 14 days. The initial cure at 105°C was necessary as studies have shown that elevated temperatures accelerate reaction and significantly improve strength [14]. Also, extended curing at room temperature was conducted as alkali activation of natural clay minerals is time dependent as a result of the low reactivity of the clay minerals [14]. After 14 days curing at room temperature, the samples were subjected to physical and mechanical characterisation including microstructural analysis.

5.3 Characterization of physical and mechanical properties

After curing, a minimum of six samples was subjected to physical tests: apparent density and water absorption were determined according to ASTM C948:

$$Apparent\ Density\left(g/cm^3\right)=\left(\frac{M_{dry}}{M_{sat}-M_i}\right)\times\rho \qquad (1)$$

$$Water\ Absorption\left(\%\right)=\left(\frac{M_{sat}-M_{dry}}{M_{dry}}\right)\times 100 \qquad (2)$$

where M_{sat} is the saturated specimen's mass with a dry surface, M_{dry} is the dry specimen's mass after 24 h at 105ºC, M_i is the specimen's mass immersed in water and ρ is the density of water (1 g/cm^3).

Flexural tests were performed on a minimum of six specimens using a universal testing machine Emic DL-30000 equipped with 5 kN load cell. A four-point bending configuration (Figure 5.3) with outer and inner support spans of 45 mm and 135 mm respectively was adopted, using a displacement control testing procedure at a rate of 1 mm/min. The effect of moisture content on earth-based materials made it necessary to standardize moisture conditions during testing. Composites were tested in dry condition where samples were subjected to 60˚C for 24 h; as well as saturated condition where another set of samples were fully immersed in water for 24 h, prior to testing. Measured mechanical properties were: modulus of rupture (MOR) and specific energy (SE). Mechanical properties were obtained using equations (3) & (4) respectively.

$$MOR = \frac{Fl}{b\,d^2} \quad (3)$$

$$SE = \frac{Energy}{bd} \quad (4)$$

where *F* is the maximum load, *l* is the major span length, *b* and *d* are the sample's respective width and depth, and m is the tangent of the slope angle of the load-deflection plot in the elastic behavior region. SE was defined as the area under the load-deflection curve to the point corresponding to a 90% reduction of the peak load during the flexural test divided by the specimen cross-sectional area.

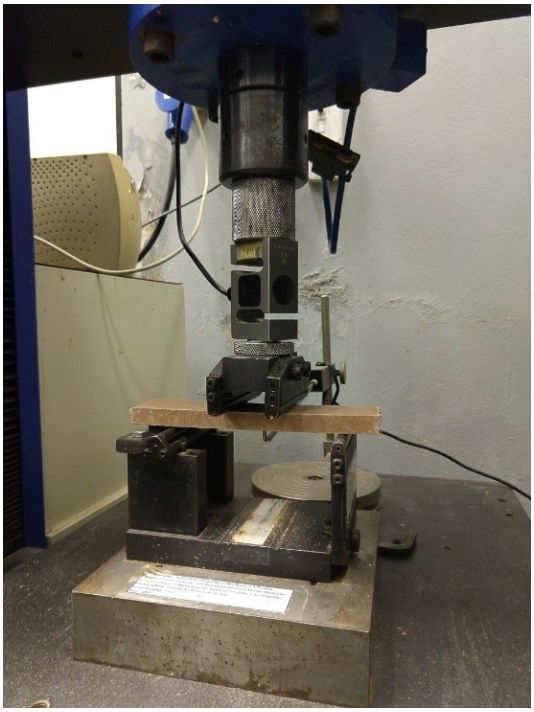

Figure 5:28 Flexural test Set up

5.3.1 Statistical analysis of physical and mechanical properties

To aid in the interpretation of results, statistical analysis was performed using ANOVA analysis in order to ascertain the effect of the reinforcing fibres on the physical and mechanical properties of the composites. One-way ANOVA tests was used to determine if differences existed between population means obtained at varying fibre volumes for a specific fibre reinforcement. The procedure tested the null hypothesis (H_o) that the average results at all fibre dosages are equal (suggesting that the incorporation of fibres had no effect on the performance) against the alternative hypothesis (H_a) that at least one average result was different i.e

$$H_0 : \mu_1 = \mu_2 = \mu_3 = \mu_4$$

$$H_a : At\ least\ one\ mean\ is\ different ¿ the\ others \quad (5)$$

where μ_1, μ_2, μ_3 and μ_4 are population means corresponding to different fibre volume fractions. A significance level of 5% was adopted for this study indicating that if the p-value of a statistical test was less than 0.05, at least one of the population means was statistically different from the others and the null hypothesis (H_o) was rejected. If H_o was rejected, a post-hoc test (Tukey's Honestly Significance Difference (HSD) test) was performed to determine which means were statistically different from each other. This test was performed to ascertain if varying fibre contents had any statistical effect on the performance of the composites.

5.3.2 Microstructural Analysis

Microstructure of the samples was analyzed using a Hitachi Tabletop Microscope TM3000 with a backscattered electron image (BSE) detector, operated at 15 kV accelerating voltage. Sample preparation comprised of impregnation with epoxy resin and manually polishing with a Struers TegraPol-11 machine using silicon carbide abrasive paper with grit sizes 320, 600, 1000 for 6 min. A final polishing was carried out using a diamond polishing compound with 6, 3, 1 µm for 6 min with each size.

5.4 Results and Discussion

5.4.1 Effect of fibre type and content on physical properties

Apparent Density

Density has been mentioned as a significant indicator of strength and durability in earth-based building materials. Figure 5.4 presents average values of density (as bars) and standard deviation (as error bars) of density variation with fibre type and content. Table 5.4 presents results of Tukey HSD comparisons of mean densities obtained for varying fibre and content.

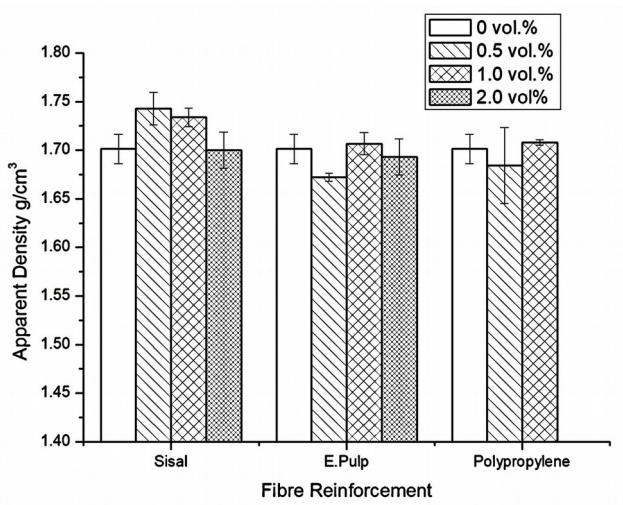

Figure 5:29 Variation of apparent density of composites with different fibre type and content

Table 5:12 Results of Tukey's HSD Comparison of mean densities for different fibre types and contents

Fibre vol.%	**Sisal**			**Eucalyptus pulp**			**Polypropylene**	
	0	*0.5*	*1.0*	*0*	*0.5*	*1.0*	*0*	*0.5*
0	--	--	--	--	--	--	--	--
0.5	1.635E-4*	--	--	0.007*	--	--	0.193	--
1.0	0.002*	0.672	--	0.743	7.789E-4*	--	0.389	0.016*
2.0	0.997	2.485E-4*	0.003*	0.845	0.046*	0.289		

Note: Numbers with asterix indicate statistically significant differences at 0.05 level

There was a significant effect of sisal fibre reinforcements on the density of the composites for the different fibre volume fractions as determined by one way ANOVA [F (3,20) = 15.178 , p = 2.2×10^{-5}]. Post-hoc comparisons using the Tukey HSD indicated that the average density at 0.5 and 1.0 vol.% sisal fibre content was significantly different from the unreinforced matrix whilst density at increased fibre content of 2 vol.% was not statistically different from the unreinforced matrix. Statistically, increasing sisal fibre content from 0.5 vol.% to 1.0 vol.% was not significant on apparent density. However, difference of means of densities obtained at 2.0 vol.% sisal fibre content was statistically significant from lower fibre contents. These results suggest that sisal fibres reinforcements significantly modified the density of the unreinforced matrix leading to more compact composites. The initial increase in density of composites with sisal fibre reinforcements may be attributed to improved packing densities associated with these fibre reinforcements. Similarly, inclusion of pulp fibres had a significant effect on apparent density of the composites as determined by one-way ANOVA [F (3,20) = 8.068, p = 0.001]. Post hoc comparisons show only average density at 0.5 vol.% pulp content was significantly different from the unreinforced matrix and other pulp fibre contents. These results suggest that effect of pulp fibre reinforcements on apparent density of composites was not as significant as their ligno-cellulosic (sisal) counterparts with regards to improved packing density. On the other hand, one way ANOVA analysis on means of densities obtained from polypropylene reinforced composites show that the means at varying fibre contents are significantly different at the 0.05 level [F (2,15) = 5.111 , p = 0.02]. However, the difference of means of densities obtained at 0.5 vol.% and 1.0 vol.% was not statistically different from that of the unreinforced matrix. This suggests that polypropylene reinforcement had no significant effect on the density of the matrix.

Comparison of effect of fibre reinforcements on density indicates that at the highest volume fraction of ligno-cellulosic fibres investigated in this study (2.0 vol.%), densities of composites were equivalent to the unreinforced matrix. Similarly, incorporation of polypropylene (up to 1.0 vol.%) had no significant effect on the apparent density of the composite. This behaviour is not consistent with results which have been reported in literature [23-25]. With soil-fibre mixtures, replacement of soil particles with fibres, which have lower densities, results in a reduction of overall density of composite. The behaviour observed in this study could be explained using moisture-density relationship concept of soils as well as the extrusion technique. Extrusion moulding is a material processing method, which has been reported to produce well-consolidated fibre cement composites with low porosities and fibre matrix bonds [26]. Furthermore, extrusion of fibre-soil mixtures was carried out at plastic limit of plain soil matrix, which corresponds to moisture content at which the soil begins to behave like a plastic material. However, the optimum moisture content of soil, which corresponds to the highest packing density, is typically lower than the plastic limit. This implies that a reduction of moisture content from the plastic limit would bring the soil closer to the optimum moisture content resulting in improved packing density. As observed during sample production, the inclusion of fibres stiffened the matrix and may have placed a water demand on the soil thereby resulting in reduced moisture content and a higher density. The effect is more pronounced in sisal fibre reinforced composites and this may be attributed to high hydrophillicity relative to the other fibres. Studies have reported water absorption values of 200% associated with sisal fibres [27]. Furthermore, variation in the initial moisture content as a result of fibre reinforcements may affect the alkali activation of the clay minerals leading to a variation of alkali activated products in the composites.[28]
Correlation of these results with flexural strength show that these optimum fibre contents for apparent density correspond to optimum fibre content for flexural strengths as presented in the following section. Increase in soil dry density indicates increased contact conditions between soil particles and therefore an increased interfacial contact area between fibre and soil matrix which improves interfacial bond strength (Tang et al., 2016). However, preferred fibre contents should correspond to lighter composite materials. In this regard, 2% vol. fraction of ligno-cellulosic fibre reinforcements with enhanced mechanical properties will have implications in the development of lightweight construction materials.

Water Absorption

Values of average water absorption (presented as bars) and standard deviation (presented as error bars) are presented in figure 5.5. Water absorption characteristic of earth-based materials is significant as it is an indicator of durability of materials [30] given the moisture sensitivity of earth. In earthen-based composites reinforced with vegetable fibres, water absorption in composites may be attributed to the porosity of matrix as well as absorption of water by hydrophilic vegetable fibres. In this study, the high water absorption (20%) observed with the unreinforced matrix suggests the former to be a major contribution. This water absorption value is indicative of high porosity of the matrix and/or presence of unreacted clay minerals after alkali activation. This can be attributed to the low reactivity of the clay minerals as well as low molarity of alkali activator solutions utilized. Table 5.5 presents results of Tukey's HSD Comparison of mean values of water absorption for different fibre types and contents.

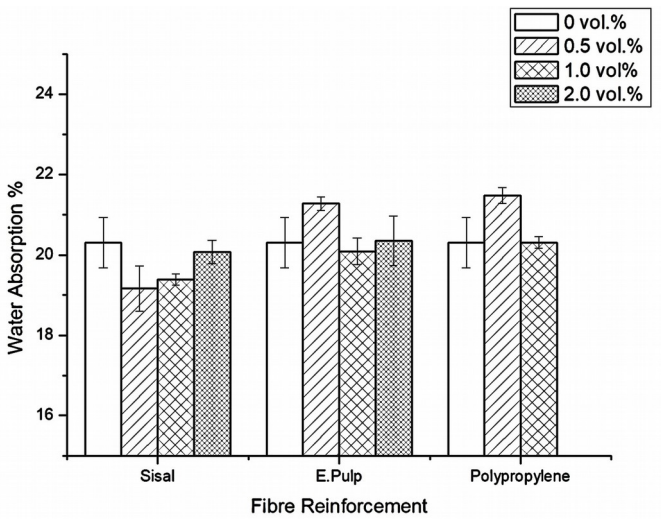

Figure 5:30Variation of water absorption of the composites with different fibre type and

Table 5:13 Results of Tukey's HSD Comparison of mean values of water absorption for different fibre types and contents

Fibre vol.%	**Sisal**			**Eucalyptus pulp**			**Polypropylene**	
	0	*0.5*	*1.0*	*0*	*0.5*	*1.0*	*0*	*0.5*
0	--	--	--	--	--	--	--	--
0.5	3.137E-4*	--	--	0.008*	--	--	0.224	--
1.0	0.004*	0.675	--	0.729	7.307E-4*	--	0.325	0.015*
2.0	0.674	0.004*	0.048*	1.000	0.007*	0.732		

Note: Numbers with asterix indicate statistically significant differences at 0.05 level

There was a statistically significant difference between means of water absorption values obtained with varying sisal fibre reinforcements [$F(3,20) = 11.215$, $p = 1.56\times10^{-4}$]. The results from the Tukey post hoc analysis show that incorporation of sisal fibres at 0.5 vol.% and 1.0 vol.% significantly modified the water absorption of the matrix, whilst water absorption at 2.0 vol.% fibre content was not statistically different from the unreinforced matrix. These results suggest that sisal fibres reinforcements significantly modify the water absorption of the unreinforced matrix and this may be attributed to improved packing densities as observed in the previous section. Similarly, incorporation of eucalyptus pulp reinforcements significantly modified the water absorption characteristics of the composite as determined by one way ANOVA [$F(3,20) = 8.52$, $p = 7.616\times10^{-4}$]. However, results from the post hoc analysis show that only 0.5 vol.% pulp reinforcement significantly modified the matrix and was also statistically different from the means of water absorption obtained at higher fibre reinforcements. With polypropylene reinforcements, ANOVA results indicate water absorption values were also statistically different for the different fibre contents [$F(2,15) = 5.207$, $p = 0.019$] However, results from post hoc analysis show that inclusion of polypropylene had no effect on water absorption of the unreinforced matrix even though the means of water absorption with polypropylene reinforcement were statistically different.

Generally, hydrophilic nature of ligno-cellulosic fibres creates pathways through the soil, thereby increasing water absorption with increase in fibre content [27]. In addition, ligno-cellulosic fibres have free hydroxyl groups on the surface, which bind with water and increase water absorption capacities. Consequently, fibre reinforcements are expected to result in increased water uptake. Inclusion of sisal fibres at 0.5 and 1.0 vol.% resulted in a reduction of water absorption relative to the matrix with lowest values obtained at 0.5% vol. fraction fibre content. Similarly, inclusion of E. pulp fibres resulted in an initial increase in water absorption and subsequent decrease with increasing fibre content to values almost equivalent to unreinforced matrix. This trend is not in agreement with studies on ligno-cellulosic fibre-earth composites where high water absorption values have been recorded (Danso et al., 2015; Ismail & Yaacob, 2011). However, as observed in the previous section, inclusion of fibres improved packing density between fibres and particles. This would promote a compact fibre-matrix system with less permeable pores, which prevents the penetration of water and consequent absorption by the fibres.

At the highest volume fraction investigated in this study, water absorption values of composites were not statistically different from that of the unreinforced matrix irrespective of

fibre type. With ligno-cellulosic fibres, this should not be the case owing to the hydrophilic nature of these fibres relative to their synthetic counterpart. A possible explanation may be that interactions occur at the interface between the vegetable fibre surface and alkali solution within the matrix with consequent effect on the water absorption capacity of vegetable fibres within the composites. Sodium hydroxide treatment (often termed mercerization) of ligno-cellulosic fibre has been extensively used to modify surface properties of these fibres in the development of ligno-cellulosic fibre-polymer matrices. It has been reported that reaction between hydrophilic hydroxyl groups in ligno-cellulosic fibres and NaOH solution results in a reduction of water absorption capacity as shown in equation (6) [32]

$$Fibre-OH+NaOH \rightarrow Fibre-O-Na+H_2O \quad (6)$$

Results from this study suggest the possibility of interactions between ligno-cellulosic fibres and alkali activated matrix, which modifies the hydrophilic nature of fibres in the composites. This behaviour in earth-based matrices has implication on the dimensional stability of cellulose fibres. Studies have focused on improving dimensional stability of vegetable fibres in composites by treatment of fibres to reduce the transfer of water between the matrix and fibre [33]. Hence, the reduction of water absorption potential of fibre reinforced earthen building materials with alkali-activated matrices has significant impact on the durability of these composites.

5.4.2 Effect of fibre type and content on Mechanical Properties

Flexural Properties in Dry Condition

Figure 5.6 presents average values of modulus of rupture (MOR) represented by bars as well as standard deviations presented as error bars for composites tested with different fibre reinforcements at varying fibre content. Table 5.6 presents results of Tukey's HSD Comparison of mean values of MOR for different fibre types and contents in the dry condition

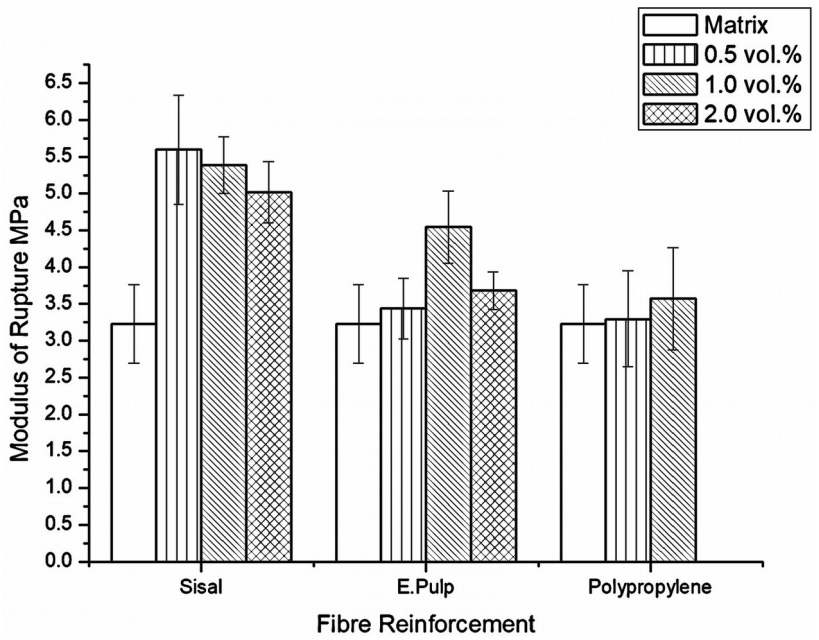

Figure 5:31 Variation of average modulus of rupture in dry condition with different fibre reinforcements and fibre content

Table 5:14 Results of Tukey's HSD Comparison of mean values of MOR for different fibre types and contents in the dry condition

Fibre vol.%	**Sisal**			**Eucalyptus pulp**			**Polypropylene**	
	0	*0.5*	*1.0*	*0*	*0.5*	*1.0*	*0*	*0.5*
0	--	--	--	--	--	--	--	--
0.5	3.94E-4*	--	--	0.929	--	--	0.988	--
1.0	0.001*	0.909	--	0.019*	0.09	--	0.757	0.768
2.0	0.002*	0.404	0.792	0.617	0.952	0.128		

Note: Numbers with asterix indicate statistically significant differences at 0.05 level

Flexural strength of fibre reinforced earth composites is dependent on two main factors: flexural strength of natural soil matrix (without fibres) and the fibre reinforcement benefit. The former is controlled mainly by the nature of the bonding at contact points between soil particles and by the number of such contacts, i.e. particle packing, whilst the latter is largely dependent on the fibre-matrix interfacial shear strength. Average MOR obtained for the unreinforced matrix was 3.25 MPa, which is significantly higher than values recorded for earth-based construction materials. Typical values reported in literature range between 0.13-1.67 MPa [13,34]. Improved flexural strength recorded in this study could be attributed to binding mechanism adopted as well as extrusion moulding. Typical moulding technique adopted in earth-based construction is compression moulding. However, enhanced

mechanical properties of extruded fibre-reinforced composites has been attributed to strengthened fibre-matrix bond associated with extrusion moulding. Despite improved flexural strength of composites, mode of failure of these unreinforced specimens was characterized by immediate failure after peak load i. e. mechanical behaviour of brittle matrices. It was recorded with a single crack at the mid span and complete separation of the specimens into two halves at the end of the test.

There was a statistically significant effect of sisal fibre reinforcements on the MOR as determined by one way ANOVA [$F(3,20) = 13.294$, $p = 4.02\times10^{-4}$]. Post hoc comparisons from Tukey HSD indicate that there was a significant effect of sisal fibre content on the MOR of the unreinforced matrix at all fibre contents investigated. However, the difference of means between MOR at varying fibre contents was not statistically significant. This suggests that a minimum volume fraction of fibres was sufficient to significantly modify the MOR of the matrix and increase of sisal fibre content was not significant with regards to flexural strength. Similarly, inclusion of eucalyptus pulp fibres resulted in a statistically significant effect on the MOR of the composites from the one way ANOVA result [$F(3,20) = 5.793$, $p = 0.021$]. Further comparisons of means using Tukey HSD indicate that only 1.0 vol.% pulp fibre content significantly modified the MOR of the unreinforced matrix. Increase in pulp fibre content did not yield any statistically different effect on the MOR. In comparison to sisal reinforcements, these results suggest that pulp reinforcement was not as effective in the improvement of flexural strength of composites. On the other hand, there was no statistically significant effect of polypropylene reinforcement on MOR of the composites as determined by one way ANOVA [$F(2,15) = 0.347$, $p = 0.714$]. Comparing with effect of polypropylene reinforcement on apparent density, this results that although the inclusion of polypropylene resulted in a more compact composite, excess fibre-fibre interactions weakened the matrix with attendant effect on the MOR.

A comparison between ligno-cellulosic fibre types shows that highest improvement in MOR was achieved with sisal fibres (≈74% increase compared to matrix) whilst maximum increase associated with pulp fibres was 29%. Superior performance in sisal reinforced composites may be attributed to the presence of a strong interaction between sisal fibres and the alkali activated clay matrix. Rough surface morphologies observed with sisal fibres may facilitate mechanical anchorage which plays an important role in the bond strength and interfacial performance of composites [35]. Furthermore, due to hydrophilic nature of vegetable fibres, possibility of development of hydrogen bonds between hydrophilic surface groups and oxygen containing species within the alkali activated matrix [36] may also provide additional

chemical adhesion between fibres and matrix. In addition, sisal fibre had the lowest number of reinforcing filaments for an equivalent volume fraction of fibres. This would suggest that matrix-rich regions would dominate the fibre-soil mixture. Consequently, improved fibre-matrix interactions are expected to lead to good bond strength and overall composite strength. A combination of all these factors is expected to yield improved fibre-matrix interactions between sisal fibre and the alkali activated matrix as a result of improved stress transfer between both phases. These same factors are expected to result in improved performance of pulp reinforced composites. However, inferior performance of Eucalyptus pulp relative to sisal reinforced composites could be attributed to the fact that given the dimensions of pulp fibres, a higher number of filaments of pulp fibre would be present for an equivalent volume fibre content resulting in higher fibre-fibre interactions compared to fibre-matrix interactions. This decreases the potential of the formation of fibre-matrix interaction in the process [37] as fibre-fibre interactions break up the cohesion in the soil matrix thereby weakening the soil-fibre matrix. In addition, relative smooth morphologies of pulp fibres may not favour anchorage. In contrast, polypropylene reinforcement did not significantly influence the MOR of the matrix as compared to the ligno-cellulosic fibres and this may be attributed to a poor fibre-matrix adhesion with increased fibre-fibre interactions. Smooth surface morphology as well as alkali resistance of polypropylene fibres would contribute to poor matrix-fibre interactions. These results are in agreement with results obtained by Puertas et al. [38] where inferior flexural performance was attributed to poor workability due to addition of polypropylene fibres in an alkali activated matrix.

Post-Crack Behaviour in Dry Condition

Much of the expected performance benefits due to fibre inclusion are observed in the post-peak load portion of the stress–strain behavior. Hence, typical stress stain curves are presented in Figure 5.7, which gives an indication of the quality of the material from the point of view of crack control.

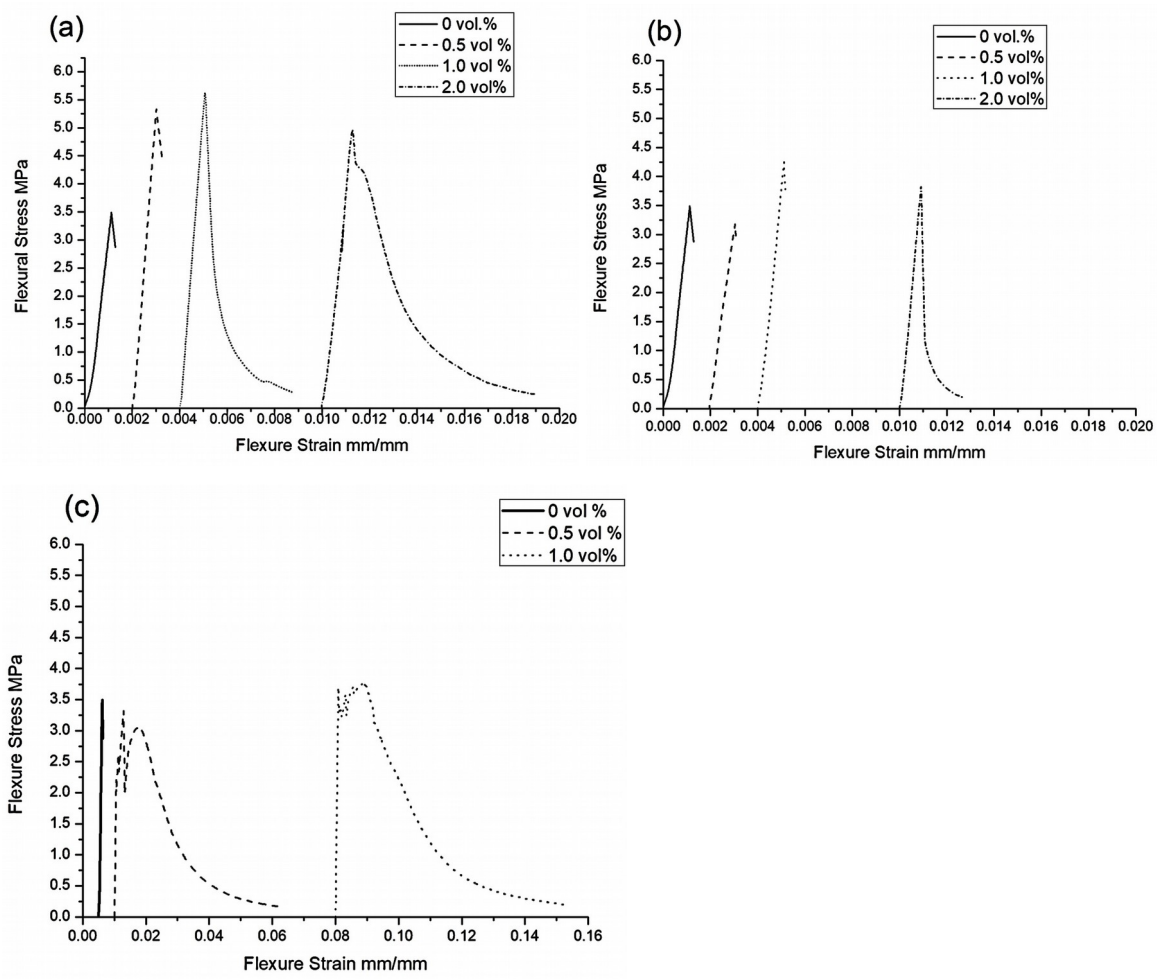

Figure 5:32 Typical flexural stress-Strain Curves in oven dry condition (a) Sisal reinforced composites (b) E.Pulp reinforced composites (c) Polypropylene reinforced

Despite satisfactory performance in flexural strength at low vegetable fibre contents (0.5 & 1.0 vol.%), flexure stress-strain curves at these fibre contents show an abrupt load drop with loss of load carrying capacity at peak strength. In the case of sisal fibre reinforcements, variation of MOR with fibre content was not statistically significant. However, specific energy absorbed at 2 vol.% was 37% higher than energy absorbed at 1 vol.% fibre content (Table 5.7). As presented in Figure 8, 2 vol.% fibre content yielded a characteristic deflection softening behavior after first cracking indicating that loading was transmitted to the ligno-cellulosic fibres with possible crack bridging. Similarly, Figure 5.7 shows significant energy absorption capacity was only introduced at 2 vol.% pulp reinforcement. This indicates that 2 vol.% ligno-cellulosic fibre content presents a satisfactory balance of flexural strength as well as ductility in the development of robust extruded earth-based materials. A similar deflection softening behaviour was observed with non-continuous ligno-cellulosic fibre-cement

composites with fiber volume fractions less than 4% and fibre lengths less than 25-30 mm [39].

The high number of reinforcing filaments of E. pulp was expected to favour debonding in the post crack response. However, evaluation of post-crack response shows that Eucalyptus pulp reinforced composites exhibited an almost brittle failure. This behavior is not in tandem with results from pulp reinforced fibre cement composites which demonstrate improved behavior as a result of pulp fibre reinforcements [40, 41] . However, these studies adopt volume fractions as high as 8-10%. Given their dimensions relative to the matrix, pulp microfibers provide reinforcing mechanism at the micro level by arresting cracks before they propagate to unstable dimensions [42]. This implies they are expected to modify intrinsic mechanical performance of matrix by increasing cracking strength. Studies by Mustapha et al. (2016) on straw fibre reinforced earth-based matrices have noted pull-out (debonding and sliding) and crack bridging to contribute to the overall toughness of these composites. If toughness influence of fibres may only come into effect when macrocracks are wide enough to activate these toughness mechanisms, such as pull-out and bridging, this explains why reinforcing effect of pulp fibres was not observed as a result of insufficient embedment length to resist high pull out loads. This suggests that a minimum critical fibre content and dispersion/distribution challenges are required to efficiently introduce and exploit potential toughness mechanisms with pulp reinforcement of this class of materials.

On the other hand, stress-strain curves show that polypropylene fibre reinforcement satisfy condition of deflection hardening where average MOR value is greater than the first crack strength and deflection at peak load is higher than that at first load [17]. Consequently, failure of specimen was characterized by multiple cracking and large deflections. Although, increase of fibre content from 0.5 vol.% to 1.0 vol.% had not statistical effect on the MOR, specific energy increased by about 175% with increase in fibre content (Table 5.8). As a result, whilst fracture mode of vegetable fibre reinforced composites was characterized by sole cracks, polypropylene reinforced composites presented multiple cracking. Consequently, composite deformation measured at the middle of the span at peak load was 0.1% for both sisal and eucalyptus pulp reinforcements which was almost equivalent to deformation of the unreinforced matrix. Polypropylene reinforcements, on the other hand exhibited composite deformations up to 1.0% at peak load. This significant improvement in ductility and energy absorption capacity observed with polypropylene reinforced earth composites presents the potential of increasing the versatility of earth as a building material.

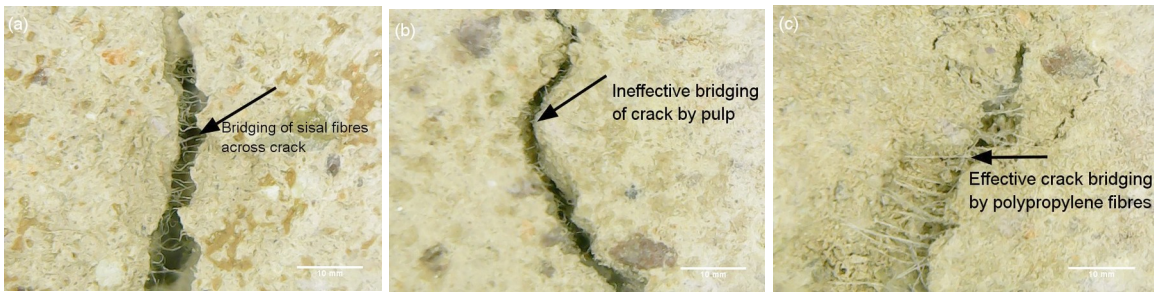

Figure 5:33 Optical images of cracked specimens showing evidence of crack bridging by sisal and polypropylene fibres in (a) Sisal (b) Eucalyptus Pulp and (c) Polypropylene reinforced composites tested in the dry condition

The post-peak behaviour for sisal and polypropylene reinforced composites can be attributed to the bridging effect of fibres as presented in Figure 9 indicating that crack growth was impeded by the fibres. This bridging effect by sisal and polypropylene fibres effectively reduces the crack driving force and promotes shielding of the crack tip. [43,44]. However, Fig 9b shows eucalyptus pulp fibres were not as effective in bridging crack and effectively transferring stress between both phases. This explains brittle behaviour of these composites. Deflection softening behaviour observed with sisal reinforcements suggest that performance can be significantly affected by an increase in fibre length which would further improve the bridging effect. Longer embedment lengths would correspond to better energy absorption capacities as direct consequence of higher loads required for fibre debonding and frictional pullout. Furthermore, a higher fibre content may result in a weakened fibre-matrix interaction which would favor debonding alongside the crack bridging effect and cause a transition from deflection softening to deflection hardening as a direct consequence of increased energy dissipation during debonding and frictional pull-out [45]. In comparison to polypropylene fibres, higher aspect ratio of polypropylene fibres relative to ligno-cellulosic fibres resulted in a higher number of filaments for a more effective crack bridging.

Flexural Properties in Saturated Condition

In order to determine the resilience of these composites as building materials, the effect of full saturation of the composites was investigated. Saturated conditions have a significant effect on the mechanical properties of both soil and vegetable fibres. In soil, clay minerals absorb water which leads to development of significant pore water pressures with corresponding reduction of effective stress between particles [46] whilst ligno-cellulosic fibres absorb moisture via lumen and porous surface and in the process, loose stiffness. [17] In the dry state, the soil suction is relatively high and the formed water bridges at particle–

particle contact points are strong resulting in high bonding force between particles, contributing to the soil flexural strength [47] . With saturation, the soil suction decreases and the bonding force developed through the bridge system gradually disappears resulting in a weakened matrix. Hence, the true test of any binding mechanism may only be evaluated when samples are fully saturated.

Figure 5.9 presents average values of MOR presented as bars and corresponding standard deviation presented as error bars for samples tested in the saturated condition. In comparison to MOR values obtained in the dry condition, there is a significant drop in average MOR value of the unreinforced matrix (saturated MOR to dry MOR ratio = 13%) when samples are tested in the saturated condition. This could be attributed to the presence of voids within the matrix and/or the presence of unreacted clay minerals in the matrix. This agrees with results from water absorption tests presented in the preceding section. Absorbed water molecules act as lubricant resulting in a reduction in the overall strength and increased deformation. Despite this significant drop, saturated MOR value does not fall below range of typical values obtained in literature 0.13-1.67 MPa [13,34]. However, this significant loss in strength suggests that application of this class of materials should be limited to moisture-controlled environments to preserve structural integrity.

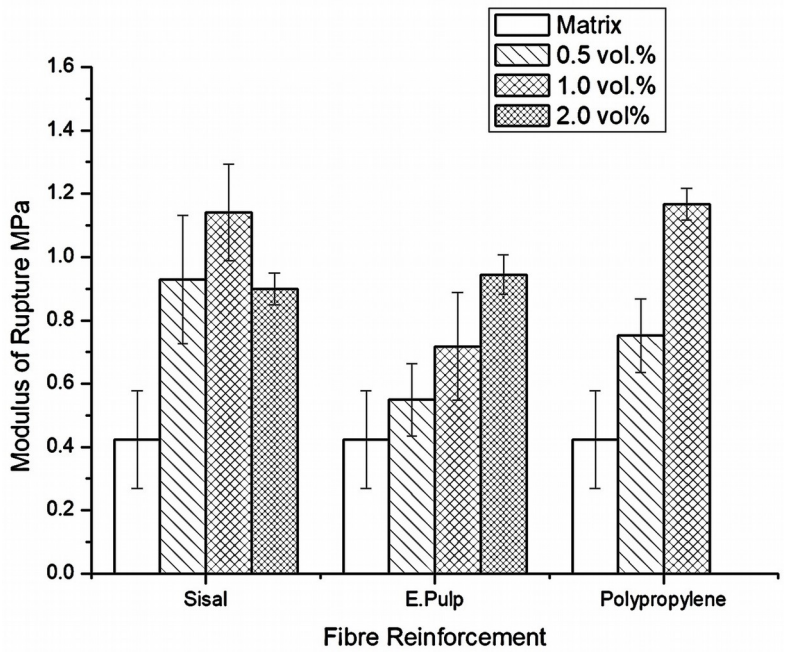

Figure 5:34 Variation of average modulus of rupture in saturated condition with different fibre types and content.

.

Table 5:15 Results of Tukey's HSD Comparison of mean values of MOR for different fibre types and contents in the saturated condition

Fibre vol.%	**Sisal**			**Eucalyptus pulp**			**Polypropylene**	
	0	*0.5*	*1.0*	*0*	*0.5*	*1.0*	*0*	*0.5*
0	--	--	--	--	--	--	--	--
0.5	5.70E-4*	--	--	0.543	--	--	0.059	--
1.0	1.79E-5*	0.148	--	0.022*	0.269	--	1.15E-4*	0.004*
2.0	0.002*	0.989	0.102	2.01E-4*	0.003*	0.07		

Note: Numbers with asterix indicate statistically significant differences at 0.05 level

Results from the one way ANOVA analysis indicate that inclusion of sisal fibres had a statistical effect on the MOR of the composites in the saturated condition [$F(3,20) = 16.712$, $p = 3.47\times10^{-5}$]. Post hoc comparison of means using the Tukey HSD indicate that the difference of means between saturated MOR of the unreinforced composite compared to all fibre reinforced composites was statistically significant. However, the difference of means between MOR values at each fibre content was not statistically significant. These results further confirm that inclusion of sisal fibre reinforcements significantly modified the flexural response of the unreinforced matrix but the matrix was not sensitive to the change in fibre content. Similar trends observed with sisal reinforced samples tested in the dry and saturated conditions suggest that water saturation did not significantly alter interactions between sisal fibre reinforcements and earth-based matrix. Samples reinforced with pulp fibres also showed a statistically significant effect on the saturated MOR as determined by one way ANOVA [$F(3,20) = 13.23$, $p = 2.26\times10^{-4}$]. However, only samples reinforced with 1.0 and 2.0 vol.% pulp fibres demonstrated a statistically significant effect on the saturated MOR of the unreinforced matrix. These results suggest that low pulp fibre contents (0.5 vol.%) were not sufficient to significantly modify the matrix as was the case with sisal fibre reinforcements. Also, the unreinforced matrix was sensitive to changes in pulp volume fraction as means of differences of saturated MOR at 1.0 vol.% and 2.0 vol.% were statistically different from each other. Like sisal fibre reinforcements, pulp fibre reinforced composites did not show any significant deviation of soil-fibre effect on MOR when comparing samples tested in the dry and saturated condition. This behaviour with ligno-cellulosic fibre reinforcements may be attributed to chemical interactions between fibres and alkali activated matrices. In contrast, unlike in the dry condition, inclusion of polypropylene fibres demonstrated a statistically significant effect on the saturated MOR of the composites as determined by one way ANOVA [$F(2,15) = 22.09$, $p = 1.41\times10^{-4}$]. Results from the comparison of means test shows

that only 1.0 vol.% polypropylene fibre content significantly modified the saturated MOR of the unreinforced matrix. Given the hydrophobic nature of polypropylene fibres, moisture sensitivity is expected to be reduced relative to ligno-cellulosic counterparts. However, the possibility of increased porosities attributed to higher aspect of ratio enhances water absorption which could play an important role in lubricating the layer at the fiber/particle interface. [17].

With fibre reinforcements, resilience to the damaging effect of moisture on the composites was slightly improved; average ratio of saturated MOR to dry MOR observed was 18%, 19% and 29% for sisal, pulp and polypropylene reinforced composites respectively. In the dry state, ligno-cellulosic fibres are brittle/strong with a significant fibre-matrix bond. These combined effects tend to lead to higher strength and lower toughness in ligno-cellulosic fiber reinforced composites in the dry condition [17]. In the saturated state, particles on a shear interface are easily disturbed and the pull-out resistance of fibers in soil is weakened (Tang et al., 2007). This weakening of the matrix would result in weakened fibre-matrix interactions as a result of lower contact points and would lower the fibre pull-out load. Consequent effect would be a drop in the average MOR value of the fibre reinforced composites in the saturated condition. The significant drop in MOR observed with ligno-cellulosic reinforced composites tested in the saturated condition could be therefore be attributed to a loss of strength in the fibres as well as weakening of the fibre matrix bond. However, effect of ligno-cellulosic fibre inclusion on the unreinforced matrix appears to be insensitive to moisture testing condition as determined by the one way ANOVA analysis. This suggests that effect of moisture on the matrix may be much greater than effect induced by the hygroscopic nature of the ligno-cellulosic fibres. On the other hand, average loss of strength due to saturation was not as high with polypropylene reinforcements. Higher aspect ratio resulting in a high number of reinforcing filaments would provide a dense skeleton of fibres as major resistance to flexure within the weakened matrix resulting in improved resilience. In the saturated condition, 1 vol. % polypropylene reinforced composites demonstrate the highest MOR which corresponds to a 150% increase relative to the matrix.

Post-Crack Behaviour in Saturated Condition

Figure 5.10 presents typical stress-strain curves for composites tested in the saturated condition.

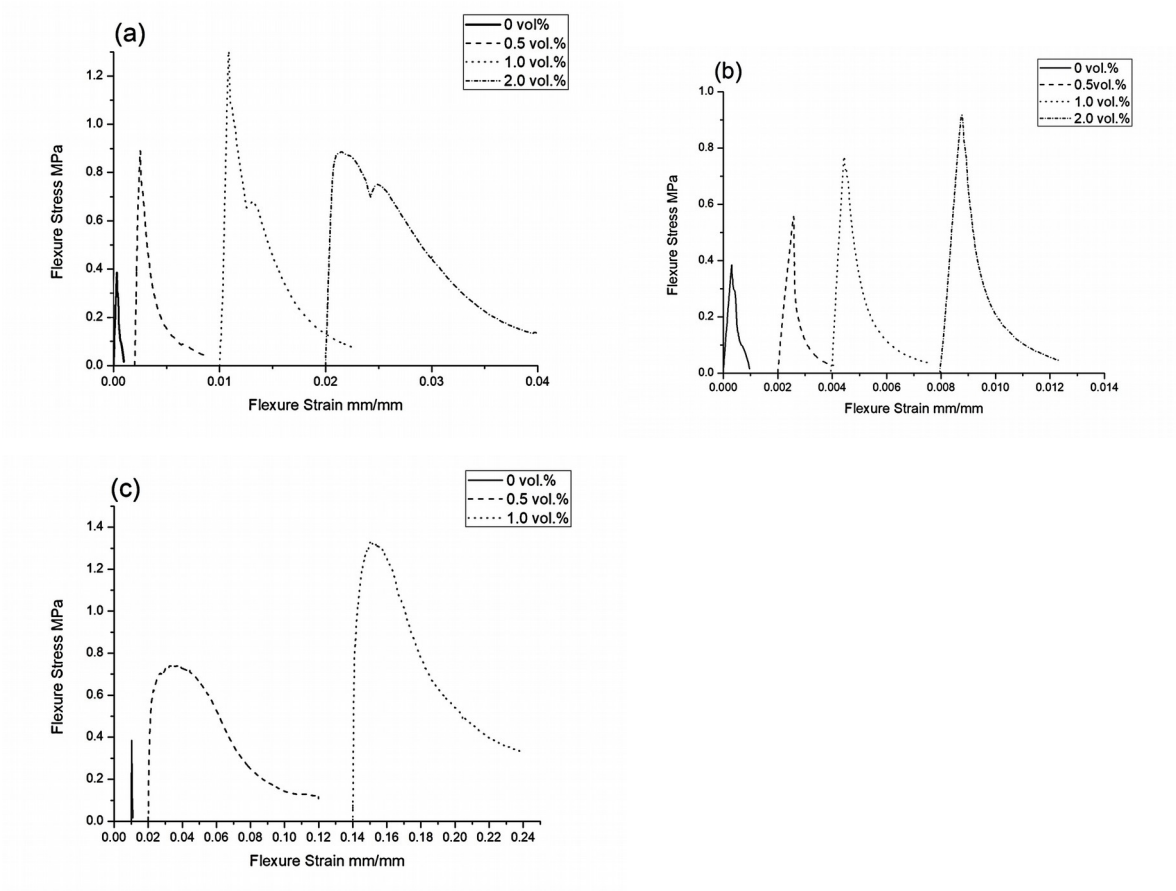

Figure 5:35 Results of Tukey's HSD Comparison of mean values of MOR for different fibre types and contents in the saturated condition

Despite significant loss in flexural strength with water saturation, stress strain exhibit a much more noticeable effect of fiber inclusion in the post-peak region. The figures illustrate the effect of moisture on the deformation behaviours of both ligno-cellulosic and synthetic fibre reinforcements. At maximum fibre volume fraction investigated, composite deformation measured at the middle of the span at peak load was 0.16% and 0.08% for sisal and eucalyptus pulp reinforcements respectively. Polypropylene reinforcements, on the other hand exhibited composite deformations up to 1.2% at peak load.

In all cases, increase in fibre content results in increased deflection capacity of samples with a marked increase in energy absorption capacity. For instance, brittle failure observed in the failure of pulp reinforced composites in the dry condition transformed to ductile failure with corresponding deflection softening in the post peak region. With sisal fibre reinforcements, a transition to graceful failure is observed from 1 vol.% of fibre content, whereas a sharp load drop after peak load is observed with pulp reinforcements. Again, this can be attributed to difference in fibre lengths confirming that with reinforcement of earth-based materials, fibre

length is more critical compared to aspect ratio as both fibres possessed almost similar aspect ratios.

Table 5:16 Specific energy of composites in dry and saturated testing conditions

	Specific Energy (J/m^2)					
Fibre Content (%)	**Dry**			**Saturated**		
	Sisal	E.Pulp	PP	Sisal	E.Pulp	PP
0	--	--	--	7.1	7.1	7.1
0.5	--	--	1375	42.5	10	1151
1	281.9	--	3789	133	17.5	2296
2	385.3	86.8	--	208.7	27.9	--

The specific energy for all fibre-soil composites, which was computed as the area under the load-deflection curve divided by the specimen cross-sectional area, is presented in Table 5.8 and gives an indication of the toughness of each material. Toughness, which is a composite property, has implications for structural elements, which may be exposed to high dynamic loads such as earthquakes or wind loads. A comparison of ligno-cellulosic fibre reinforced composites shows that at equal fibre contents, energy absorption capacity of sisal reinforced composites was about 4 times higher than the Eucalyptus pulp counterparts. This further confirms the impact of fibre length in the reinforcement of these matrices. As a result of superior deflection capacity, polypropylene reinforced composites demonstrate energy absorption capacities, which is an order of magnitude higher than vegetable fibre counterparts.

5.4.3 Microstructural Analysis

SEM images presented in Figure 5.11 show the microstructure of composites with different fibre reinforcements. These images reveal a heterogeneous bulk matrix comprising of large sized grains with a binder phase surrounding the grains. Energy Dispersive X-ray Spectroscopy mapping of these large sized grains identified silica dense particles as quartz and silica/potassium dense particles as orthoclase. Fibre reinforcements appear to modify the bulk matrix as sisal and polypropylene reinforced samples appear more consolidated than Eucalyptus pulp counterparts. These could be attributed to the number of reinforcing filaments present in Eucalyptus pulp reinforced samples which may result in weaker matrices. The relative difference in microstructure confirms variation in the initial moisture

content as a result of fibre reinforcements may have affected the alkali activation of the clay minerals leading to a variation of alkali activated products in the composites. Presence of voids and linear cracks in the microstructures explains the significant water absorption observed in the composites. More linear cracks are observed around polypropylene and pulp reinforced samples. These linear cracks observed may be attributed to residual dehydration associated with thermal curing which may amplify porosities introduced by fibres.

Fibre distribution at the microstructural scale gives more insight of composite physical and mechanical performance. Sisal fibre reinforced composites showed an increase in matrix-rich regions, compared to polypropylene or Eucalyptus pulp counterparts; confirming tendency of increased fibre matrix interactions. This correlates well with the flexural strength and density performance in the previous sections. More fibre reinforcements observed with Eucalyptus pulp and polypropylene reinforcements explains tendency of these composites to be fibre-controlled. Linear cracks appear running through fibre-matrix interface for Eucalyptus pulp and polypropylene reinforced composites not observed with sisal reinforced composites which correlates with increased water absorption observed with these samples.

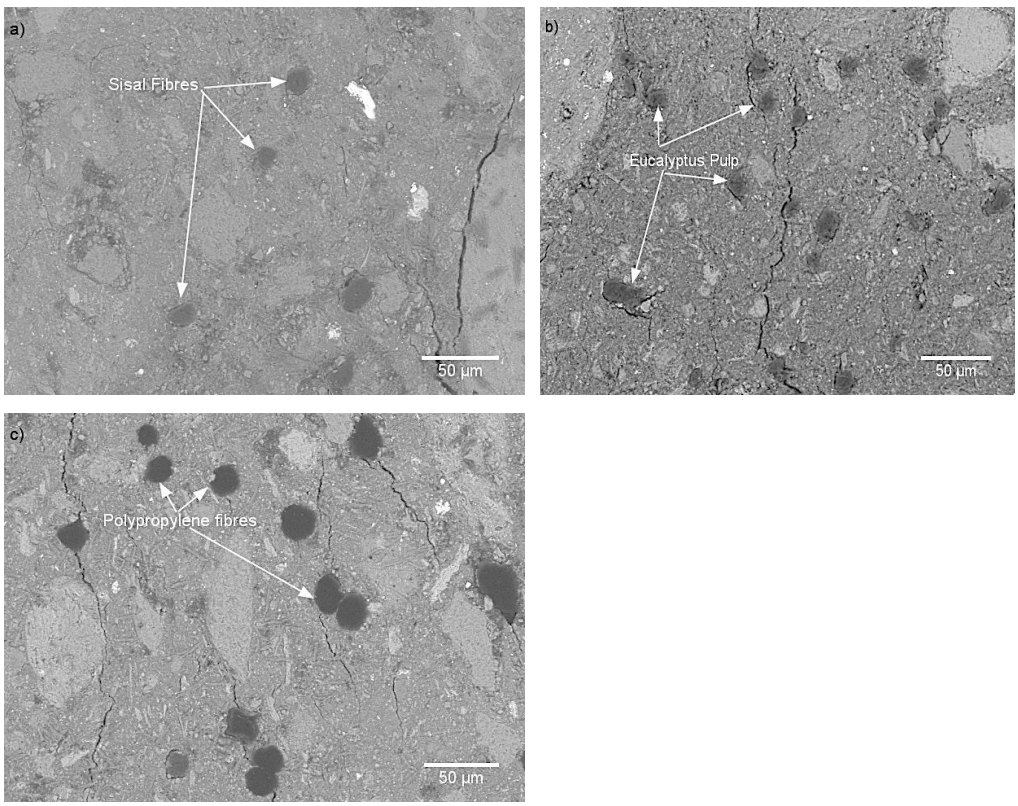

Figure 5:36SEM images of composites reinforced with different fibres (a) Sisal (b) E. Pulp and (c) Polypropylene

Comparison of the matrix with fibre reinforced samples show that the inclusion of fibres modifies the matrix and this is evident in the distribution of elements in the Energy

Dispersive X-Ray Spectroscopy (EDS) maps (Figure 5.12). EDS maps show a variation in the elemental distribution in the matrix with the different fibre types. This justifies the variation in composite densities observed in the previous section. Varied microstructure of fibre reinforced demonstrates the sensitivity of matrix to fibre inclusion. This may be attributed to moisture content variation [28].

Fibre matrix interface (Figure 5.12) shows an overall good adhesion between both fibres and the matrix. This is not in agreement with behaviour of ligno-cellulosic fibres in soil matrices which are typically characterized by dimensional changes of the fibre as a result of variation in moisture and temperature. During mixing, the hydrophilic nature of fibres leads to moisture absorption and consequent expansion whilst during the drying stage, the loss of absorbed moisture results in fibre shrinkage leaving a void around the periphery of the fibre [27]. This behavior was demonstrated in studies by Danso et al. (2017) on earth-based composites reinforced with ligno-cellulosic fibres (bagasse, coconut and oil palm) where microstructural analysis revealed gaps between the periphery of the fibres and matrix within the range of 18 -77 µm for the different fibres. The absence of significant voids around the periphery of vegetable fibres in this study could be attributed to extrusion moulding which has been reported to improve fibre packing in fibre-cement composites. Furthermore, EDS mapping/distribution of Na elements show the presence of Na within sisal fibres and Eucalyptus pulp fibres confirming chemical interaction between the fibres and the matrix. Negative charge of OH bonds from cellulose molecules may have formed a bond between flocculated Na ions from within the matrix leading to additional chemical adhesion between fibre and matrix. The absence of Na in polypropylene fibres, which is largely alkali resistant, confirms this trend. A combination of chemical and physical adhesion between ligno-cellulosic fibres and matrix justify higher flexural strengths and smaller deflection capacities observed with natural fibres reinforcements. It also confirms water absorption characteristics of composites reinforced with ligno-cellulosic fibres.

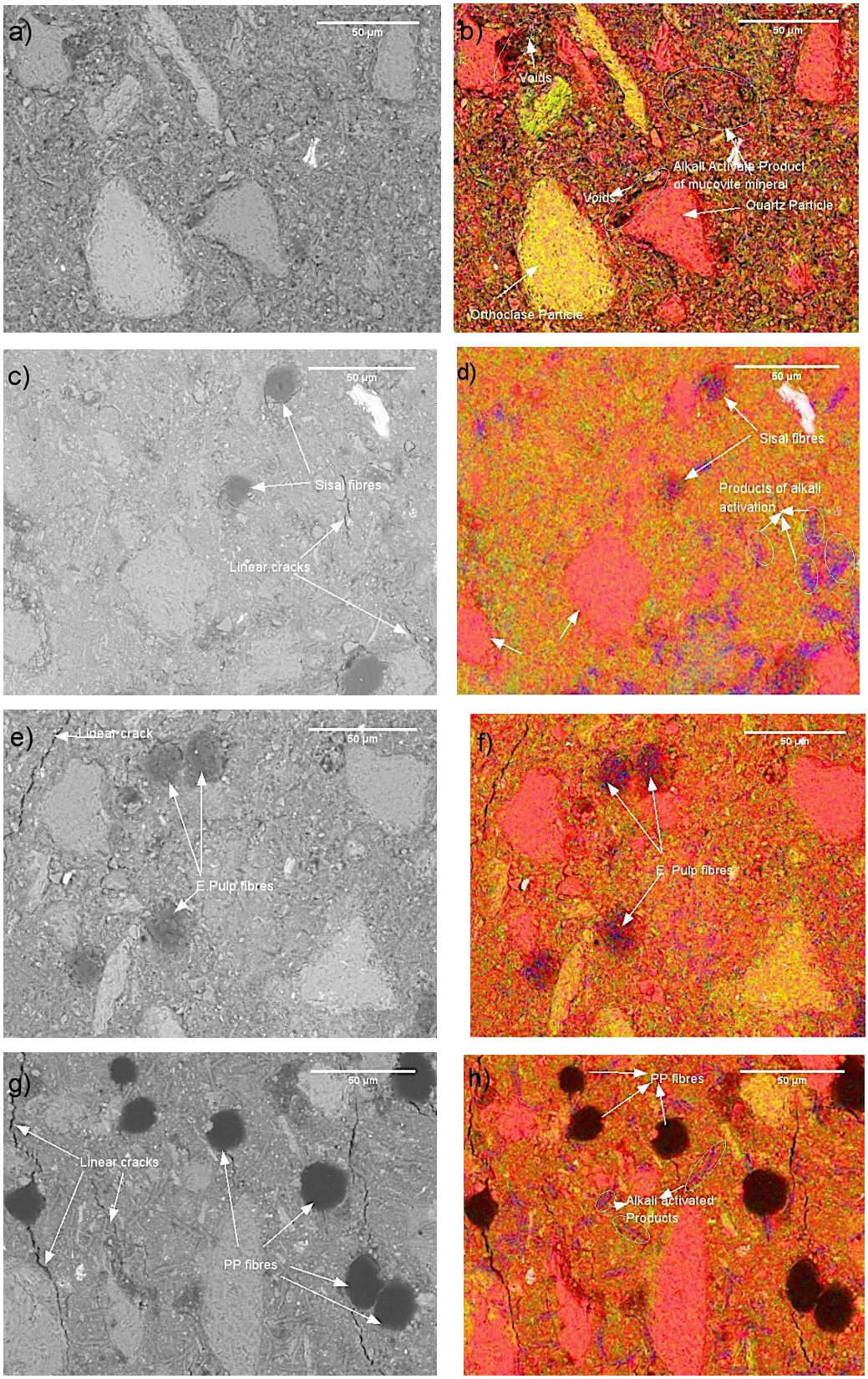

Figure 5:37 SEM images and EDS mapping of composites with different fibre reinforcements: (a) Unreinforced matrix (b) EDS map of unreinforced matrix (c) Sisal fibre reinforced composite (d) EDS map of sisal reinforced composite (e) Eucalyptus pulp reinforced c *(EDS Map Key: Silicon – Red, Aluminum – Green, Sodium – Blue)*

5.5 Implications

The results from this investigation has presented the improvement of mechanical and physical properties of alkali activated clay based composites reinforced with fibres in a bid to encourage further research into similar alkali activated earth-based matrices given the lack of studies on these composites. Most studies on earthen construction have focused on applications where compressive strength requirements govern applications. With fibre reinforcements, the scope of these materials maybe expanded to panels, claddings and pavements. Results from this study have demonstrated significant energy absorption capacities may be introduced with a combination of alkali activated clay matrices reinforced with various fibres. This energy absorption capacities have significance in earthquake prone regions. Based on these results, mechanism of failure of alkali activated earth-based composites reinforced with ligno-cellulosic fibres is primarily controlled by fibre-matrix interactions with fibre length playing a critical role in crack bridging mechanisms. A combination of mechanical and chemical adhesion as a result of surface roughness and hydrophilic nature of sisal fibres are presumed to be responsible for improved flexural strengths observed. On the other hand, synthetic fibres which are largely alkali resistant, demonstrated low flexural strengths attributed to weak fibre matrix interactions. Consequently, deflection hardening behaviours were observed in the flexural response attributed to large number of filaments and fibre debonding.

The use of ligno-cellulosic macrofibres as reinforcements presents a more eco-friendly construction material and significant fibre-matrix interactions results in materials with improved flexural strength. In this study, 10 mm long sisal fibres were used in the production of soil composite. It would be interesting to investigate longer fibres in order to establish the optimal length for maximum improvement. On the other hand, beneficial reinforcing effects of pulp microfibers may not be exploited in earth-based matrices as a result of inadequate fibre length. However, superior performance of polypropylene in ductility (as a result of weak fibre-matrix interactions) compared to ligno-cellulosic fibres, suggests that applications of earth-based building materials may be broadened to applications where ductility (and not necessarily strength/cost) is critical.

In a bid to develop a low impact earth-based building material, alkali activation of clay minerals was performed using a relatively low molarity alkaline solution. Consequently, presence of unreacted clay minerals in the matrix resulted in a significant drop in strength performance when samples were tested under saturated conditions. Notwithstanding, MOR values recorded were within the range of typical values reported in literature demonstrating

the potential of this binding mechanism. Nonetheless, applications of this class of materials may be restricted to protected/moisture-controlled environments in order to preserve structural integrity during application.

5.6 Conclusions

This study presents an experimental study on a novel construction material to give insight on effect of fibre type and dosage on physical and mechanical properties of an alkali activated clay matrix. Alkali activation of natural clay minerals is a promising alternative binding mechanism for unfired earth-based building material and it is remarkable how different types of reinforcement will influence properties of extruded composites. Three different fibre reinforcements (sisal, eucalyptus pulp and polypropylene) were studied at varying fibre volume fractions (0, 0.5, 1.0 & 2.0%). Based on the test results, the following conclusions can be drawn:

- Statistically, inclusion of sisal fibre reinforcements significantly modified the matrix attributed to improved packing density obtained during extrusion moulding resulting in an initial increase in density. Effect of pulp and polypropylene reinforcements on the density of the unreinforced matrix was not statistically significant. Replacement of soil with fibres of relatively lower densities was expected to reduce overall composite densities. However, at highest fibre content investigated in this study, density of unreinforced composite was statistically equivalent to the reinforced composites.
- Improved packing densities obtained with sisal fibre reinforcement resulted in statistically significant reductions in water absorption as a result of a more compact fibre-matrix system relative to other fibre reinforcements. Contribution of hydrophilic nature of ligno-cellulosic fibres to water absorption of composites was not significantly observed. SEM/EDS analysis revealed the presence of sodium within ligno-cellulosic fibres indicating chemical reactions between hydroxyl groups on ligno-cellulosic fibres and sodium compounds from the alkali activated matrix, which may have modified hydrophilic nature of ligno-cellulosic fibres.
- Average flexural strength of unreinforced alkali activated clay matrix (3.2 MPa) tested in the dry condition was significantly higher than typical range of values obtained from literature (0.13 – 1.67 MPa) for unfired earth, demonstrating the potential of extrusion moulding as well as alkali activation binding mechanism for the production of earthen composites. However, due to low alkalinity of solutions utilised

in the study, a significant drop in MOR was observed when samples were tested in saturated conditions. This moisture sensitivity restricts application of this class of materials to moisture-controlled environments.

- Highest improvement in MOR was achieved with sisal fibres (≈74% increase compared to unreinforced matrix) whilst maximum increase associated with pulp was 29%. In contrast, polypropylene reinforcement demonstrated no significant effect on the MOR of the composites and this may be attributed to a poor fibre-matrix adhesion with increased fibre-fibre interactions. Superior performance in sisal reinforced composites indicate improved fibre-matrix interactions between sisal fibre and the alkali activated matrix which would facilitate effective stress transfer between both phases. Due to improved fibre-matrix interactions, mechanism for crack control potential was achieved via crack bridging as observed via optical images.
- Pulp reinforcement presented the highest number of reinforcing filaments for an equivalent fibre content. However, beneficial action of fibre reinforcements was not effectively exploited with pulp fibres largely because of fibre length as toughness mechanism was based on crack bridging. Higher reinforcing filaments potentially break up the cohesion in the soil matrix thereby weakening the soil fibre matrix. Consequently, flexural strengths as well as post-crack response were low compared to sisal fibre reinforcements.
- Whereas ligno-cellulosic fibres introduced deflection softening to the brittle matrices, polypropylene reinforcements transformed unreinforced brittle matrices to deflection hardening composites with failure mode characterized by multiple cracking. This was attributed to high aspect ratio as well as weak fibre matrix interactions. Post-crack behavior was characterized by crack bridging as well as fibre debonding and pull-out.
- This paper has focused on physico-mechanical properties of fibre reinforced earth-based composites. Further tests to elucidate/confirm fibre matrix interactions such as fibre pull-out tests would need to be developed. Furthermore, long term interactions between fibre and alkaline matrix through accelerated ageing tests and attendant effect on composite properties are being developed to determine the practicability of this technique.

References

[1] K. Ghavami, A. Azadeh, Nonconventional Materials (NOCMAT) for Ecological and Sustainable Development, MRS Adv. 1 (2016) 3553–3564. doi:10.1557/adv.2016.613.

[2] H. Savastano, S.F. Santos, J. Fiorelli, V. Agopyan, Sustainable use of vegetable fibres and particles in civil construction, Second Edi, Elsevier Ltd., 2016. doi:10.1016/B978-0-08-100370-1.00019-6.

[3] J.-C. Morel, K. Ghavami, A. Mesbah, Theoretical and Experimental Analysis of Composite Soil Blocks Reinforced with Sisal Fibres Subjected to Shear by, Mason. Int. 13 (2000) 54–62.

[4] S.M. Hejazi, M. Sheikhzadeh, S.M. Abtahi, A. Zadhoush, A simple review of soil reinforcement by using natural and synthetic fibers, Constr. Build. Mater. 30 (2012) 100–116. doi:10.1016/j.conbuildmat.2011.11.045.

[5] C. Tang, B. Shi, W. Gao, F. Chen, Y. Cai, Strength and mechanical behavior of short polypropylene fiber reinforced and cement stabilized clayey soil, Geotext. Geomembranes. 25 (2007) 194–202. doi:10.1016/j.geotexmem.2006.11.002.

[6] M. Bouhicha, F. Aouissi, S. Kenai, Performance of composite soil reinforced with barley straw, Cem. Concr. Compos. 27 (2005) 617–621. doi:10.1016/j.cemconcomp.2004.09.013.

[7] K. Mustapha, E. Annan, S.T. Azeko, M.G. Zebaze Kana, W.O. Soboyejo, Strength and fracture toughness of earth-based natural fiber-reinforced composites, J. Compos. Mater. 50 (2016) 1145–1160. doi:10.1177/0021998315589769.

[8] J.L. Provis, Alkali-activated materials, Cem. Concr. Res. (2016). doi:10.1016/j.cemconres.2017.02.009.

[9] V. Correia, S. Santos, H. Savastano Jr, V. John, Utilization of vegetable fibers for production of reinforced cementitious materials, RILEM Tech. Lett. 2 (2018). doi:10.21809/rilemtechlett.2017.48.

[10] H.E. Gram, P. Nimityongskul, Durability of natural fibres in cement-based roofing sheets, J. Ferrocem. 17 (1987) 328–334.

[11] R.D. Toledo Filho, F. de A. Silva, E.M.R. Fairbairn, J. de A.M. Filho, Durability of compression molded sisal fiber reinforced mortar laminates, Constr. Build. Mater. 23 (2009) 2409–2420. doi:10.1016/j.conbuildmat.2008.10.012.

[12] A. Heath, P. Walker, M. Lawrence, Compressive strength of extruded unfired clay masonry units, (2009) 105–112. doi:10.1680/coma.2009.162.

[13] P.J. Walker, Strength, durability and shrinkage characteristics of cement stabilised soil blocks, Cem. Concr. Compos. 17 (1995) 301–310. doi:10.1016/0958-9465(95)00019-9.

[14] J. Davidovits, Geopolymer : chemistry and applications, Institut G�opolym�re, Saint-Quentin, 2011.

[15] Y. Li, Y.-W. Mai, L. Ye, Sisal fibre and its composites: a review of recent developments, Compos. Sci. Technol. 60 (2000) 2037–2055. doi:10.1016/S0266-3538(00)00101-9.

[16] B.N. Barra, S.F. Santos, P.V.A. Bergo, C. Alves, K. Ghavami, H. Savastano, Residual sisal fibers treated by methane cold plasma discharge for potential application in cement based material, Ind. Crops Prod. 77 (2015) 691–702. doi:10.1016/j.indcrop.2015.07.052.

[17] A. Bentur, S. Mindess, Fibre Reinforced Cementitious Composites, Second Edition, Taylor & Francis, 2006.

[18] H. Savastano, S.F. Santos, M. Radonjic, W.O. Soboyejo, Fracture and fatigue of natural fiber-reinforced cementitious composites, Cem. Concr. Compos. 31 (2009) 232–243. doi:10.1016/j.cemconcomp.2009.02.006.

[19] G.H.D. Tonoli, S.F. Santos, A.P. Joaquim, H. Savastano, Effect of accelerated carbonation on cementitious roofing tiles reinforced with ligno-cellulosic fibre, Constr. Build. Mater. 24 (2010) 193–201. doi:10.1016/j.conbuildmat.2007.11.018.
[20] J.E.M. Ballesteros, V. dos Santos, G. Mármol, M. Frías, J. Fiorelli, Potential of the hornification treatment on eucalyptus and pine fibers for fiber-cement applications, Cellulose. 24 (2017) 2275–2286. doi:10.1007/s10570-017-1253-6.
[21] G. Araya-Letelier, J. Concha-Riedel, F.C. Antico, C. Sandoval, Experimental mechanical-damage assessment of earthen mixes reinforced with micro polypropylene fibers, Constr. Build. Mater. 198 (2019) 762–776. doi:https://doi.org/10.1016/j.conbuildmat.2018.11.261.
[22] D. Maskell, A. Heath, P. Walker, Laboratory scale testing of extruded earth masonry units, Mater. Des. 45 (2013) 359–364. doi:10.1016/j.matdes.2012.09.008.
[23] H. Danso, D.B. Martinson, M. Ali, J.B. Williams, Physical , mechanical and durability properties of soil building blocks reinforced with natural fibres, Constr. {&} Build. Mater. 101 (2015) 797–809. doi:10.1016/j.conbuildmat.2015.10.069.
[24] Ş. Yetgin, Ö. ÇAVDAR, A. Çavdar, The effects of the fiber contents on the mechanic properties of the adobes, Constr. Build. Mater. 22 (2008) 222–227. doi:10.1016/j.conbuildmat.2006.08.022.
[25] I. Demir, An investigation on the production of construction brick with processed waste tea, Build. Environ. 41 (2006) 1274–1278. doi:10.1016/J.BUILDENV.2005.05.004.
[26] R.S. Teixeira, S.F. Santos, A.L. Christoforo, H. Savastano, F.A.R. Lahr, Extrudability of cement-based composites reinforced with curauá (Ananas erectifolius) or polypropylene fibers, Constr. Build. Mater. 205 (2019) 97–110. doi:https://doi.org/10.1016/j.conbuildmat.2019.02.010.
[27] K. Ghavami, R.D. Toledo Filho, N.P. Barbosa, Behaviour of composite soil reinforced with natural fibres, Cem. Concr. Compos. 21 (1999) 39–48. doi:10.1016/S0958-9465(98)00033-X.
[28] J. Xie, O. Kayali, Effect of initial water content and curing moisture conditions on the development of fly ash-based geopolymers in heat and ambient temperature, Constr. Build. Mater. 67 (2014) 20–28. doi:https://doi.org/10.1016/j.conbuildmat.2013.10.047.
[29] C. Tang, D. Wang, Y. Cui, B. Shi, J. Li, Tensile Strength of Fiber-Reinforced Soil, J. Mater. Civ. Eng. 28 (2016) 04016031. doi:10.1061/(ASCE)MT.1943-5533.0001546.
[30] A. Seco, P. Urmeneta, E. Prieto, S. Marcelino, B. García, L. Miqueleiz, Estimated and real durability of unfired clay bricks: Determining factors and representativeness of the laboratory tests, Constr. Build. Mater. 131 (2017) 600–605. doi:10.1016/j.conbuildmat.2016.11.107.
[31] S. Ismail, Z. Yaacob, Properties of laterite brick reinforced with oil palm empty fruit bunch fibres, Pertanika J. Sci. Technol. 19 (2011) 33–43.
[32] R. Agrawal, N.S. Saxena, K.B. Sharma, S. Thomas, M.S. Sreekala, Activation energy and crystallization kinetics of untreated and treated oil palm fibre reinforced phenol formaldehyde composites, Mater. Sci. Eng. A. 277 (2000) 77–82.
[33] M. Segetin, K. Jayaraman, X. Xu, Harakeke reinforcement of soil-cement building materials: Manufacturability and properties, Build. Environ. 42 (2007) 3066–3079. doi:10.1016/j.buildenv.2006.07.033.
[34] C. Galán-Marín, C. Rivera-Gómez, J. Petric, Clay-based composite stabilized with natural polymer and fibre, Constr. Build. Mater. 24 (2010) 1462–1468. doi:10.1016/j.conbuildmat.2010.01.008.
[35] F.D.A. Silva, B. Mobasher, C. Soranakom, R.D.T. Filho, Effect of fiber shape and morphology on interfacial bond and cracking behaviors of sisal fiber cement based

composites, Cem. Concr. Compos. 33 (2011) 814–823. doi:10.1016/j.cemconcomp.2011.05.003.
[36] M. Alzeer, K. MacKenzie, Synthesis and mechanical properties of novel composites of inorganic polymers (geopolymers) with unidirectional natural flax fibres (phormium tenax), Appl. Clay Sci. 75–76 (2013) 148–152. doi:10.1016/j.clay.2013.03.010.
[37] P. Donkor, E. Obonyo, Earthen construction materials: Assessing the feasibility of improving strength and deformability of compressed earth blocks using polypropylene fibers, Mater. Des. 83 (2015) 813–819. doi:10.1016/j.matdes.2015.06.017.
[38] F. Puertas, T. Amat, A. Fernández-Jiménez, T. Vázquez, Mechanical and durable behaviour of alkaline cement mortars reinforced with polypropylene fibres, Cem. Concr. Res. 33 (2003) 2031–2036. doi:10.1016/S0008-8846(03)00222-9.
[39] F. de A. Silva, R.D. Toledo Filho, J. de A. Melo Filho, E. de M.R. Fairbairn, Physical and mechanical properties of durable sisal fiber–cement composites, Constr. Build. Mater. 24 (2010) 777–785. doi:https://doi.org/10.1016/j.conbuildmat.2009.10.030.
[40] H. Savastano, P.G. Warden, R.S.P. Coutts, Brazilian waste fibres as reinforcement for cement-based composites, Cem. Concr. Compos. 22 (2000) 379–384. doi:10.1016/S0958-9465(00)00034-2.
[41] A.E.F.S. Almeida, G.H.D. Tonoli, S.F. Santos, H. Savastano, Improved durability of vegetable fiber reinforced cement composite subject to accelerated carbonation at early age, Cem. Concr. Compos. 42 (2013) 49–58. doi:10.1016/j.cemconcomp.2013.05.001.
[42] N. Banthia, J. Sheng, Fracture toughness of micro-fiber reinforced cement composites, Cem. Concr. Compos. 18 (1996) 251–269. doi:https://doi.org/10.1016/0958-9465(95)00030-5.
[43] M.E. Launey, R.O. Ritchie, On the Fracture Toughness of Advanced Materials, Adv. Mater. 21 (2009) 2103–2110. doi:10.1002/adma.200803322.
[44] W. Soboyejo, Mechanical Properties of Engineered Materials, CRC Press, 2002.
[45] F. Aymerich, L. Fenu, P. Meloni, Effect of reinforcing wool fibres on fracture and energy absorption properties of an earthen material, Constr. Build. Mater. 27 (2012) 66–72. doi:10.1016/j.conbuildmat.2011.08.008.
[46] D.G. Fredlund, H. Rahardjo, H. Rahardjo, Soil Mechanics for Unsaturated Soils, Wiley, 1993.
[47] C.S. Tang, B. Shi, L.Z. Zhao, Interfacial shear strength of fiber reinforced soil, Geotext. Geomembranes. 28 (2010) 54–62. doi:10.1016/j.geotexmem.2009.10.001.
[48] H. Danso, D.B. Martinson, M. Ali, J.B. Williams, Mechanisms by which the inclusion of natural fibres enhance the properties of soil blocks for construction, (2017). doi:10.1177/0021998317693293.

6.0 Chapter 6: Multiscale Characterisation of Fibre Reinforced Alkali Activated Un-Calcined Earth-based Composites

This chapter presents the results of a multi-scale study of the mechanical properties of model earth-based composites. The local mechanical properties of the fibers, binder and matrix materials are characterized at the nano- and micro-scales using nano-indentation and statistical deconvolution techniques. The macro-mechanical properties are also elucidated using a combination of flexural strength testing, and resistance-curve experiments. The underlying strengthening and toughening mechanisms are explored using a combination of *in-situ/ex-situ* observations of crack interactions and micro-mechanical models.

6.1 Introduction

Due to their eco-friendly indices, enhanced by their availability, earth-based construction materials have re-emerged as an attractive and viable construction material in recent times[1]. However, like other quasi-brittle materials, low energy absorption capacity and poor fracture resistance of this class of materials presents limitations on their use in structural applications. Furthermore, poor resistance to abrasion, weathering and water erosion of earth, further restricts applications to moisture-controlled environments. These challenges have stimulated researchers to develop various binding/reinforcing solutions using a wide range of binders and fibre reinforcements to improve durability and mechanical performance of earthen construction; biopolymers and natural fibres [2–4]; cement and natural fibres[5] Coal ash [6]; Metakaolin/cement [7]; Lime activated GGBS [8]; Agricultural by-products -Rice husk ash/bagasse ash [9]. It is well documented that the presence of fibres in soil matrices enhances ductility of the composite [10,11]. However, studies have shown that fibre-matrix interactions which could be based on physical/chemical adhesion, friction and/or mechanical anchorage; largely determine the effectiveness of fibres in enhancing the mechanical performance of brittle matrices[12]. Whilst significant effort has been made to characterize enhanced ductility of earth-based matrices as a result of fibre reinforcements, the underlying strengthening and toughening mechanisms induced by fibre reinforcements in within the binder systems are still partly understood. The understanding of the mechanisms of stress transfer provides a basis for the development of improved composites through the tailoring of fibre-matrix interactions.

A class of binders which has received much attention in recent times, is that of alkali activation.

In alkali activated systems, binding mechanisms are achieved via a reaction of solid aluminosilicates under alkaline conditions to synthesize semi-crystalline to amorphous inorganic gel binders that have been classified as geopolymers [13] or inorganic polymers [14]. These alkali activated aluminosilicates have been reported to possess superior mechanical/durability properties over conventional binders. The alkaline cations act as catalysts in the destruction of Si-O-Si, AlO-Al and Si-O-Al bonds [15] and subsequently serve as partners in the formation of water resistant alkaline or alkaline-alkaline earth aluminosilicate hydrates analogous to natural zeolites and micas [13]. It is well known that earth consists of a wide range of aluminosilicates suggesting that alkali activator solutions may provide in situ binding mechanisms with the potential to improve mechanical properties of earth-based construction materials. However, it is not clear how alkali activated earth-based matrices would interact with various fibre types typically used as reinforcement in this class of materials and how these interactions would ultimately control strengthening and toughening mechanisms in the composite.

Nanoindentation has been used for the identification of the mechanical effects of elementary chemical components of composites at a scale where physical chemistry meets mechanics [16,17]. This implies that micromechanical effects of fibre reinforcements in alkali activated matrices may also be characterized via nanoindentation. However, literature is scarce on such multiscale characterization of earth-based construction materials. This current effort seeks to evaluate the reinforcing efficiency of two fibre types on alkali activated soil based on enhancement in strength and fracture resistance compared to the brittle matrix as well as evaluate the modification in micromechanical response associated with these fibre reinforcements. Fundamental understanding of these mechanisms is essential in order to tailor and optimize the properties of these composites for various structural applications.

This paper reports the results of a multiscale characterization aimed at studying the reinforcing efficiency of two different fibre types (sisal and polypropylene) on an alkali activated natural soil matrix. At the macroscale, a combined experimental and analytical investigation evaluated the modification in strength/toughness and post-crack behavior induced by the fibres. Based on the underlying strengthening and toughening mechanisms, predictions of flexural properties and resistance curve behaviour from existing micro-mechanical models were compared with experimental measurements. A combined grid nano-indentation/statistical deconvolution

technique was adopted on the nano-scale to identify mechanical properties of binder phases and corresponding volumetric fractions associated with each fibre type to evaluate how fibre reinforcements control formation of binding phases. A comparative analysis is presented on the efficiency of the fibre reinforcements based on the of the use of natural fibres and synthetic fibres as reinforcements.

6.2 Materials and Methods

6.2.1 Materials

Soil

The soil used for this study was supplied by Top Telha Ceramic Tile Company, Leme and sourced from Brazilian quarries in the State of Sao Paulo, Brazil. The soils are typical source materials used for the production of fired roof tiles. The particle size distribution was determined using laser particle analyser and show wide spread of particle sizes (Figure 6.1); particles range in diameter from as high as 0.4mm to a few micrometers. Characterization was carried out by Scanning Electron Microscopy with chemical analysis by Energy Dispersive X-ray Spectroscopy (EDX). Fig 6.2 shows the Back Scatter Electron image of the as-received samples showing wide variation of particle sizes. Particles are predominantly irregular shaped and with smaller sized particles agglomerating over larger particles.

Alkali Activator Solution

Alkaline activator used in this study was a solution of sodium hydroxide and sodium silicate as studies have shown that the addition of sodium silicate accelerates the activation of aluminosilicates and improve mechanical properties[13]. Sodium Hydroxide used was of caustic soda pellets with 97% purity whilst sodium silicate used was in the powder form and were both supplied by Dinamica Quimica Contemporanea Ltd, Brazil

In this study a low concentration alkali activator solution (*4M* NaOH Solution) was used to ensure that building units had minimal environmental impact. This would also minimise alkalinity of the matrix which has detrimental effect on long term structural integrity of ligno-cellulosic fibres. Gram he

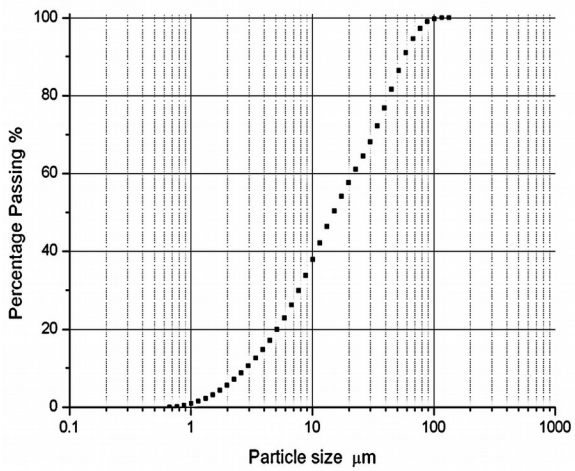

Figure 6:38 Particle size distribution

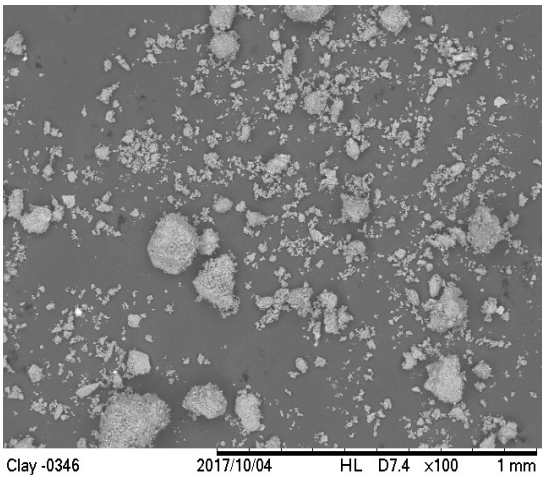

Figure 6:39 SEM-BSE images of soil particles

Fibres

Sisal (Agave sisalana) fibers used in this study were extracted from the waste of baler twine cordage and was donated by the Association for the Sustainable Development of the Sisal Producing Region, Valente, Bahia State, Brazil. Fibres were cut to a length of 10mm.

Polypropylene fiber is the most widely used synthetic fibre used as reinforcement for soil [11] and was selected for the purpose of comparison. They possess improved ductility and are resistant to alkaline attack relative to cellulose fibres. Polypropylene fibre produced by Saint-Gobain, Brazil was used in this study. As observed in Figure 6.3, the fibres present varying surface morphologies which is expected to play a role in fibre-matrix interactions.

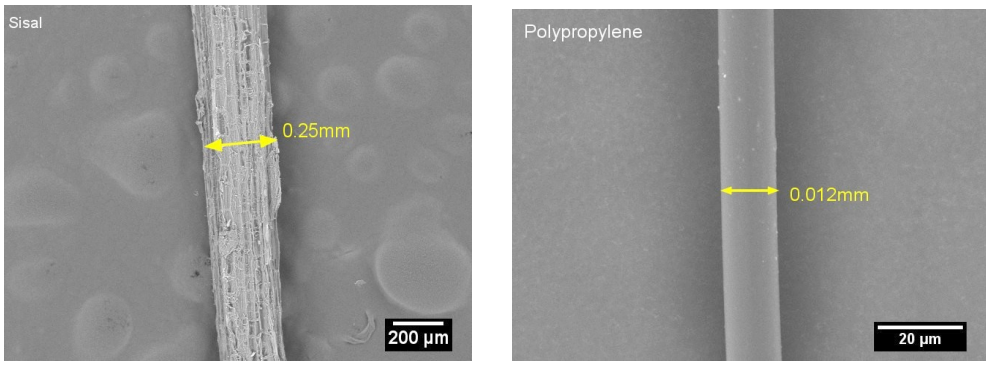

Figure 6:40 BSE images of fibres showing morphology

6.2.2 Preparation of specimens

Composites with fibre volume fractions of 1% were prepared in the laboratory using extrusion technique. Selection of fibre content was based on optimum levels allowing for effective paste extrusion. Alkaline activator solution was produced by dissolving sodium hydroxide and sodium silicate powder in deionized water in mass ratios of 3% and 0.75% respectively by dry weight of soil. The paste was obtained by mixing alkali activator solution with the soil in a mass ratio (i.e. soil moisture content) of 25%, which corresponds to the plastic limit of the soil. This moisture content was selected based on findings from Maskell et al. [18]. In the preparation sequence, the dry soil -fibre mixture was homogenised using a high energy intensive Eirich mixer (capacity 10l) for 5mins at high speed before the introduction of the alkali activator solution with additional mixing for 5mins. The fibre-soil paste was transferred to a Gelenski MVIG-05 laboratory extruder with a cross section die width/height ratio of 3.3 and operating at a linear speed of approximately 4mm/s. Plates of 200mm×50mm×15mm were produced. Samples were cured initially at elevated temperature of 105°C for 5hrs and left in the laboratory at room temperature of 24C±2 and RH of 60% and tested after 14 days in accordance with procedures developed in [19].

6.2.3 Experimental Methods

Grid Nanoindentation

Grid nano-indentation array consisting of a large number of indentations was performed at random locations. For heterogeneous materials composed of N different phases, this technique can provide both quantitative and qualitative data on the mechanical properties in the material [17]. Samples for nanoindentation (10mm sized cubes) were embedded in epoxy resin and allowed to harden over a 24hr period. The hardened samples were ground sequentially using SiC papers with grit sizes #500, #1000, #2000 & #4000 followed by finer polishing using diamond abrasives. Specimen surfaces were cleared by washing in alcohol and ultrasonic bath to remove lose debris on the surfaces. By using such procedures, satisfactorily smooth surfaces have been obtained for cement based composites [20].

Indentation was performed using a T1 950 Hysitron TriboIndenter with a berkovich tip. For the grid indentation to be representative of mechanical phases present and not be a function of bulk material properties, loads were chosen such that indentation depths satisfied conditions governed

by length scales i.e indentation depths are shallow enough to satisfy the criterion $\frac{h}{D}<0.1$ where h is indentation depth and D is characteristic particle size. As a result, a peak load of 500μN was selected which led to maximum penetration depth ranging from 500 to 700nm. Information was obtained from a matrix of 100 indents covering a representative area of 70×70μm^2. Due to varying heterogeneous composition of all samples, at least three grid indentation series were performed on each sample on separate locations to ensure that the results were representative and reproducible. Elastic properties were evaluated from the Load-displacement curves according to Oliver and Pharr method [21].

Statistical Deconvolution

Following grid indentation, individual phase properties were determined by statistical deconvolutions applied to histograms. Modulus and hardness values followed the same trends and hence only Modulus values were analysed statistically. Using a bin size of 1GPa which is reasonable for structural materials [22], histograms were plotted against frequency density. Experimental probability density function (PDF) was computed as

$$p_i^{\exp}=\frac{f_i^{\exp}}{N^{\exp}}.\frac{1}{b} \qquad \text{(i)}$$

where p_i^{exp} = experimental PDF, f_i^{exp} = frequency of values, N^{exp} = effective indentation experiments and b = bin size. Deconvolution of M phases involves finding $j = 1,2,3\ldots M$ individual PDFs related to a single material phase. Assuming a normal distribution, PDF for a single phase can be written as

$$p_j(x)=\frac{1}{\sqrt{2\pi s_j^2}}\exp\frac{-(x-\mu_j)^2}{2s_j^2} \qquad \text{(ii)}$$

where p_j is the theoretical PDF of the jth phase with μ_j and s_j as the mean and standard deviations of the jth phase respectively. The overall PDF covering all M phases is then represented by

$$C(x)=\sum_{j=1}^{M} f_j p_j(x) \qquad \text{(iii)}$$

where f_j is the volume fraction of a single phase.

Deconvolution into phases was conducted under the assumption that values of E ≥ 20GPa could be attributed to silt inclusions and were not considered due to their random occurrence in different grids.

Mechanical Testing

Mechanical tests were performed within a laboratory environment after hygroscopic stabilisation to a relative humidity of ≈ 60% and a temperature of ≈26°C using a servo-hydraulic mechanical testing machine MTS model 370.02. With the aid of a diamond saw blade, prismatic specimens (80 mm×13 mm ×13 mm) were prepared after which grinding and polishing of the specimen sides was carried out. A three point bending test configuration with span of 52 mm was used to determine flexural strengths and stress intensity values of the samples. For each composite formulation, a minimum of five specimens were tested.

Modulus of Rupture (MOR) values were obtained using samples without notch based on the equation:

$$\sigma_f = \frac{3PS}{2BH^2} \qquad \text{(iv)}$$

where P is the maximum load, S is the loading span, B and H are specimen breadth and height respectively. Tests were conducted using a crosshead speed of 1 mm/min.

Fracture toughness (under Mode 1 loading, K_{1C}) was determined to evaluate the materials resistance to crack propagation and was performed using Single Edge Notched Bend (SENB) type specimens. Notches to a depth equal to 45% of the specimen height were prepared using a diamond disc of 0.5mm thick to initiate a sharp crack. A crosshead speed of 15 mm/min was applied. The values of the maximum load P from the load displacement curves were applied in the calculation of K_{1C} using the following equation in accordance with ASTM E399

$$K = \frac{PSf\left(\frac{a}{w}\right)}{BW^{1.5}} \qquad \text{(v)}$$

where $$f\left(\frac{a}{W}\right)=\frac{3(a/W)^{0.5}\left[1.99-(a/W)(1-a/W)\left(2.15-3.93(a/w)+2.7\left(a^2/W^2\right)\right)\right]}{2(1+2a/W)(1-a/W)^{1.5}}$$ (vi)

and P is the maximum applied load, B and W are specimen thickness and depth respectively, S is the span and a is the crack length. This equation was adopted under the assumption that plastic deformations are limited and the material is substantially brittle such that Linear Elastic Fracture Mechanics (LEFM) can be applied satisfactorily.

Resistance curve experiments were conducted to evaluate the toughening contributions induced by the fibres. Resistance curve experiments were performed on SENB specimen configurations used for fracture toughness tests. Crack growth was monitored using an optical microscope (Miscropio Digital) and connected to a video monitoring system. Stress intensity factors corresponding to crack extensions were obtained from equation 5.

6.3 Results And Discussion

6.3.1 Grid Nanoindentation

In order to determine the validity of each indentation, indentation load-depth (P-h) curves were viewed prior to statistical deconvolution to ensure that criterion of length scales was satisfied. Typical P-h curves are illustrated in Figure 6.4 showing maximum penetration depth of 550 nm.

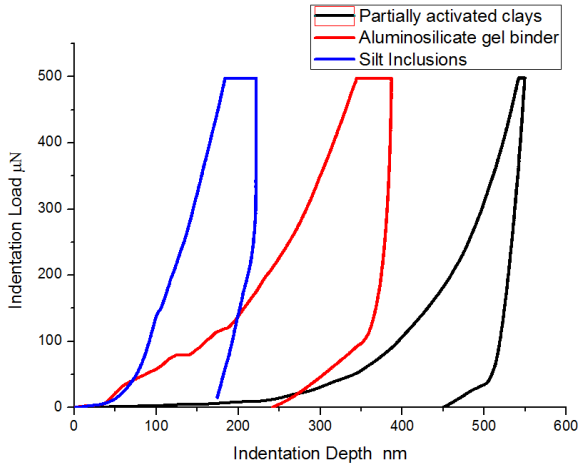

Figure 6:41 Typical indentation load-depth curves

The results of a grid indentation array on the unreinforced matrix is presented in Figure 6.5. The optical micrograph shows the location were the grid array was performed and the corresponding mechanical property maps. Discrete data from each grid was transformed into a continuous distribution of mechanical properties by linearly interpolating the grid point values over the grid region. Spatial representation of mechanically distinct phases shows morphological arrangement of the different phases. Matrix is predominantly characterized by areas of low modulus and hardness indicating large fraction of areas of low porosities. The maps show a general correlation between indentation modulus and hardness properties/distribution.

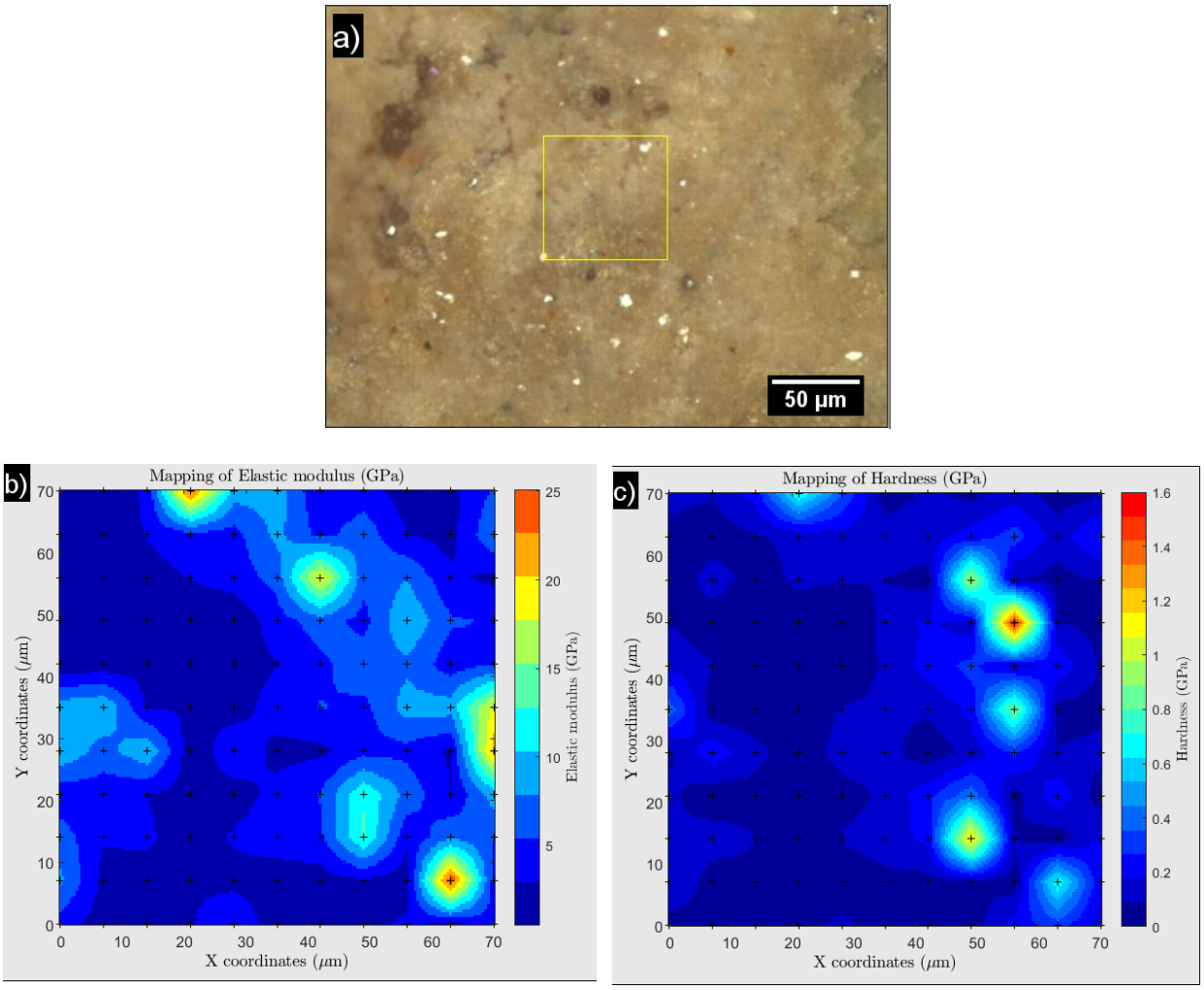

Figure 6:42 (a) Optical image of unreinforced matrix showing location of grid indentation; (b) corresponding indentation modulus map and (c) hardness map

6.3.2 Statistical Deconvolution

The experimental frequency plots of indentation modulus is presented in Figure 6.6.

Hardness data are consistent with indentation moduli peaks and are presented in supplementary article. Following deconvolution of the histograms of the indentation modulus and hardness with reference to previous studies [23,24], two distinct phases can be categorized as follows:

- Partly activated minerals: $2 \leq M \leq 5.5$ GPa and $0.1 \leq H \leq 0.35$ GPa
- Aluminosilicate gels: $5.5 \leq M \leq 20$ GPa and $0.35 \leq H \leq 1.5$ GPa

The aluminosilicate gel is the binder phase and the main product of alkali activation of muscovite minerals within the soil. Frequency plots for unreinforced matrix as well as sisal reinforced composites show single modal peaks which correspond to partially alkali activated binders. On the other hand, inclusion of polypropylene reinforcements results in multimodal peaks which correspond to alkali activated phases alongside partially activated phases. Variation of mechanical properties at this scale suggests that binder phase formation was influenced by the presence of fibres.

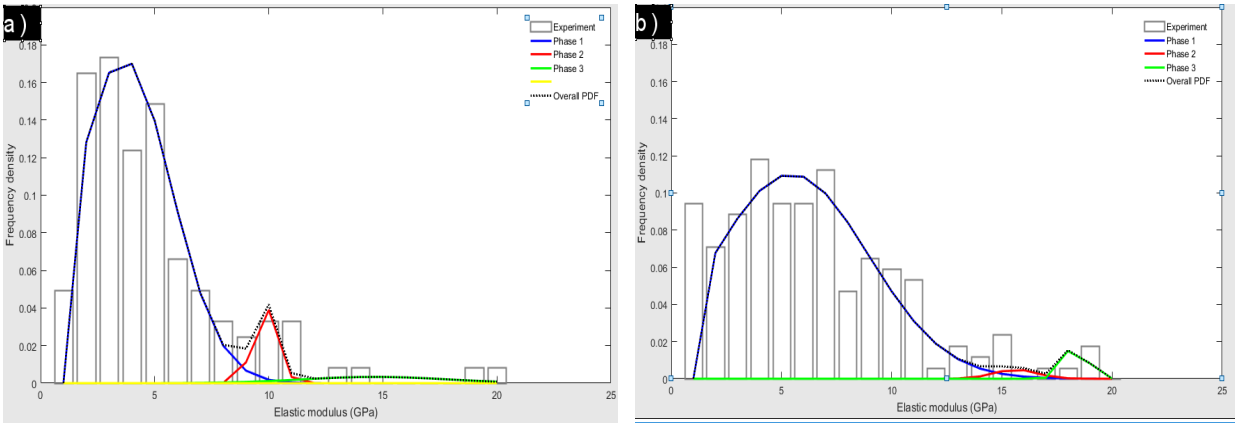

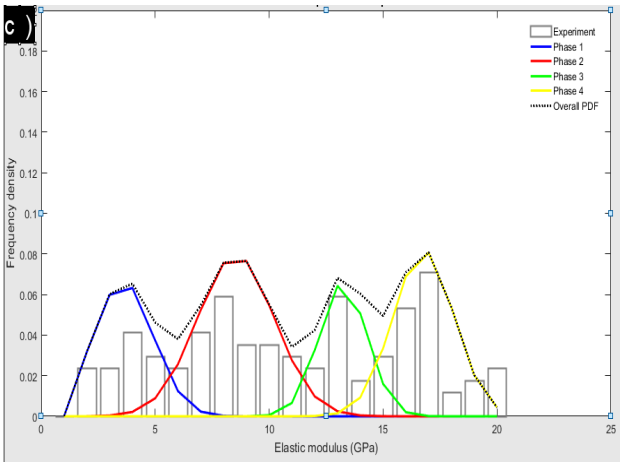

Figure 6:43 Experimental PDF and deconvolution results of (a) unreinforced matrix (b) sisal reinforced composite and (c) polypropylene reinforced composite

Alkaline activation of aluminosilicates is essentially a moisture dependent process[25] and the presence of hydrophilic sisal fibres may have placed a moisture demand on the alkali activators resulting in partial activation of muscovite minerals. The extracted indentation moduli and respective volume fractions are presented in the Table 6.1 which shows very low volume fractions of fully reacted phases in sisal reinforced composites. These fully reacted phases have been directly associated with strength gain suggesting that higher volumes would result in better mechanical strength [24].

Table 6:17 Indentation Modulus and volume fractions for different phases

Reinforcement type	Unreinforced		Sisal reinforced		Polypropylene reinforced	
	Modulus GPa	Vol. %	Modulus GPa	Vol. %	Modulus GPa	Vol. %
Partially activated phases 2 ≤ M ≤ 5.5 GPa 0.1 ≤ H ≤ 0.35 GPa	*4.16 ± 2.32*	*74.6*	*5.38 ± 3.42*	*96.4*	*5.69 ± 2.33*	*38.8*
Alkali activated phases 5.5 ≤ M ≤ 20 GPa 0.35 ≤ H ≤ 1.5 GPa	*13.33 ± 3.6*	*25.4*	*17.44 ± 1.52*	*3.6*	*16.47 ± 4.23*	*61.2*

6.3.3 Flexural Characteristics

The results of the comparative three point flexure tests are presented in Figure 6.7 and shows that fibre reinforcement leads to a 47% increase in Modulus of Rupture relative to the unreinforced matrix. Although there was no significant difference observed in the MOR values obtained with sisal and polypropylene reinforcements, there was a significant difference in their post cracking behaviour. Analysis of representative load-deflection curves in the post-cracking zone presents an indication of the quality of the composite from a crack control perspective as it represents the strain capacity and toughness of the composite which may be more significant than flexural strength [12]. Whilst failure of the unreinforced matrix was characterised by localisation at peak load with sudden drop of load carrying capacity of the matrix, incorporation of polypropylene fibres slightly modified the first cracking stress observed in the unreinforced matrix. This was followed by a deflection hardening region where strength carried by the matrix was imposed on the bridging fibres and strength carrying capacity increased beyond the matrix cracking stress to a maximum value which corresponded to the ultimate strength of composite. Strain capacity was considerably enhanced in the deflection hardening region. This behaviour is consistent with results from other studies [26]. This flexural response observed with polypropylene fibres suggests that fibre volume fraction was equivalent or higher than the critical volume fraction for this class of materials. Polypropylene reinforcement transformed brittle matrix to a quasi-brittle material with significantly modified ductility and present an attractive combination of strength, modulus and ductility at fibre volume fraction as low as 1%.

On the other hand, sisal reinforcement significantly modified matrix cracking strength which coincided with MOR of composite and subsequently exhibited deflection softening behaviour where it gradually lost load carrying capacity. Hence, with sisal fibres, higher stresses would be required for matrix crack initiation. Consequently, strain at peak load corresponded to matrix strain. Strengthening effect due to sisal fibres could be attributed to higher stiffness of sisal fibres which resulted in a higher modulus of elasticity of the composite relative to the unreinforced matrix. The implication of the drop in peak load after first cracking in sisal reinforced composites is that load bearing capacity of the sisal fibres was lower than the load on the composite at first crack. Inability of the fibres to sustain the load indicate that volume fraction of fibres was not sufficient to redistribute the load between the matrix and fibres. As a result, the composites were matrix controlled and failure mode was characterised by propagation of a single

crack. This behaviour is consistent with reinforcement of earth/concrete with macrofibres where large dimensions of fibres are only able to bridge and interact with macrocracks [27]. In addition, low aspect ratio implies smaller number of fibres which are spaced to far apart to interact and arrest small cracks [27]. This suggests that using longer lengths of sisal fibres would result in higher aspect ratios therefore resulting in longer bridging lengths to generate a stresses equal to the fibre strength leading to deflection hardening behaviour.

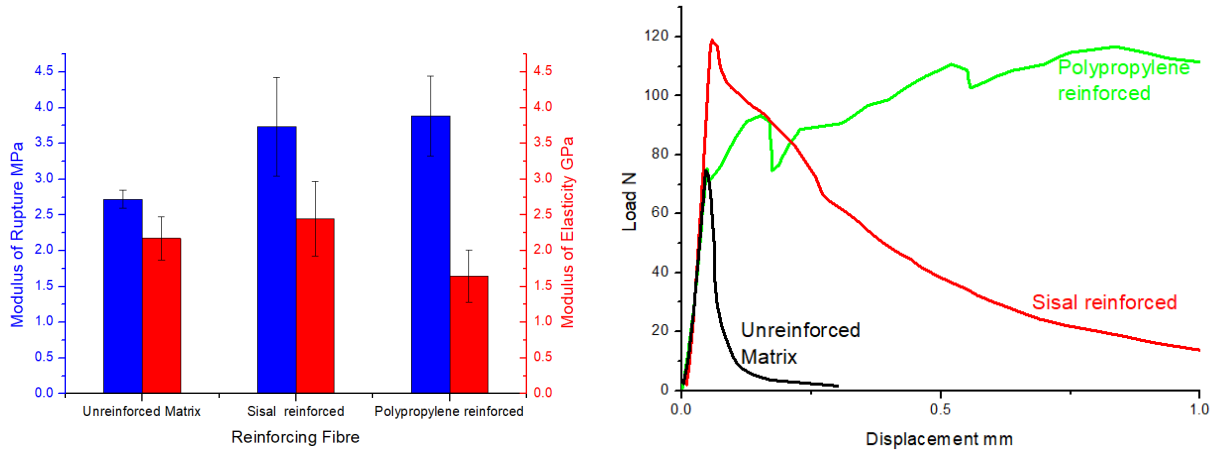

Figure 6:44 Variation of MOR with fibre reinforcement for un-notched specimens

6.3.4 Strengthening mechanisms in Composites

The stress-strain curves observed with the composites elucidates the different mechanisms which control the behaviour of the composites. Strengthening induced by sisal fibres takes place in the linear elastic region whereas strengthening with polypropylene counterparts was observed in the post-crack region. Based on analysis of load-deflection curves, composite strength and modulus were rationalised using existing analytical micromechanical models based on fibre-matrix stress transfer mechanisms. Flexural behaviour of sisal reinforced composites (where MOR of composites corresponds to LOP and matrix failure strain does not change) indicates elastic stress transfer as the dominant stress transfer mechanism. This implies elastic shear transfer at the fibre matrix interface may be used to predict the overall strength of the composite. As a result, the rule of mixture aligned and discontinous fibres (eqn vii) and shear lag model (eqn viii) which characterises stress transfer in the elastic zone, were used to rationalise the flexural response in sisal reinforced composites.

$$E_c = E_m V_m + n_{ı} E_f V_f \; ; \qquad \sigma_c = \sigma_m V_m + n_{ls} \sigma_f V_f \qquad \text{(vii)}$$

$$\frac{E_c}{E_m} = V_m + V_f \left(\frac{E_f}{E_m} \right) \left[1 - \frac{\tanh(x)}{x} \right] \; ; \qquad \frac{\sigma_c}{\sigma_m} = 0.5 V_f \left(2 + \frac{l}{d} \right) + (1 - V_f) \qquad \text{(viii)}$$

where $x = \frac{l}{d} \left[(1 + \upsilon_m) \frac{E_f}{E_m} \ln (V_f)^{-1/2} \right]^{-1/2}$

and E_c, E_m and E_f are the respective Young's moduli of the composite, matrix and fibre; V_m and V_f are the respective volume fractions of matrix and fibre; and σ_c, σ_m and σ_f are the respective flexural strengths of the composite, matrix and fibre; $\frac{l}{d}$ is the fibre aspect ratio; $n_{ı}$, n_{ls} are fibre efficiency factor for discontinous fibres for stiffness and strength and υ_m is Poisson's ratio of the matrix.

These models were originally developed for composites subjected to tensile loading, but have shown potential in the prediction in flexural strength of composites. On the other hand, post-cracking flexural behaviour observed with polypropylene reinforced composites indicates that contribution of matrix to overall composite strength is negligible and failure in the post-cracking zone occurs primarily by pull-out. Hence, process controlling stress transfer is frictional slip since frictional stress develops at the interface after debonding assuming a constant frictional bond strength, flexural strength of the composite was rationalised using a modified equation in [12,28]

$$\sigma_c = \tau_{fu} V_f \frac{l}{d} \qquad \text{(ix)}$$

where τ_{fu} is the frictional bond strength

A comparison between experimental observations and predicted values is presented in Table 6.2.

Table 6:18: Comparison between experimental and predicted flexural properties of composites

		Experimental	Simple ROM	Shear Lag	Modified ROM
Sisal	Modulus (GPa)	2.44	2.34	2.32	
	Strength (MPa)	3.89	3.72	3.87	3.54

Polypropylene	Modulus (GPa)	1.66	2.25	2.25	
	Strength (MPa)	3.88	5.15	10.71	3.52

ROM and shear lag models show good correlation with experimental data obtained for sisal reinforced composites but over estimate values for polypropylene reinforced composites. This is expected since overall contribution of matrix to flexural strength is negligible and hence the modified equation which is dependent on frictional bond strength gives a better correlation with experimental data. The fit of experimental data to these models suggests that composite strength can be engineered by improving fibre strength with sisal fibres and aspect ratio of pp fibres even at volume fractions as low as 1%.

6.3.5 Fracture Toughness

Effects of fibre reinforcement on the fracture toughness of alkali activated earth-based matrices are presented in Figure 6.8. In toughening, key concept is the shielding of crack tip from applied forces such that higher levels of remote stresses can be applied before critical conditions are reached [29]. Low value of fracture toughness of unreinforced matrix confirms high sensitivity of these materials to defects at low stress levels. Reinforcement with polypropylene leads to significant improvement (over 200%) in the fracture behaviour of the unreinforced matrix. Smaller, but significant (72%) improvements were observed with sisal reinforced composites. Significant improvement associated with fibre reinforcements indicates that fibres present enhanced shielding under a remotely applied stress despite the presence of microcracks and flaws which may act as stress risers. High aspect ratio of polypropylene fibres increases the probability of intersection with the crack thereby enhancing toughening by creating a larger shielding zone of continuous bridges in the crack wake [30]. With fibre reinforcements, mechanisms that take place in the crack wake and the crack bridging effect may shield the crack-tip from the far-field applied stresses thereby toughening the brittle materials[31]. This crack wake mechanisms because of their cumulative nature give rise to a rising r-curve behaviour where fracture resistance increases with crack extension.

Load-deflection curves show peak load observed with the notched sisal reinforcement is not significantly different from matrix peak load further confirming that composite is matrix

controlled and hence, notch sensitive. However, energy absorption associated with sisal reinforcement is significantly higher relative to the matrix. On the other hand polypropylene reinforcement shows increase in peak load as well as energy absorption over the unreinforced matrix.

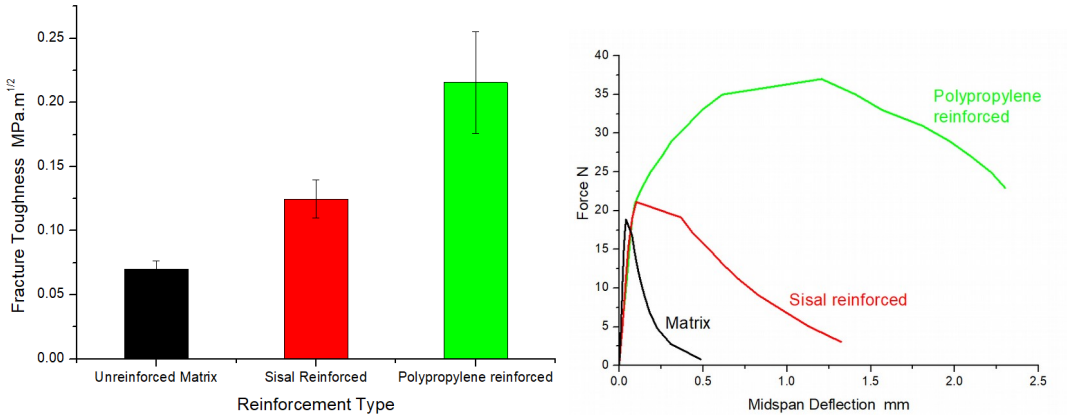

Figure 6:45 Variation of Fracture Toughness with fibre reinforcement for notched specimens

6.3.6 Toughening Mechanisms in Composites

From experimental observations, the source of toughening in the composites was associated principally with crack tip shielding arising from fibre bridging. Optical images taken during experiments are presented in Figure 6.9 and show such as bridging associated with both fibres. Synergistic fibre bridging and pull-out toughening mechanisms have been reported as predominant mechanisms in natural fibre reinforced earth-based matrices [32].

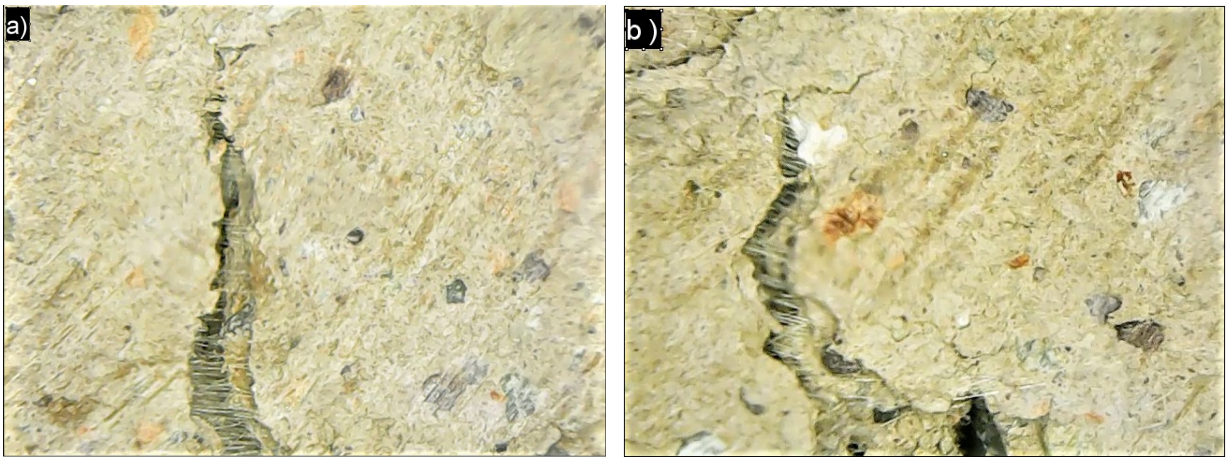

Figure 6:46 Crack bridging by fibres in composites reinforced with (a) Sisal and (b) Polypropylene

Quantitatively, the toughening contribution due to crack bridging by the different fibres was rationalised using crack bridging models to explore the extent to which measured resistance curves can be predicted by micromechanical bridging models. Bridging models based on an idealized elastic-plastic spring model originally proposed by Budiansky et al. [33], has been used by various studies [34–37] to study toughening due to small scale bridging (SSB). For SSB conditions, the bridge length corresponds to values below 0.5mm and the ductile phase toughening contribution to fracture toughness may be expressed as

$$\Delta K_{SSB} = \sqrt{\frac{2}{\pi}\alpha V_f \int_0^L \frac{\sigma_y}{\sqrt{x}} dx} \qquad \text{(x)}$$

where ΔK_{SSB} is toughening due to SSB, α is the constraint/triaxiality factor, V_f is the volume fraction of the fibres, L is the length of bridging ligament, σ_y is the uniaxial yield stress and x corresponds to the distance from the crack tip.

For large scale bridging (LSB) conditions, i.e where bridge lengths exceed 0.5mm, toughening due to ligament bridging developed by Bloyer was used and is given by

$$\Delta K_{LSB} = V_f \int_0^L \alpha \sigma_y h(a, x)\, dx \qquad \text{(xi)}$$

where ΔK_{LSB} is toughening contribution due to LSB, and *h(a,x)* is the weighting function given by Fett and Munz [38] as

$$h(a,x)=\sqrt{\frac{2}{\pi a}\frac{1}{\sqrt{1-\frac{x}{a}}}\left(1+\sum_{(v,u)}\frac{A_{v,u}\left(\frac{a}{W}\right)}{\left(1-\frac{a}{W}\right)}\left(1-\frac{x}{a}\right)^{v+1}\right)} \qquad \text{(xii)}$$

where the coefficients $A_{v,u}$ for and SENB specimen can be found in Fett and Munz.

Initiation fracture toughness K_i was determined using stress intensity equations for SENB specimens in accordance with ASTM E399. Hence, composite fracture toughness, $K_R$was determined by the following expression

$$K_R=K_i+\Delta K_B \qquad \text{(xiii)}$$

where ΔK_B represents toughening contribution for either SSB or LSB conditions.

6.3.7 Resistance Curve Behaviour

Figure 6.10 presents rising R-curve behaviour of composites and demonstrates the rising stress intensity factors with crack growth. Whilst single value parameter (K_{1C}) have traditionally been used to characterise fracture resistance, they do not adequately evaluate the toughening arising from fibre reinforcement. Compared with fracture toughness of 0.07 MPa$\sqrt{m}$ for the unreinforced matrix, addition of sisal and polypropylene fibres resulted in an initiation toughness of 0.11 MPa$\sqrt{m}$ and 0.14 MPa$\sqrt{m}$ respectively. Both SSB and LSB models capture general trends of experimental R-curves confirming that crack bridging is the dominant crack tip shielding mechanism and toughening can be reasonably predicted by crack bridging models. Bridging models give a closer prediction of resistance curve behaviour of sisal reinforced composites suggesting crack bridging to be predominant toughening mechanism. This is understandable given morphology of sisal fibres which would favour anchoring. On the other hand, weak fibre matrix interactions with polypropylene fibres would suggest debonding and pull-out may also contribute to toughening.

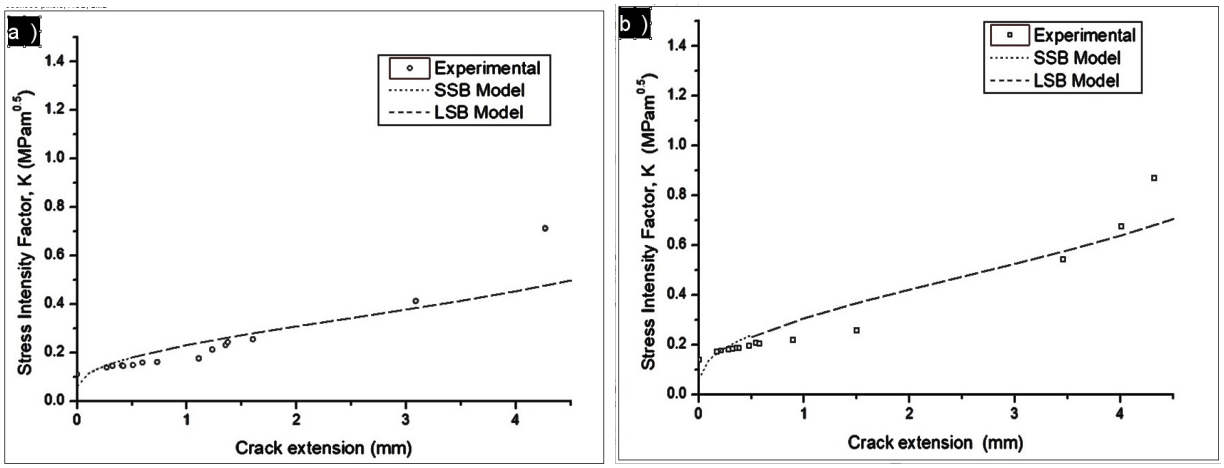

Figure 6:47 Experimentally measured r-curves with predictions from bridging models for composites with reinforced with a) sisal and b) polypropylene

6.4 Summary/Conclusions

In this study, earthen based composites were produced using uncalcined clays and weak alkali activator solutions with two different types of fibre reinforcements; sisal and polypropylene. They were characterized at multiscales by macro-mechanical and nano grid indentation to evaluate reinforcing efficiency of fibres for this class of materials. Nano-mechanical properties of composites was determined via a combination of nanoindentation and statistical deconvolution techniques to enable identification of distinct binder phases as well as respective volume fractions associated with different fibre reinforcements. Strength and resistance curve behaviour of the composites were analysed based on existing micromechanical models and attempts were made to predict the composite flexural properties and resistance curve behaviour. Efficiency of fibre reinforcement type was judged based on enhancement in strength and fracture resistance relative to the unreinforced matrix.

The following conclusions can be drawn based on this study:

- Significant strengthening as well as stiffening of the unreinforced earthen matrix was observed with sisal fibre reinforcements. This strengthening contribution was via an elastic stress transfer mechanism attributed to fibre-matrix interactions. Predictions from simple rule of mixtures and shear lag models provide compared satisfactorily with experimental measurements.

- Significant strength and ductility were introduced in the earth-based matrix due to reinforcement with polypropylene fibres. Brittle matrix was transformed to a quasi-brittle materials with multiple cracking and deflection hardening beyond the point of first cracking with an attendant increase in energy absorption capacity at volume fraction as low as 1% polypropylene. Strengthening contribution was observed in the post-cracking region, as a result contribution of matrix to composite strength was negligible. Modified ROM model based on frictional slip was used to rationalise composite strength and modulus with satisfactory correlations with experimental measurements.
- Crack-tip shielding was predominantly due to crack bridging and prediction from bridging models correlate with experimental values for both sisal and polypropylene fibres.
- At the scale where mechanics meets chemistry, results from the nanoindentation showed fibre reinforcements altered microstructure by influencing the formation of binder phases within the alkali activated systems. Hydrophillic sisal fibres absorbed alkali activation solutions thereby reducing the degree of alkali activate binder phases in the matrices.

References

[1] F. Pacheco-Torgal, S. Jalali, Earth construction: Lessons from the past for future eco-efficient construction, Constr. Build. Mater. 29 (2012) 512–519. doi:10.1016/j.conbuildmat.2011.10.054.

[2] C. Galán-Marín, C. Rivera-Gómez, J. Petric, Clay-based composite stabilized with natural polymer and fibre, Constr. Build. Mater. 24 (2010) 1462–1468. doi:10.1016/j.conbuildmat.2010.01.008.

[3] C.A. Dove, F.F. Bradley, S. V. Patwardhan, Seaweed biopolymers as additives for unfired clay bricks, Mater. Struct. Constr. 49 (2016) 4463–4482. doi:10.1617/s11527-016-0801-0.

[4] J. Nakamatsu, S. Kim, J. Ayarza, E. Ramírez, M. Elgegren, R. Aguilar, Eco-friendly modification of earthen construction with carrageenan: Water durability and mechanical assessment, Constr. Build. Mater. 139 (2017) 193–202. doi:10.1016/j.conbuildmat.2017.02.062.

[5] H. Danso, D.. Martinson, M. Ali, J.. Williams, Physical, Mechanical, Durability Properties of soil building blocks reinforced with natural fibres, Constr. Build. Mater. 101 (2015) 797–809.

[6] M.C.N. Villamizar, V.S. Araque, C.A.R. Reyes, R.S. Silva, Effect of the addition of coal-ash and cassava peels on the engineering properties of compressed earth blocks, Constr. Build. Mater. 36 (2012) 276–286. doi:10.1016/j.conbuildmat.2012.04.056.

[7] D. Maskell, A. Heath, P. Walker, Use of metakaolin with stabilised extruded earth masonry units, Constr. Build. Mater. 78 (2015) 172–180. doi:10.1016/j.conbuildmat.2015.01.041.

[8] J.E. Oti, J.M. Kinuthia, R.B. Robinson, The development of unfired clay building material using Brick Dust Waste and Mercia mudstone clay, Appl. Clay Sci. 102 (2014) 148–154. doi:10.1016/j.clay.2014.09.031.
[9] S.A. Lima, H. Varum, A. Sales, V.F. Neto, Analysis of the mechanical properties of compressed earth block masonry using the sugarcane bagasse ash, Constr. Build. Mater. 35 (2012) 829–837. doi:10.1016/j.conbuildmat.2012.04.127.
[10] J.-C. Morel, K. Ghavami, A. Mesbah, Theoretical and Experimental Analysis of Composite Soil Blocks Reinforced with Sisal Fibres Subjected to Shear by, Mason. Int. 13 (2000) 54–62.
[11] S.M. Hejazi, M. Sheikhzadeh, S.M. Abtahi, A. Zadhoush, A simple review of soil reinforcement by using natural and synthetic fibers, Constr. Build. Mater. 30 (2012) 100–116. doi:10.1016/j.conbuildmat.2011.11.045.
[12] A. Bentur, S. Mindess, Fibre Reinforced Cementitious Composites, Second Edition, Taylor & Francis, 2006.
[13] J. Davidovits, Geopolymer : chemistry and applications, Institut Geopolymere, Saint-Quentin, 2011.
[14] P. Duxson, A. Fernández-Jiménez, J.L. Provis, G.C. Lukey, A. Palomo, J.S.J. Van Deventer, Geopolymer technology: The current state of the art, J. Mater. Sci. 42 (2007) 2917–2933. doi:10.1007/s10853-006-0637-z.
[15] P. Krivenko, Why alkaline activation - 60 years of the theory and practice of alkali-activated materials, J. Ceram. Sci. Technol. 8 (2017) 323–333. doi:10.4416/JCST2017-00042.
[16] G. Constantinides, F.-J. Ulm, K. Van Vliet, On the use of nanoindentation for cementitious materials, Mater. Struct. 36 (2003) 191–196. doi:10.1007/BF02479557.
[17] G. Constantinides, K.S. Ravi Chandran, F.-J. Ulm, K.J. Van Vliet, Grid indentation analysis of composite microstructure and mechanics: Principles and validation, Mater. Sci. Eng. A. 430 (2006) 189–202. doi:https://doi.org/10.1016/j.msea.2006.05.125.
[18] D. Maskell, A. Heath, P. Walker, Laboratory scale testing of extruded earth masonry units, Mater. Des. 45 (2013) 359–364. doi:10.1016/j.matdes.2012.09.008.
[19] E.B. Ojo, K. Mustapha, R.S. Teixeira, H. Savastano, Development of unfired earthen building materials using muscovite rich soils and alkali activators, Case Stud. Constr. Mater. 11 (2019) e00262. doi:https://doi.org/10.1016/j.cscm.2019.e00262.
[20] R.S. Teixeira, G.H.D. Tonoli, S.F. Santos, E. Rayón, V. Amigó, H. Savastano, F.A. Rocco Lahr, Nanoindentation study of the interfacial zone between cellulose fiber and cement matrix in extruded composites, Cem. Concr. Compos. 85 (2018) 1–8. doi:https://doi.org/10.1016/j.cemconcomp.2017.09.018.
[21] W.C. Oliver, G.M. Pharr, An improved technique for determining hardness and elastic modulus using load and displacement sensing indentation experiments, J. Mater. Res. 7 (1992) 1564–1583. doi:DOI: 10.1557/JMR.1992.1564.
[22] J. Němeček, V. Šmilauer, L. Kopecký, Nanoindentation characteristics of alkali-activated aluminosilicate materials, Cem. Concr. Compos. 33 (2011) 163–170. doi:https://doi.org/10.1016/j.cemconcomp.2010.10.005.
[23] M. Zhang, M. Zhao, G. Zhang, T. El-Korchi, M. Tao, A multiscale investigation of reaction kinetics, phase formation, and mechanical properties of metakaolin geopolymers, Cem. Concr. Compos. 78 (2017) 21–32. doi:10.1016/j.cemconcomp.2016.12.010.
[24] H. Lee, V. Vimonsatit, P. Chindaprasirt, Mechanical and micromechanical properties of

alkali activated fly-ash cement based on nano-indentation, Constr. Build. Mater. 107 (2016) 95–102. doi:https://doi.org/10.1016/j.conbuildmat.2015.12.013.
[25] J. Xie, O. Kayali, Effect of initial water content and curing moisture conditions on the development of fly ash-based geopolymers in heat and ambient temperature, Constr. Build. Mater. 67 (2014) 20–28. doi:https://doi.org/10.1016/j.conbuildmat.2013.10.047.
[26] G. Araya-Letelier, J. Concha-Riedel, F.C. Antico, C. Sandoval, Experimental mechanical-damage assessment of earthen mixes reinforced with micro polypropylene fibers, Constr. Build. Mater. 198 (2019) 762–776. doi:https://doi.org/10.1016/j.conbuildmat.2018.11.261.
[27] C. Yi, C.P. Ostertag, Strengthening and toughening mechanisms in microfiber reinforced cementitious composites, J. Mater. Sci. 36 (2001) 1513–1522. doi:10.1023/A:1017557015523.
[28] Y.W. Mai, Strength and fracture properties of asbestos-cement mortar composites, J. Mater. Sci. 14 (1979) 2091–2102. doi:10.1007/BF00688413.
[29] W. Soboyejo, Mechanical Properties of Engineered Materials, CRC Press, 2002.
[30] D.R. Bloyer, R.O. Ritchie, K.T. Venkateswara Rao, Fracture toughness and R-Curve behavior of laminated brittle-matrix composites, Metall. Mater. Trans. A. 29 (1998) 2483–2496. doi:10.1007/s11661-998-0220-0.
[31] M. Sakai, R.C. Bradt, Fracture toughness testing of brittle materials, Int. Mater. Rev. 38 (1993) 53–78. doi:10.1179/imr.1993.38.2.53.
[32] K. Mustapha, S.T. Azeko, E. Annan, M.G. Zebaze Kana, L. Daniel, W.O. Soboyejo, Pull-out behavior of natural fiber from earth-based matrix, J. Compos. Mater. 50 (2016) 3539–3550. doi:10.1177/0021998315622247.
[33] B. Budiansky, J.C. Amazigo, A.G. Evans, Small-scale crack bridging and the fracture toughness of particulate-reinforced ceramics, J. Mech. Phys. Solids. 36 (1988) 167–187. doi:https://doi.org/10.1016/S0022-5096(98)90003-5.
[34] K. Mustapha, E. Annan, S.T. Azeko, M.G. Zebaze Kana, W.O. Soboyejo, Strength and fracture toughness of earth-based natural fiber-reinforced composites, J. Compos. Mater. 50 (2016) 1145–1160. doi:10.1177/0021998315589769.
[35] H. Savastano, S.F. Santos, M. Radonjic, W.O. Soboyejo, Fracture and fatigue of natural fiber-reinforced cementitious composites, Cem. Concr. Compos. 31 (2009) 232–243. doi:https://doi.org/10.1016/j.cemconcomp.2009.02.006.
[36] H. Jr Savastano, A. Turner, C. Mercer, W.O. Soboyejo, Mechanical behavior of cement-based materials reinforced with sisal fibers, J. Mater. Sci. 41 (2006) 6938–6948. doi:10.1007/s10853-006-0218-1.
[37] T. Tan, S.F. Santos, H. Savastano, W.O. Soboyejo, Fracture and resistance-curve behavior in hybrid natural fiber and polypropylene fiber reinforced composites, J. Mater. Sci. 47 (2012) 2864–2874. doi:10.1007/s10853-011-6116-1.
[38] T. Fett, D. Munz, Stress lntensity Factors and Weight Functions for One-dimensional Cracks Kernforschungszentrum Karlsruhe, (1994).

7.0 Chapter 7: Concluding Remarks and Suggestions for Future Work

7.1 Summary and Concluding Remarks

This thesis has presented and explored efforts to use a material science and engineering approach to engineer earth-based materials with improved properties for applications in building construction. The primary objective was to elucidate the synthesis (processing)-composition-property relationship and how it controls the performance of earth-based composites that are relevant to construction. Research into earthen construction is currently witnessing a boost due to its potential to solve increasing infrastructural challenges in a more sustainable manner. The application of alkali activation as binder mechanism for earthen construction has demonstrated great potential for the development of robust engineered earth based composite. Topics covered in this thesis include: synthesis of alkali activated binders using natural in-situ aluminosilicates in earth-based building materials; rheological characterization of fresh fibre reinforced alkali activated earth-based pastes; physico-mechanical characterization of fibre reinforced composites; strengthening/toughening mechanisms associated with fibre reinforcements.

The main results and conclusions from the above topics are highlighted below in line with the initial objectives of study highlighted in section 1.3

Chapter one presented background leading to unresolved issues associated with the use of alkali activation as binding mechanism in earth-based composites as well as objectives and scope of the work. A study approach on the engineering of earth-based composite based on the materials science and engineering paradigm was presented.

Chapter two presented a state of the art review of literature which presented concepts on the development of earth-based composites as building materials. Attention was given to major drawbacks with focus on binding mechanisms as well as strengthening/toughening improvements using fibre reinforcements, which have been studied. Description of characterization techniques typically used in evaluating these modifications as well as micromechanical models, which describe strengthening and toughening contributions, were discussed. Rheological characterisation techniques associated with fibre reinforcements which control extrudability of fresh paste with respect to extrusion moulding as a processing technique was also discussed.

Chapter three explored the feasbility of producing sustainable building materials from natural aluminosilicate minerals present in soil using low concentration alkali activator solutions. Small scale samples were subjected to different curing regimes to ascertain the effect of initial curing temperature as well as curing duration on the alkali activation and consequent strength development in uncalcined muscovite based soils. The results reveal alkali activation of these clays to be a satisfactory mechanism for the stabilisation of these soils and was evident in the impressive mechanical properties obtained in the dry state relative to other stabilisation mechanisms. These materials may be suitable for load-bearing masonry applications. However, in the saturated condition, sufficient binding for the production of water stable units was achieved only at elevated initial curing temperatures of 105˚C for 5hrs revealing the temperature dependence of the process. This suggests that the scope of application of building units may be expanded to moisture susceptible environments with proper optimisation. Analysis of XRD spectra reveal unreacted clay minerals after alkali activation confirming the low reactivity of the starting clays. However, the presence of this residual clays suggest that the alkali activated clays may retain hygroscopic and moisture buffering properties which is associated with earthen construction thereby enhancing the thermal efficiency of the building. Further studies would need to be conducted to clearly establish the porosity-thermal conductivity behaviour of alkali activated clays. Porous and graded microstructure reveal limitations associated with extrusion moulding and suggest that optimisation of moisture content during moulding will result in enhanced packing density and consequently improved mechanical and physical properties. SEM-EDX/FTIR analysis reveal the formation of phases which are presumably Na-aluminosilicates formed as a result of a dissolution of muscovite and responsible for the binding observed. The variation of the formation of phases with increasing curing temperature further confirm the need of higher temperatures to facilitate the dissolution of alumina and silica species from natural aluminosilicates.

Chapter four presented the results of experimental and analytical studies on the rheological behavior and characterization of a range of soil pastes comprising an alkali activated fresh paste containing different fibres at varying proportions. This enabled the effects of fibre addition on the bulk and interfacial rheology behaviour of earth-based composites to be studied using ram extrusion. The results show that the Benbow-Bridgwater model can be satisfactorily used to characterise the contribution of parallel and convergent fluxes associated with the incorporation

of different fibre reinforcements in an alkali activated earth paste. Fresh alkali activated earth-based composites showed Bingham plastic behaviour at low extrusion rates and demonstrated satisfactory extrudability without the need for rheology modifiers. Introduction of fibres into the fresh paste resulted in two counteracting effects on the extrusion pressures: increase in die entry pressures due to fibre-matrix interaction in the barrel which increased paste viscosity; and reduction in die land wall resistance due decreased wall slip as a result of the presence of longitudinally oriented fibres along the wall-extrudate interface. However, rheological parameters show that convergent flow in the die entry region is the dominant contributor to extrusion pressures for all fibres studied. Fresh pastes incorporating polypropylene fibres showed both greater die entry and die land pressure than that reinforced with sisal fibres of the same fibre length and dosage due to difference in aspect ratio and stiffness. In addition, convergent flows were strongly dependent on fibre content and extrusion velocities. Consequently, polypropylene-soil pastes recorded the highest extrusion pressures at 80% increase relative to the plain soil paste. Addition of E.Pulp fibres caused a slight variation in rheological response indicating that rheological behaviour of soil pastes dominates and fibre content can be varied over a considerable range without unduly affecting pastes extrusion behaviour.

Chapter five presented insights on effect of fibre type and dosage on physical and mechanical properties of the alkali activated soil. Statistically, inclusion of sisal fibre reinforcements significantly modified the matrix attributed to improved packing density obtained during extrusion moulding resulting in an initial increase in density. Effect of E.pulp and polypropylene reinforcements on the density of the unreinforced matrix was not statistically significant. Replacement of soil with fibres of relatively lower densities was expected to reduce overall composite densities. However, at highest fibre content investigated in this study, density of unreinforced composite was statistically equivalent to the reinforced composites. Improved packing densities obtained with sisal fibre reinforcement resulted in statistically significant reductions in water absorption as a result of a more compact fibre-matrix system relative to other fibre reinforcements. Contribution of hydrophilic nature of ligno-cellulosic fibres to water absorption of composites was not significantly observed. SEM/EDS analysis revealed the presence of sodium compounds within ligno-cellulosic fibres indicating chemical reactions between hydroxyl groups on ligno-cellulosic fibres and sodium compounds from the alkali

activated matrix, which may have modified hydrophilic nature of ligno-cellulosic fibres. Average flexural strength of unreinforced alkali activated clay matrix (3.2 MPa) tested in the dry condition was significantly higher than typical range of values obtained from literature (0.13 – 1.67 MPa) for unfired earth, demonstrating the potential of extrusion moulding as well as alkali activation binding mechanism for the production of earthen composites. However, due to low alkalinity of solutions utilised in the study, a significant drop in MOR was observed when samples were tested in saturated conditions. This moisture sensitivity restricts application of this class of materials to moisture-controlled environments. Highest improvement in MOR was achieved with sisal fibres (≈74% increase compared to unreinforced matrix) whilst maximum increase associated with pulp was 29%. In contrast, polypropylene reinforcement demonstrated no significant effect on the MOR of the composites and this may be attributed to a poor fibre-matrix adhesion with increased fibre-fibre interactions. Superior performance in sisal reinforced composites indicate improved fibre-matrix interactions between sisal fibre and the alkali activated matrix which would facilitate effective stress transfer between both phases. Due to improved fibre-matrix interactions, mechanism for crack control potential was achieved via crack bridging as observed via optical images. Pulp reinforcement presented the highest number of reinforcing filaments for an equivalent fibre content. However, beneficial action of fibre reinforcements was not effectively exploited with pulp fibres largely because of fibre length as toughness mechanism was based on crack bridging. Higher reinforcing filaments potentially break up the cohesion in the soil matrix thereby weakening the soil fibre matrix. Consequently, flexural strengths as well as post-crack response were low compared to sisal fibre reinforcements. Whereas ligno-cellulosic fibres introduced deflection softening to the brittle matrices, polypropylene reinforcements transformed unreinforced brittle matrices to deflection hardening composites with failure mode characterized by multiple cracking. This was attributed to high aspect ratio as well as weak fibre matrix interactions.

Chapter six presented a multi-scale characterization of composites by macro-mechanical and nano grid indentation to evaluate reinforcing efficiency of fibres for this class of materials. Efficiency of fibre reinforcement type was judged based on enhancement in strength and fracture resistance relative to the unreinforced matrix. Significant strengthening as well as stiffening of the unreinforced earthen matrix was observed with sisal fibre reinforcements. This strengthening contribution was via an elastic stress transfer mechanism attributed to fibre-matrix interactions.

Predictions from simple rule of mixtures and shear lag models compared satisfactorily with experimental measurements. On the other hand, significant strength and ductility were introduced in the earth-based matrix due to reinforcement with polypropylene fibres. Strengthening contribution was observed in the post-cracking region, as a result contribution of matrix to composite strength was negligible. Modified ROM model based on frictional slip was used to rationalise composite strength and modulus with satisfactory correlations with experimental measurements. Brittle matrix was transformed to quasi-brittle materials with multiple cracking and deflection hardening beyond the point of first cracking with an attendant increase in energy absorption capacity at volume fraction as low as 1% polypropylene. Crack-tip shielding associated with both types of reinforcements was predominantly due to crack bridging and prediction from bridging models correlate with experimental values for both sisal and polypropylene fibres. At the scale where mechanics meets chemistry, results from the nanoindentation showed fibre reinforcements altered microstructure by influencing the formation of binder phases within the alkali activated systems. Hydrophillic sisal fibres absorbed alkali activation solutions thereby reducing the degree of alkali activate binder phases in the matrices.

7.2 Suggestions for future work

Based on major findings from the study, the following areas for future work have been highlighted:

7.2.1 Durability performance tests to characterise deterioration mechanisms

The results from this study have shown that with proper optimisation, alkali activation of aluminosilicates may provide sufficient binding required for development of robust earth based building products. However, the durability of this mechanism is still considered an unproven issue to be elucidated before wide scale adoption. Hence, there is a need to investigate the durability performance of these composites to understand degradation mechanisms. Furthermore, studies on fibre-cement composites have demonstrated deleterious effects of alkaline compounds in the matrix on the reinforcing effect of ligno-cellulosic fibre. This raises questions as to long-term behavior of ligno-cellulosic fibres used as reinforcements in alkali activated earth-based composites. Hence, there is also a need to investigate long term effects of alkaline soil matrix on the structural integrity of this class of fibres. Characterisation of long term interactions between fibre and alkaline matrix through accelerated ageing tests and attendant effect on composite

properties need to be developed to determine the practicability of this technique for the development of durable and robust building materials.

7.2.2 Characterisation of fibre-matrix Interactions

The efficiency of fibres in enhancing the mechanical properties of earth-based materials is largely controlled by the nature of fibre-matrix interactions. As shown in this study, the nature of the fibre plays a critical role in determining the nature of stress transfer at the fibre-matrix interphase. Further tests (such as pull-out or push-in tests) need to be performed to quantify stresses at these interfaces to provide more insight on the fibre-matrix interactions such that these composites can be tailored to fully harness the reinforcing effects of fibres.

7.3 Contribution to Knowledge

The following salient points have been summarised as the major contributions of this study to the existing body of knowledge:

a. This study has demonstrated the feasibility of alkali activation as a binding mechanism of muscovite rich soils via the partial dissolution of muscovite minerals and the formation of sodium-aluminosilicate gels.
b. The study has demonstrated the unique reinforcing effects of different fibre types in the alkali activated soil and the sensitivity of the earth based matrix to variations in fibre volume fraction. This reinforcing efficiency is largely controlled by distinct fibre-matrix interactions.
    - Sisal fibres significantly improved the MOR of the unreinforced matrix indicating improved interactions between sisal fibre and the alkali activated soil which would facilitate effective stress transfer between both phases and introduced a deflection softening behaviour in the post-crack region.
    - Polypropylene reinforcements transformed unreinforced brittle matrices to deflection hardening composites with failure mode characterized by multiple cracking. This was attributed to high aspect ratio of fibres as well as weak fibre-matrix interactions.
    - Beneficial action of fibre reinforcements was not effectively exploited with pulp fibres largely because of limited fibre length and increased fibre-fibre interactions. Consequently, flexural strength modification as well as post-crack response were low compared to sisal fibre.
c. The study has demonstrated significance of moisture condition during testing for this class of earth-based composites.
d. The study has demonstrated synergistic reactions between ligno-cellulosic fibres and alkali activator solutions which control water absorption capacity of composites.
e. Fresh alkali activated earth based composites showed Bingham plastic behaviour at low extrusion rates and demonstrated satisfactory extrudability without the need for rheology modifiers.
f. Introduction of fibres into the fresh paste resulted in two counteracting effects on the extrusion pressures: increase in die entry pressures due to fibre-matrix interaction in the

barrel which increased paste viscosity; and reduction in die land wall resistance due decreased wall slip as a result of the presence of longitudinally oriented fibres along the wall-extrudate interface. However, rheological parameters show that convergent flow in the die entry region is the dominant contributor to extrusion pressures for all fibres studied.

g. Hydrophillic sisal fibres interacted with alkali activated matrices, thereby reducing the degree of alkali activated binder phases in the matrices. Consequently, increased volume fractions of binder phases were observed with polypropylene due to its relatively alkali resistant behavior.

h. Significant strengthening as well as stiffening of the unreinforced earthen matrix was observed in the sisal fibre-reinforced composites. This strengthening occurred via an elastic stress transfer mechanism, which was attributed to fibre-matrix interactions. Predictions from simple rule of mixtures and shear lag models compared satisfactorily with experimental measurements

i. Strengthening contribution from polypropylene fibres was observed in the post-cracking region; as a result, contribution of matrix to composite strength was negligible. Modified ROM model based on frictional slip was used to rationalise composite strength and modulus with satisfactory correlations with experimental measurements

j. The predictions of toughening/resistance-curve behavior obtained for the sisal and polypropylene fibre-reinforced composites were also comparable to the measured resistance curves in the small scale bridging (SSB) and long scale bridging (LSB) regimes indicating that toughening mechanism was predominantly via crack bridging